Studies on fatty acid oxidation in trout liver

Naomi Fawcett

University of St Andrews

A thesis presented for the degree of Doctor of Philosophy

at the University of St Andrews,. November 2004

DECLARATION

I, Naomi Fawcett, hereby certify that this thesis, which is approximately 30,000 words in length, has been written by me, that it is the record of my work carried out by me and that it has not been submitted in any previous application for a higher degree.

Date 30/11/04..... Signature of candidate

I was admitted as a research student in September 2000 and as a candidate for the degree of Doctor of Philosophy in September 2000; the higher study for which this record was carried out in the University of St. Andrews between 2000 and 2004.

Date 30/11/04..... Signature of candidate

I hereby certify that the candidate has fulfilled the conditions of the Resolution and Regulations appropriate for the degree of Doctor of Philosophy in the University of St. Andrews and that the candidate is qualified to submit this thesis in application for that degree.

Date 30/11/04..... Signature of supervisor

In submitting this thesis to the University of St. Andrews I understand that I am giving permission for it to be made available for use in accordance with the regulations of the University library for the time being in force, subject to any copyright vested in the work not being affected thereby. I also understand that the title and abstract will be published, and that a copy of the work may be made and supplied to any *bona fide* library or research worker.

Date 30/11/04..... Signature of candidate

To my parents

AKNOWLEDGEMENTS

I express my greatest thanks to Dr Rona Ramsay, my supervisor for excellent tuition, guidance and help throughout all aspects of the PhD programme.

My gratitude to Dr Val Smith and her group at the Gatty Marine Laboratory, St Andrews for the provision of samples and helpful discussions.

Thanks are also due to Dr Nigel Price for supervision during my time at the Hannah Research Institute in Ayr. Advice on the write-up of chapter six was also appreciated.

Special thanks are due to Irene Tinto for her considerate help, especially with the transport of samples.

The Cobb Scholarship, made available through the University of St Andrews, provided financial support. Thanks to Arthur and Alan Cobb, the trustees. The Student Support Services also assisted in funding and I would like to thank Ailsa Ritchie and her team for their thoughtful help.

I would like to thank my lab colleagues for providing a pleasant and social working environment. A special mention goes to Ana Paula Vintém, Teresa Carlos and Sitheswaran Nainamalai, whose friendship has extended beyond the lab.

Finally, I wish to convey my deepest gratitude to my family for their constant love, encouragement and good humour.

'Thanks be unto God for his unspeakable gift'
2 Corinthians 9:15

ABSTRACT

The driving force for this project was a desire to understand metabolic regulation of fat oxidation in fish, a global goal that was modified by reality to this study of aspects of fatty acid oxidation in trout liver, and, in particular, the carnitine acyltransferase enzymes involved.

Without the need to produce ketone bodies that necessitates high rates of fatty acid oxidation in mammalian liver, the rates of fatty acid oxidation in livers from Oncorhynchus mykiss (rainbow trout) were relatively low. Mitochondria and peroxisomes (35-45%) both contribute to the oxidation. Preliminary data suggest that the metabolic cost of mounting an immune response induces a short term increase in fatty acid oxidation, particularly in the mitochondrial rate. In contrast, food deprivation invoked no short-term (less than fourteen days) response in fatty acid oxidation rates.

The main regulatory point of fatty acid oxidation in mammals is carnitine palmitoyltransferase 1 (CPT1) on the mitochondrial outer membrane. Trout CPT1 was malonyl-CoA sensitive but there was no change in the sensitivity after food deprivation. In mammals enrichment of CPT1 in the mitochondrial contact sites alters it properties in favour of increased rates of fatty acid oxidation. In trout liver, there was no enrichment in the contact sites and no change in malonyl-CoA sensitivity.

In peroxisomes, carnitine octanoyltransferase (COT) specificity defines the optimum transfer of chain shortened fatty acids to the mitochondria. Trout COT was isolated and characterized to show its chain length specificity for longer fatty acids (>C8) and, as for all other species, its lack of malonyl-CoA sensitivity. The COT protein was

subjected to mass spectral analysis and some partial sequence obtained. This confirmed and extended slightly the deduced sequence obtained from cDNA and allowed a comparison of COT between fish and mammals.

ABBREVIATIONS

Abs	Absorbance
BSA	bovine serum albumin (defatted)
CrAT	carnitine acetyltransferase
COT	carnitine octanoyltransferase
CPT	carnitine palmitoyltransferase
CPT1	carnitine palmitoyltransferase of the mitochondrial outer membrane
CPT2	carnitine palmitoyltransferase of the mitochondrial inner membrane
DTT	dithiothreitol
EDTA	ethylenediaminetetra-acetic acid
KCN	potassium cyanide
KPi	potassium phosphate
mPTP	mitochondrial permeability transition pore
PDS	4,4-dithiobispyridine

Chapter 1. INTRODUCTION

3. FATTY ACID OXIDATION IN TROUT LIVER

Chapter 4 Contact sites and CPT1 in trout liver mitochondria

Chapter 1 INTRODUCTION

1.1 β-Oxidation of fatty acids - Historical background

β-Oxidation is the degradation of fatty acids leading to the production of acetyl-CoA, the principal substrate of the tricarboxylic acid cycle, which is involved in generating ATP. β-Oxidation plays a major role in providing energy for the heart and skeletal muscle. In mammals hepatic β-oxidation provides acetyl-CoA for the synthesis of ketone bodies that are used by organs such as the brain when blood glucose levels are low. This is usually during starvation or endurance exercise (Felig and Wahren, 1975).

Investigation of the pathway began in the early twentieth century with the pioneering work of Dutch biochemist Frances Knoop. He fed dogs ω-phenyl-labelled odd or even carbon-number long-chain fatty acids and concluded from the excretion of phenyl-acetylglycine and benzoylglycine respectively that metabolism of fatty acids proceeded by a process of successive removal of two-carbon chain fragments. It is termed β-oxidation because the removal of the two-carbon units occurs at the β-carbon position of the fatty acyl-CoA molecule. These findings were subsequently confirmed by Dakin and the pathway's form and function were soon established after the realisation that acetyl-CoA and not acetate represents the final product of the fatty acid oxidation pathway (reviewed in (Eaton et al., 1996)). Further research outlined the basic sequence of steps in the cycle: FAD-linked dehydrogenation, hydration, NAD^+-linked dehydrogenation and thiolytic cleavage (Lynen and Ochoa, 1989). The understanding of the role of L-carnitine in the transport of fatty acids and the function of malonyl-CoA as a regulator of transport came much later (Bremer, 1977; McGarry

and Foster, 1980). More recently interest in the pathway has been fuelled by the discovery of a secondary oxidising system in the peroxisome (Lazarow and DeDuve, 1976; Moser, 1996; Rinaldo and Matern, 2002) and by the identification of inherited metabolic disorders linked to the deficiency key enzymes involved in the β-oxidation pathway in both peroxisomes and mitochondria (Moser, 1996; Rinaldo and Matern, 2002).

The β-oxidation of fatty acids in fish is basically the same as in mammals (Bilinski, 1970). The pathways of fatty acid metabolism have been reviewed by (Meed and Kayama, 1967). The essential fatty acids and saturated and monoenoic fatty acids are all equally used by fish for energy production (Halver, 1980) in contrast to mammals where saturated fatty acids predominate as a substrate for energy production.

1.2 Mitochondrial β-oxidation

Mammalian fatty acid oxidation for energy production occurs predominantly in the mitochondria under normal physiological conditions. After the fatty acids have been activated and transported into the mitochondria (fig 1.1 and 1.2), the pathway proceeds as a spiral successively removing two carbons at a time (fig 1.3). Each round of β-oxidation produces one mole of ATP, NADH, $FADH_2$ and acetyl-CoA. NADH and $FADH_2$ are also generated during the oxidation of acetyl-CoA in the TCA cycle. They then enter the respiratory pathway for the production of ATP. The yield for one mole of palmitate is 107 moles of ATP (Berg et al., 2002).

1.2.1 Carnitine-dependent uptake of fatty acids by mitochondria

The first step in the pathway (fig 1.1) is the activation of the fatty acid to fatty acyl-coenzyme A (CoA). Long chain fatty acids must be activated in the cytoplasm before being oxidised in the mitochondria, although medium and short chain acids can be activated in the matrix. Activation is catalysed by acyl-CoA synthetase. Activation occurs in two steps. First, the fatty acid reacts with ATP to form an acyl adenylate. The sulphydryl group of CoA then attacks the acyl adenylate, which is tightly bound to the enzyme, to form acyl-CoA and AMP (Fritz and Marquis, 1965).

Activated long-chain fatty acids are carried across the inner mitochondrial membrane as their L-carnitine esters (fig 1.2). The acyl group is transferred from the sulphur group in CoA to the hydroxyl group in L-carnitine, forming acyl-L-carnitine. This reaction is catalysed by carnitine palmitoyltransferase 1 (CPT1). Acyl-L-carnitine is then transported across the inner mitochondrial membrane by a translocase (Ramsay and Tubbs, 1975). The acyl group is then transferred back to the CoA on the matrix side of the membrane, a reaction that is catalysed by carnitine acyltransferase 2 (Clarke, 1981). Finally, L-carnitine is returned to the cytosolic side of the membrane by the translocase.

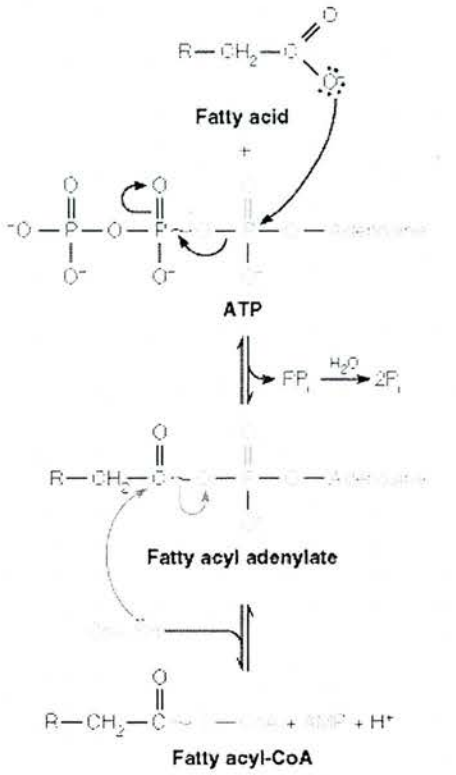

Fig 1.1 Activation of fatty acid to fatty acyl –CoA

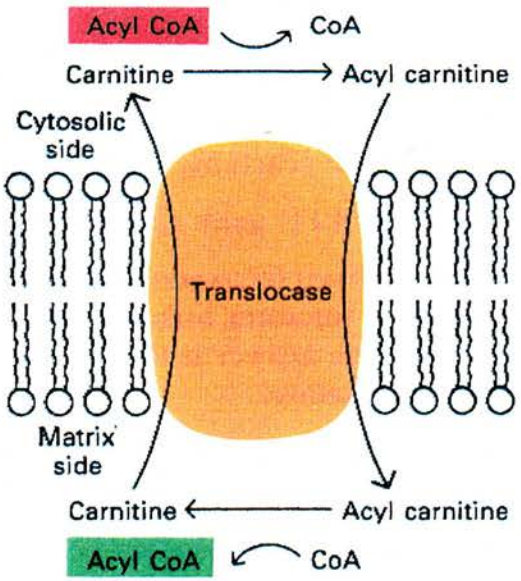

Fig 1.2 Transport of acylcarnitine by carnitine: acylcarnitine translocase (Stryer, 1988).

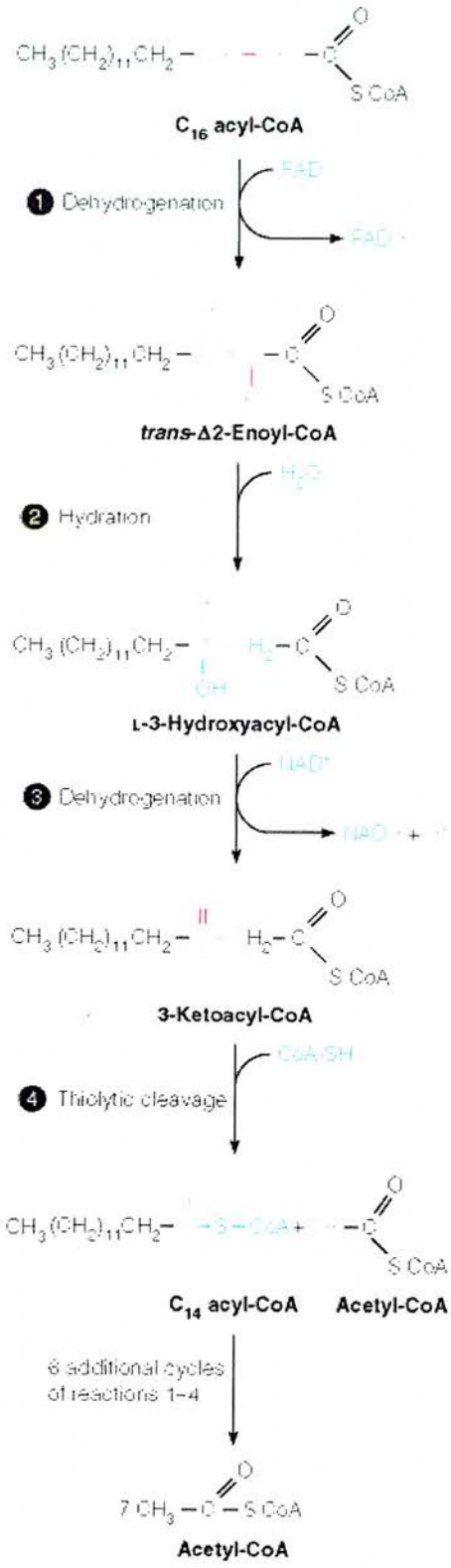

Fig 1.3 β-oxidation spiral

1.2.2 Regulation of mitochondrial β-oxidation

The rate of fatty acid oxidation is primarily determined by the availability of substrate but there are intracellular controls for modulation of fuel use in the cell. (Clark et al., 2004) showed that physiological concentrations of fatty acids perfused through rat hearts increased the activity of AMP protein kinase, resulting in increased phosphorylation of acetyl-CoA carboxylase and decreased malonyl-CoA. This pathway is proposed to be a feed-forward mechanism to up-regulate fatty acid import into the mitochondrion for oxidation.

The regulated step in mitochondrial β–oxidation in mammals is the reaction catalysed by CPT1 (McGarry et al., 1978). The regulator, malonyl-CoA, is formed by acetyl-CoA carboxylase in the rate-controlling step in fatty acid synthesis. Malonyl-CoA inhibits CPT I at low micromolar concentrations (Robinson and Zammit, 1982). This prevents *de novo* synthesised fatty acids from entering the mitochondria. As once the fatty acids are inside the mitochondria, they are committed to β-oxidation. The cleavage of the thioester, the final step in the β-oxidation spiral, can be inhibited by high concentrations of acetyl-CoA (McGarry and Foster, 1980). This inhibition results in a build-up of acyl-CoA derivatives that are transferred to carnitine and re-exported.

1.3 Peroxisomal β-oxidation

The recognition of the involvement of peroxisomes in metabolising fats (Lazarow and DeDuve, 1976) prompted numerous studies to characterise and understand the function of a second system. This led very quickly to the elucidation of the reactions and enzymes that make up the pathway (reviewed in (Schultz, 1991). The studies were aided largely by the use of the hypolipidemic drugs such as clofibrate and di (-2-ethylhexyl)phthalate, a plasticizer. These drugs induce both the proliferation of peroxisomes and the activity of the enzymes in the pathway (Lazarow and DeDuve, 1976). The peroxisome has evolved as a separate organelle, capable of oxidising fatty acids but has several characteristics that distinguish it from the mitochondrial system. Peroxisomal oxidation is insensitive to cyanide because it is not coupled to the electron transport system like mitochondrial fatty acid oxidation where cyanide inhibits the electron transport chain. Peroxisomes do not fully oxidise a fatty acid chain but rather shorten it and then pass it to the mitochondria to be fully oxidised (Lazarow, 1978).

1.3.1 Transport of fatty acids in the peroxisome: a carnitine-dependent system?

Fatty acid activation and β-oxidation of fatty acids in the peroxisome is shown in fig 1.4. Activation of long-chain fatty acids is catalysed by acyl-CoA synthase on the cytoplasmic face of the membrane (Singh et al., 1992). Recent reports (reviewed in (Ramsay, 1999) suggest that a carnitine system analogous to that in the mitochondria may be operational in the peroxisome (fig 1.4). Carnitine has never been found in isolated peroxisomes but this may be due to the fragile nature of its membrane. It is suggested that during isolation the peroxisome membrane is disturbed enough to

allow carnitine but not proteins to leak out (Ramsay, 1999). The presence of a carnitine carrier either identical or homologous to the mitochondrial carrier is strong evidence that carnitine dependent transfer must take place across the peroxisomal membrane (Fraser and Zammit, 1999).

Functional studies support the need for the carnitine system in peroxisomes. A study on cultured fibroblasts showed that the carnitine carrier and CPT2 were essential for complete oxidation of phytanic acid but CPT1 was not. The initial steps of oxidation take place in the peroxisomes so it was deduced that COT catalysed the transfer of the intermediates to carnitine for the export to the mitochondria (Verhoeven et al., 1998). In yeast, both citrate synthase and carnitine acetyltransferase had to be knocked out in order to inhibit peroxisomal β-oxidation, implying that transfer of the acetate group to carnitine enabled its export from the peroxisomes (Elgersma et al., 1995). This work also established that, in the cell, the peroxisomal membrane is impermeable to acetyl-CoA.

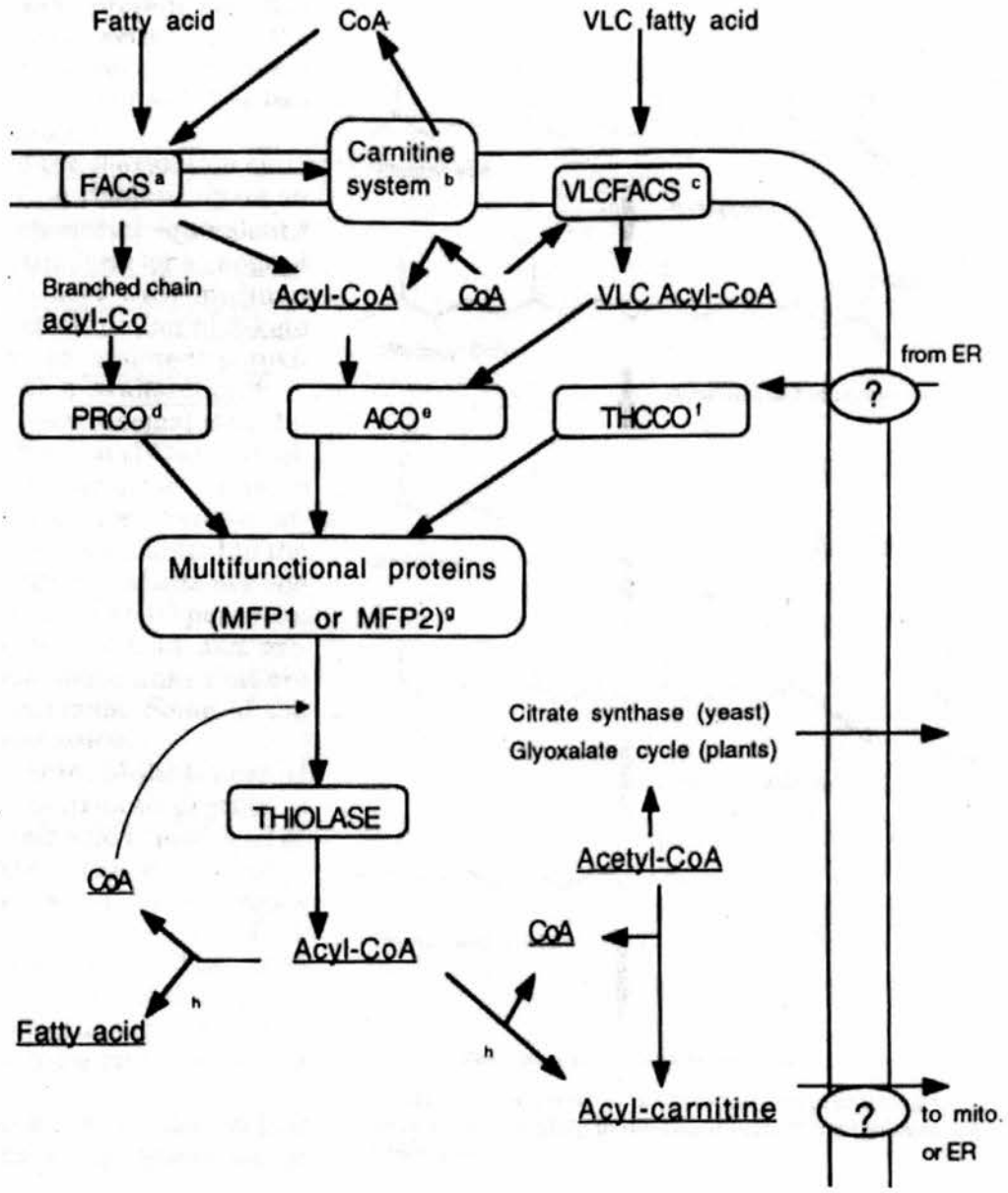

Fig 1.4 Fatty acid activation and β-oxidation in peroxisomes (Ramsay, 1999)

1.4.2 Peroxisomal β-oxidation

The cyanide-insensitive fatty acyl-CoA oxidising system is characterised by its independence from the electron-transport chain. This is because the first step in the peroxisomal pathway differs from that in the mitochondrial pathway. In contrast to the mitochondrial energy-generating dehydration step, the peroxisomal version is catalysed by acyl-CoA oxidase, which transfers electrons via its cofactor flavin adenine dinucleotide to O_2 producing H_2O_2. Fatty acyl-CoA oxidase is widely reported as being the rate limiting enzyme in the peroxisomal pathway(Hashimoto, 1990). Since catalase is present in peroxisomes, the H_2O_2 is cleaved to O_2 and H_2O.

The intermediates of peroxisomal fatty acid oxidation are identical to the mitochondrial intermediates of fatty acid oxidation shown in figure 1.5. The final stage of the peroxisomal pathway is the thioloytic cleavage of 3-ketoacyl-CoA thiolase by CoASH, catalysed by 3-ketoacyl-CoA thiolase. The end products are chain shortened acyl-CoAs, acetyl-CoA and NADH (Schultz, 1991).

All these products must be exported from the peroxisome despite the impermeability of the membrane to them. Gene disruption studies in yeast demonstrated that malate dehydrogenase was required for the shuttling of NADH out of the peroxisomes (Elgersma et al., 1995) and there may also be redox shuttling via lactate and pyruvate (McClelland et al., 2003). Both carnitine acetyltransferase and citrate synthase had to be deleted in yeast to prevent export of acetyl-CoA (Elgersma et al., 1995). CrAT catalyses the transfer of acetyl groups to carnitine and CPT is assumed to do the same for the chain shortened fatty acid products. The carnitine but CPT1-dependent oxidation of the peroxisomal products of phytanic acid breakdown was demonstrated

in cultured fibroblasts, providing evidence for this (Verhoeven et al., 1998). The presence of a carnitine exchange system in the peroxisomal membrane has now also been established by Western blot (Fraser and Zammit, 1999).

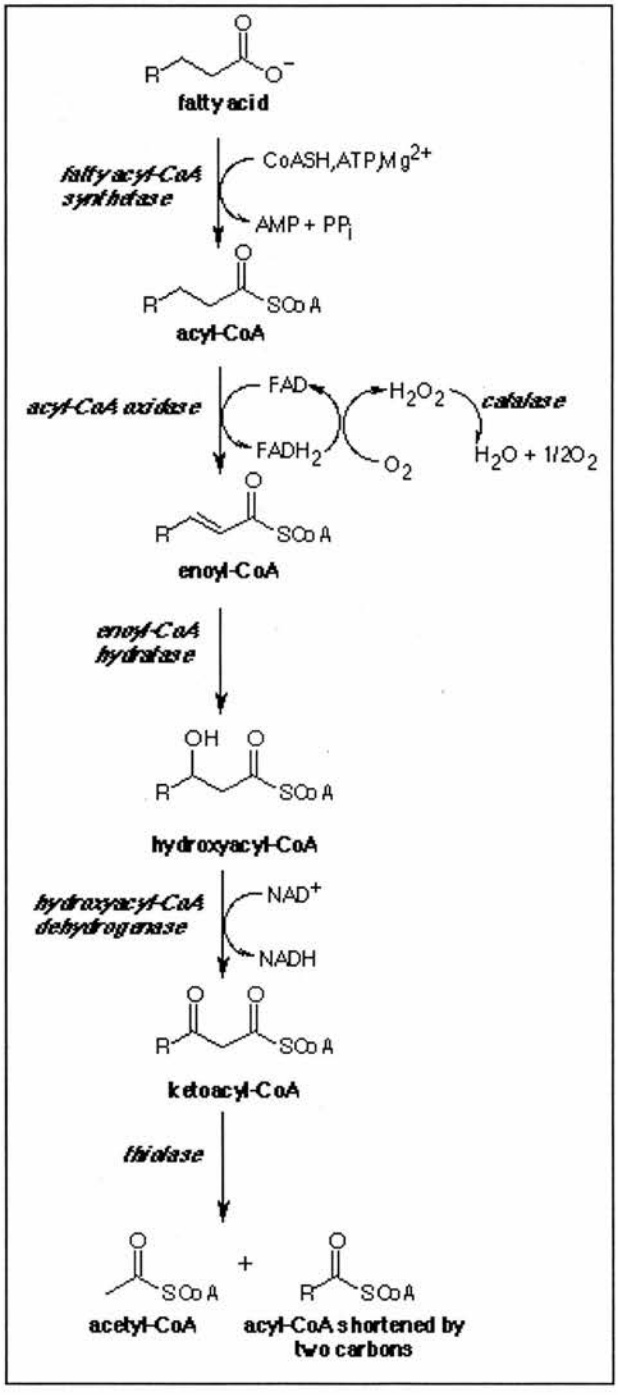

Figure 1.5: Peroxisomal β-oxidation pathway

[Courtesy of www.peroxisome.org/Scientist/Biochemistry/boxidationtext.html]

The peroxisomal β-oxidation system is active on saturated acyl-CoA derivatives of both odd and even chain lengths ranging from 7 to at least 20 carbons, being most active on lauryl-CoA (Lazarow, 1978). Although mammalian peroxisomes are capable of oxidising regular fatty acids, an important function appears to be the partial β-oxidation of very long chain fatty acids. Other functions include partial β–oxidation of prostaglandins, dicarboxylic acid, xenobiotic compounds such as phenyl fatty acids and hydroxylated 5B-choestanoic acids formed during the conversion of cholesterol to cholic acid (Schultz, 1991). Polyunsaturated long chain fatty acids (PUFA) such as docosahexanoic acid are poorly oxidised by the mitochondria and often inhibit oxidation of other fatty acids by mitochondria. PUFAs are good substrates for peroxisomal fatty acid suggesting that peroxisomes can metabolise fatty acids that the mitochondria cannot. Peroxisomes do not fully oxidise a fatty acid but rather chain shorten it and then pass it over to the mitochondria complete the process with better energy conservation. The number of cycles in the peroxisome varies. For example, using 1- and 3- radiolabelled fatty acids followed by HPLC separation of the soluble products, demonstrated that 24:5 and 24:6 polyunsaturated fatty acid were mostly beta-oxidized only one cycle in peroxisomes (Tran and Christophersen, 2002).

1.4 Lipid catabolism in fish

There are two main classes of fish: elasmobranches and teleosts. Elasmobranchs describe a family of cartilaginous fish that include sharks, skates and dogfish. Teleosts describe a large group of bony fish that are characterised by a movable upper jaw. They are found in both freshwater and saltwater environments and examples include eels, catfish, tuna, trout, cod and salmon. It is though that elasmobranches evolved from the sea whereas teleosts most likely originated from freshwater (Froese and Pauly, 2002). The processes of lipid catabolism have not been explored as extensively as they have been in mammals (Henderson and Tocher, 1987), but teleosts like higher vertebrates store a large amount of their triacylglycerol (TG) in a discrete abdominal tissue (Love, 1970). During starvation ketone bodies are an important fuel for elasmobranches but not nonesterified fatty acids whereas for teleosts nonesterified fatty acids but not ketone bodies are an important fuel during starvation (Zammit and Newsholme, 1979). Rates of fatty acid oxidation vary considerably between elasmobranches and teleosts. The mitochondria and peroxisomes both show broad chain-length specificity of hepatic β-oxidation of fatty acids in fish (Henderson and Sargent, 1985a). In one teleost (*Notothenia gibberifrons*) substrate specificities were broader for peroxisomal β-oxidation than mitochondrial β-oxidation (Crockett and Sidell, 1993b). Also, the exact metabolic partitioning between mitochondrial and peroxisomal compartments remains unclear and reported estimates vary considerably. Investigation into partitioning in the Longhorn Sculpin (a bottom dwelling marine teleost) reported that equivalent capacities for palmitoyl-CoA oxidation existed for the two organelles (Crockett and Sidell, 1993a). In fact, several lines of evidence suggest that peroxisomal β-oxidation may be a significant pathway involved in energy metabolism in the fish. Many fish consume long chain fatty acids as part of their

natural diet. Zooplankton (calenoid copepods) contain large reserves of wax esters rich in 22:1 fatty alcohol which is converted to 22:1 fatty acid in the fishes' intestinal mucosae. A significant fraction of the esters of long-chain polyunsaturated fatty acids which if not catabolised, will accumulate in the fish (Sergeant et al., 1979). As with mammals, peroxisomal β-oxidation may assist the mitochondria in lipid metabolism as well as metabolising fatty acids that the mitochondria cannot.

1.5 Control of fatty acid oxidation in fish

Very little data exists on the mechanisms involved in controlling β-oxidation in fish (Rodnick and Sidell, 1994) reported that the red muscle of striped bass (*Morone saxatilis*) was sensitive to malonyl-CoA. Moreover, (Froyland et al., 1998) showed that CPT1 present in the liver, heart, white and red muscle of Atlantic salmon (*Salmo salar)* was malonyl-CoA sensitive and studies in recombinant CPT1 in rainbow trout (Gutieres et al., 2003) also displayed malonyl-CoA sensitivity suggesting that fatty acid oxidation is regulated in a similar way to that shown in mammalian tissue.

1.5.1 Effect of seasonal variations on fatty acid metabolism

Muscle metabolic organisation in many fish undergoes seasonal variation. Female fish undergo a period of starvation during part of their reproductive cycle when they rely on lipids as a major fuel source (Kiessling et al., 1995a). During the feeding season, females reserve large amounts of lipids, which are depleted during spawning. As the fish matures, triglycerides and free fatty acids increase in the liver (Love, 1970). Cold acclimatisation can stimulate an increase in long-chain acyl-CoA synthase activity, the first enzyme required in either fatty acid oxidation or complex lipid synthesis.

(Patey and Driedzic, 1997) reported a 2-fold increase in long-chain acyl-CoA synthetase activity in heart tissue from rainbow trout acclimatised to 5°C.

1.5.2 Effect of temperature on fatty acid and mitochondrial oxidation in fish

Mitochondria of Arctic fish seem to have no adaptation of their mitochondrial function. Oxidative capacity increases with temperature up to 18C but the proton leak increases more sharply so that coupling is lost at high temperatures (Hardewig et al., 1999). The same relationship of oxidation rate to temperature was observed in a wide range of fish adapted to different temperature and it was shown that cold adaptation in evolution was achieved by increasing the volume and surface density of mitochondria in fish muscle (Johnston et al., 1998).

1.6 Mitochondrial contact sites and regulation of fatty acid influx

In liver tissue from starved animals, increased contacts between the inner and outer membranes of mitochondria were observed by electron microscopy. (Blok et al., 1971) were the first to suggest a role for contact sites in the transport of fatty acids across the membranes of the mitochondria but it was the elegant work of Zammit's group that established an enrichment of CPT1 and CPT2 in the contact sites accompanied by a change in the kinetics of CPT1 to give optimum activity for increased fatty acid flux (Fraser and Zammit, 1998).

(Hackenbrock, 1968) first described the contact sites within the mitochondria. He defined contact sites as places where fusion or semi-fusion of the inner and outer mitochondrial membrane takes place. It is believed that the contact sites allow the formation of a unique microenvironment in which specific enzymes can function in

the most efficient way. The exact structure of the contact sites is yet to be determined. In principle, the transient contact sites formed by the TIM and TOM complexes for the import of matrix proteins are also a type of contact site (Reichert and Neupert, 2002). The contact sites are often referred to as mitochondrial permeability transition pore (mPTP), because, once open, there is a change from negative potential in the matrix to a more positive potential. The mPTP has been studied intensely because of its role in apoptosis. Currently the main components of the mPTP are believed to be the voltage dependent anion channel (VDAC), adenine nucleotide translocase (ANT), cyclophilin D (CyP-D), hexokinase (HK), creatine kinase (CK) and a periphereal benzodiazepine receptor (pBzR).

1.6.1 Components of the isolatable contact sites

The voltage dependent anion channel (VDAC) is found within the outer mitochondrial membrane of the mPTP. It was first discovered in 1979 in extracts of *Paramecium* (Colombini, 1979) and has been isolated from plasma membrane and from mitochondria across the animal and plant kingdom. VDAC is a 31 kDa protein, which forms a large pore structure. The opening and closing of the channel is dependent on voltage and a 20-30mV change can produce a partially closed sub-state when applied in either direction across the phospholipids membrane (Benz et al., 1990) Further experiments with *Neurospora crasa* by (Mannella, 1990) revealed that the repeating unit is a group of six transmembrane pores each 3 - 4 nm long and 2.5 – 3 nm wide, with centre-to-centre spacing of approximately 5 nm. The overall structure is similar to that of a β–barrel.

The second major component is **the adenine nucleotide translocase (ANT)** from the inner membrane. ATP and ADP do not diffuse freely across the inner mitochondrial membrane. A specific transport protein, ANT, exchanges these highly charged molecules across this permeability barrier (Berg et al., 2002). ANT is a dimer of two identical 35 kDa proteins containing one nucleotide binding site. These proteins can exist into two conformations, allowing the ATP/ADP binding region to alternate between the matrix side and the cytosol side. ANT ligands that bind to the matrix binding site inhibit the mPTP, whereas cytosolic binding ligands activate the mPTP (reviewed in (Crompton, 1999). The binding of either ATP or ADP depends on their relative concentration, which is directly related to the membrane potential. During positive membrane potentials the shuttling of ATP from the matrix to the cytosol is greater than that of ADP because ATP has an extra negative charge.

Another component is **cyclophilin D** (CyP-D), a water-soluble protein. It is believed that the main role of cyclophilins could be in accelerating the folding of some denatured proteins (Lin et al., 1988). Its involvement within the mPTP was discovered through the experiments that indicated that the pore is blocked by cylosporin A (CSA). Cyclophilin was suggested because similar amounts of bound CSA are needed to block the pore and to inhibit the enzymatic activity of the mitochondrial CyP by sitting in its active site (Halestrap and Davidson, 1990).

Adams et al (Adams et al., 1989) demonstrated that both **hexokinase (HK)** and **creatine kinase (CK)** were exclusively enriched in the contact site of mitochondria. They proposed that depending on the bound or free state of the respective kinases they would either utilise glycolytic or mitochondrial ATP and thus affect the metabolic rate

in the respective ATP producing system. Further experiments on creatine kinase in the mPTP by Schiegel (Schlegel et al., 1988) and Schnyder (Schnyder et al., 1988) demonstrated that mitochondrial creatine kinase forms an octomer of four dimers. This ordered structure could suggest that CK might operate as an energy-sensing molecule in the mPTP.

The **peripheral benzodiazepine receptor (pBzR)** is believed to be located on the outer membrane side of the contact site. The pBzR can bind to Bcl-2, suggesting a link to the role of the mPTP in apoptosis.

1.6.2 Overall topography of the mPTP

(Szabo et al., 1993) proposed that an mPTP structure of two co-operating VDAC molecules plus two copies of the ANT and one or more copies of the 18 KDa pBzR. These components would interact, giving rise to the observed co-operative behaviour and to the various properties of the mPTP. The creatine kinase octamer has been proposed as the link between VDAC and ANT whilst the hexokinase is believed to interact on the outer membrane by binding to VDAC (reviewed in (Crompton, 1999).

1.6.3 The mitochondrial transition pore and cell death

The mitochondrial transition pore has been suggested to be involved in both necrotic cell death and apoptotic cell death. Necrosis may occur due to a tissue overload of calcium causing the mPTP to open. This opening of the pore could cause an increase in free calcium, resulting in cell death.

Apoptotic cell death is a planned shutdown of the cell. Opening of the mPTP in response to signals or a change in the redox potential triggers the release of cytochrome *c* to activate the proteases in the cytosol. The opening is regulated by the Bcl-2, which are a family of proteins that are involved in mitochondrial dependent apoptosis (Reed et al., 1998). The family consists both of inducers such as Bax, and inhibitors such as Bcl-2. The inducers of the Bcl-2 family trigger opening of the mPTP and the release of cytochrome c and apoptosis-inducing factor, proteins that causes the activation of caspases. The activated caspases can target specific aspartic acid residues and hydrolase proteins, resulting in death. ATP is needed to execute the apoptotic programme by the apoptosis-inducing factor (reviewed in (Breckenridge and Xue, 2004).

1.6.4 Fatty acids and apoptosis

Some fatty acids, in particular the metabolic products derived from poylunsaturated fatty acids, can influence signalling pathways leading to apoptosis (Tang et al., 2002).

1.6.5 The mitochondrial transition pore and fatty acid handling

(Blok et al., 1971) and (Baranska and Wojtczak, 1984), were the first to suggest a role for the mPTP in the transport of fatty acids across the membranes of the mitochondria. This hypothesis was proposed because of the unique enzyme environment of the mPTP, and the increased concentration of ATP at these sites that can cause a change in the potential across the membranes. Until recently however, little experimental data was available to reinforce this hypothesis.

1.6.6 Enrichment of CPT1 and CPT2 in contact sites

(Fraser and Zammit, 1998) investigated the distribution of CPT1 and CPT2 within the mitochondrial outer membrane, inner membrane and contact site. They found that both the CPT1 and CPT2 were in higher concentrations at the contact site than the outer or inner membrane. Furthermore, CPT1 was located towards the outer membrane surface of the contact whilst CPT2 was located towards the inner membrane surface.

In further studies, (Fraser and Zammit, 1999) conducted similar experiments to deduce the distribution of the transporter CACT. They found that CACT had a much more uniform distribution across the inner mitochondrial membrane. It was suggested that this more even distribution of CACT could be because CACT function is not solely the transport of acyl-L-carnitine formed by CPT1. It is also used to export excess activated acetyl groups as acetyl-L-carnitine and import acyl-L-carnitine formed elsewhere in the cell, e.g. peroxisomes.

1.6.7 CPT1 in the mPTP – kinetic properties and malonyl-CoA inhibition

Inhibition by malonyl-CoA has been shown to be uncompetitive in the outer membrane, but competitive in the contact sites. Uncompetitive inhibition in the outer membrane ensures that accumulating acyl-CoA required for other cytosolic functions is not converted into acylcarnitine. Competitive inhibition in the contact site allows long chain acyl-CoA to overcome malonyl-CoA inhibition and prevent accumulation permitting channelling to β-oxidation (Fraser et al., 2001).

The affinity for the acyl-CoA substrate also changed when CPT1 was located in the contact sites. The Km for palmitoyl-CoA was 2.4- fold lower, which favours transfer

to carnitine and, hence, higher transfer of the activated fatty acid into the mitochondria (Fraser et al., 2001)

1.7 Peroxisomal carnitine octanoyltransferase (COT)

COT serves to transfer the chain-shortened products of peroxisomal β-oxidation from the limited peroxisomal pool of CoA to the larger cellular pool of carnitine ready for translocation into mitochondria for complete oxidation (reviewed in (Ramsay and Arduini, 1993); (Ramsay, 1999). Even if the products are as short as C_6 or C_8 the isoenergetic process via carnitine is more likely than the futile cycle of hydrolysis followed by reactivation in the mitochondrial matrix (Ramsay and Arduini, 1993).

COT has been well characterized, purified and cloned, appearing as a soluble and presumably matrix enzyme (Ramsay, 1999). However, the purified COT properties (Ramsay, 1988) were quite different from the properties of the enzyme assayed in isolated peroxisomes (Derrick and Ramsay, 1989; Ramsay, 1996). In 1996, the existence of two catalytically active carnitine medium/long chain acyltransferases was proposed, due to the different membrane and matrix enzyme activities (Singh et al., 1996). Another feature that led to this conclusion was the observation that the enzyme in the membrane fraction showed higher malonyl-CoA sensitivity compared to the enzyme in the matrix fraction (Derrick and Ramsay, 1989; Singh et al., 1996).

1.7.1 Deduced amino acid sequences of COT

The human (Ferdinandusse et al., 1999), rat (Choi et al., 1995) and bovine (Cronin, 1997a) cDNA sequences of peroxisomal COT encode proteins of 612 or 613 amino acids with a deduced molecular weight of about 70 kDa. These proteins contain the

carboxyl-terminal sequences (THL, AHL and PHL, respectively) that serve as a peroxisomal targeting signal (PTS). However, other signals may also be involved or the folded state of the protein may contain specific information for sorting (Ramsay et al., 2001). The carboxyl-terminal THL, AHL or PHL sequence indicates that, like CrAT, the carnitine octanoyltransferase will be imported into the peroxisome by the same transporter (with the PTS-1 receptor) as the β-oxidation enzymes.

Although more is now known about defects in the human peroxisomal β-oxidation system, no human disease-causing mutations in COT are yet known (Wanders et al., 2001). Mutations that affect the activity of CPT1 and CPT2 have mild to severe affects on muscle and/of liver function in humans and so have been identified and some characterised after expression in yeast. The most common mutation in CPT2 is S113L which has only mild muscular consequences (Taroni et al., 1992). L-CPT1 deficiency presents as recurrent attacks of fasting hypoketotic hypoglycemia (Bonnefont et al., 1999). The mutation causing it was G710E which, by comparing the sequence to CrAT and its structure, is now thought to block the acyl binding site (Gobin et al., 2003).

Mutational studies in heterologously expressed proteins from several species have identified the function of several of the conserved residues (reviewed in (Ramsay et al., 2001). The catalytic histidine in COT is H327 and this residue is conserved throughout the family. The STS motif is also found in all the transferases and mutations in bovine COT established that these residues are important for carnitine binding (Cronin, 1997b) and Arg 505 is important in binding the carboxylate group of carnitine (Cronin, 1997a).

Sequence comparisons of COT with the malonyl-CoA sensitive CPT1 led to the suggestion that two histidines in COT would contribute to malonyl-CoA sensitivity. When rat COT was expressed in yeast, malonyl-CoA sensitivity was found which disappeared in these mutations. In particular, the H131 that is Y in bovine COT was thought to explain the lack of malonyl-CoA sensitivity there. However, recent work in the Ramsay lab has shown that none of the purified COT proteins (rat with H131 and human and cow with Y131) have any sensitivity to malonyl-CoA except as a competitive inhibitor (Sitheswaran et al, in preparation) and the H340Y mutation makes no difference.

Further sequence comparisons will be made in Chapter 6 with the wider evolutionary perspective provided by the trout COT information.

1.7.2 Kinetics of COT

Both CrAT and COT follow a rapid equilibrium, random mechanism and showed an equilibrium constant close to 1 (Bhaird et al., 1993). This means that the role of COT, like CrAT, is to maintain the equilibrium between the acylation state of the CoA and carnitine pools in peroxisomes (Ramsay, 1999). After perturbation of the system, the rate at which the equilibrium is achieved will depend on the level of expression of the activity and the kinetic parameters (Ramsay, 2000).

The specificity of the COT present in the peroxisomes may play a role in determining the point of chain termination (Ramsay, 1999). The relative substrate specificity (expressed as the V_{max}/K_M) for acyl-CoA varies among species, as shown in the figure

1.6. The COT from mouse liver has highest activity with C_6 acyl-CoA chain-length and almost no activity with C_{16} or longer (Farrell et al., 1984), whereas rat liver COT has an optimum at C_8 and shows good activity with C_{16} and C_{18} acyl-CoA (Miyazawa et al., 1983). Bovine COT has the longest chain-length preference, since it has good activity at C_{10} and an optimum at C_{16} (Ramsay, 1988). The physiological importance of the differences between the specificity of peroxisomal COT from different species is not yet known. However, theoretically, the ability to transfer longer chain-lengths could be advantageous, because the carnitine system has been shown to be the main route for transfer of chain-shortened products from the peroxisomes to the mitochondria, where their further oxidation is accompanied by more efficient energy conservation (Ramsay, 1999).

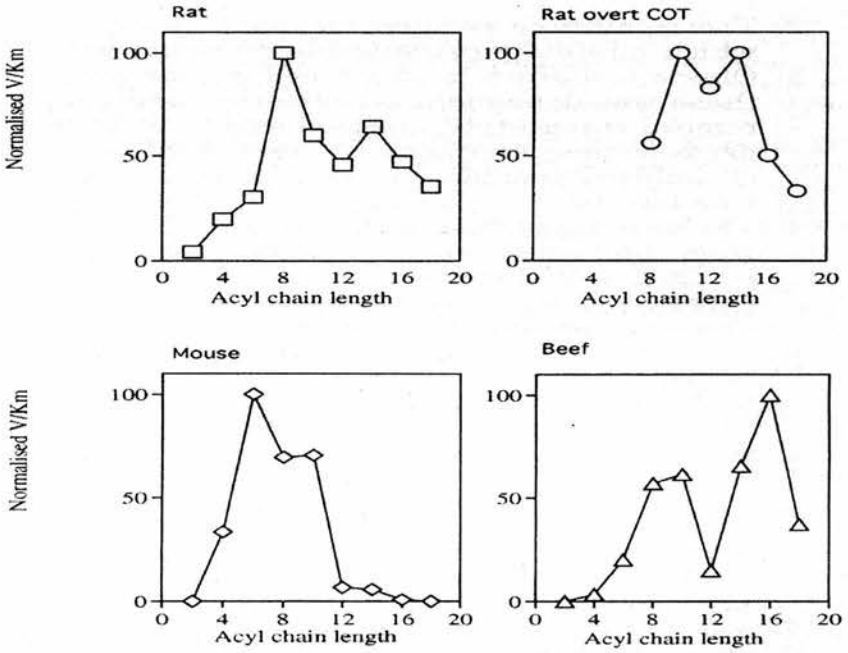

Figure 3. Comparison of the chain length specificity of peroxisomal COT from rat, mouse, and bovine liver peroxisomes. The specificity of each enzyme was calculated as V/K_m but then expressed as percentage of the maximum value for that species to allow direct comparison. Data are given for the matrix (□)[27] and overt (○)[29] COT from rat liver (*top*). The mouse (◇)[26] and bovine (△)[28] data are for the matrix COT only.

Figure 1.6: COT fatty acyl-CoA chain length specificity from rat, mouse and cow (Ramsay, 1999)

1.7.3 Structure of COT

CoA-dependent acyltransfer reactions are common within the cell, so Hegardt's group used homology modelling based on other acyltransferases to construct homology models for COT and CPT1 (Morillas et al., 2001). The model, based on the known structure of rat enoyl-CoA hydratase, showed a putative acyl-CoA binding mode and allowed identification of residues close to the active site that could be mutated to identify their function. The model is shown in Fig 1.7. In further modelling they docked malonyl-CoA to the COT model (Morillas et al., 2002).

The crystal structure of CrAT, published in 2003, superseded the models (Jogl and Tong, 2003) but allowed the Hegardt group to construct a much better model because of the close sequence homology of the carnitine acetyltransferases. Although small crystals of COT have been grown in our laboratory, no diffraction pattern has yet been obtained. The crystal structure of CrAT clearly defined the carnitine and CoA binding sites and a putative acyl binding region. This putative binding region was then given functional support by the mutation of M564 to glycine in CrAT that resulted in activity with longer chain substrates (Hsiao et al., 2004; Morillas et al., 2004) and by the mutation in COT of G553 to the larger methionine which resulted in the loss of activity with any substrate longer than acetyl-CoA (Morillas et al., 2004). The crystal structure of CrOT has now been published (Jogl et al., 2004) but is not discussed in this chapter.

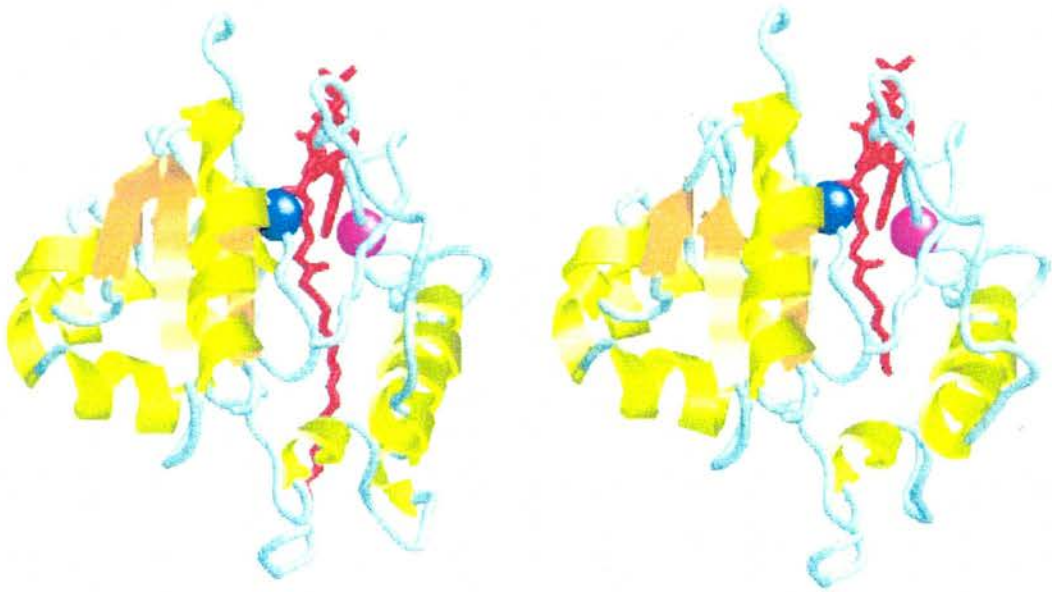

Fig 1.7 CPT1 and COT structural models. Shown is a *ribbon plot* representation of the proposed models for the catalytic surrounding regions of CPT I (*left*) and COT (*right*). β-Sheets are in *orange*, α-helices are in *yellow*. *Stick representations* of a molecule of palmitoyl-CoA (*left*) or octanoyl-CoA (*right*) are included, suggesting their putative locations at the active site. The positions of CPT I amino acids His473 (*blue*) and Ala381 (*magenta*) and their equivalent COT residues His327 (*blue*) and Ala238 (*magenta*) are also indicated as *colored spheres*. **CPT I and COT structural models.** Shown is a *ribbon plot* representation of the proposed models for the catalytic surrounding regions of CPT I (*left*) and COT (*right*). β-Sheets are in *orange*, α-helices are in *yellow*. *Stick representations* of a molecule of palmitoyl-CoA (*left*) or octanoyl-CoA (*right*) are included, suggesting their putative locations at the active site as *coloured spheres* (Fig 1.7 taken from Morillas et al, 2001).

1.7.4 Malonyl-CoA inhibition of COT

1.7.4.1 Overt COT in intact peroxisomes

The discovery of malonyl-CoA-sensitive carnitine acyltransferase activity in peroxisomes was very important as it demonstrated that regulation of acyltransferase by malonyl-CoA was not just confined to mitochondria (Derrick and Ramsay, 1989). There are three malonyl-CoA-sensitive acyltransferases: CPT1 in the mitochondrial outer membrane, COT as measured in intact peroxisomes and CPT_{ER}. All three malonyl-CoA sensitive enzymes have different properties with respect to the detergent inhibition and solubilization (Bieber, 1988). The malonyl-CoA sensitivity of peroxisomal COT, like that of mitochondrial CPT1, is reportedly lost on

solubilization of the enzyme (Derrick and Ramsay, 1989; Farrell and Bieber, 1983; Miyazawa et al., 1983). However, (Nic a'Bhaird and Ramsay, 1992) studied the inhibition of COT by malonyl-CoA and related compounds and compared the characteristics of the inhibition of the purified enzyme with the inhibition of the enzyme in intact peroxisomes. In contrast to intact peroxisomes, the purified COT was inhibited by malonyl-CoA only as a substrate analogue, with a Ki of 106 μM. The intact peroxisomes were 50% inhibited by 1 μM malonyl-CoA, similar to CPT1 and well within the physiological range (Derrick and Ramsay, 1989).

The malonyl-CoA inhibition of CPT1 and COT is strongly influenced by the particular assay conditions used, such as buffer composition, pH, acyl-CoA substrate and the presence or absence of serum albumin (Nic a'Bhaird and Ramsay, 1992). This factor is particularly important in the kinetics of the inhibition, since IC_{50} values are critically dependent on the substrate concentration used (Nic a'Bhaird and Ramsay, 1992). It was also shown by Nic a'Bhaird & Ramsay, in 1992, that the pH dependent increase in sensitivity of CPT1 by malonyl-CoA is also observed for the purified COT, which can be explained by the presence of a histidine residue in the active site. Both COT in isolated peroxisomes and the purified COT show similar K_m values for fatty acyl-CoA esters, but the Ki value for the inhibition of COT in intact peroxisomes was dramatically lower (Nic a'Bhaird and Ramsay, 1992). Two possibilities were proposed to explain this fact. The existence of a regulatory subunit with a malonyl-CoA-binding site could be lost on solubilization of the enzyme, with a subsequent decrease in sensitivity to inhibition but this is not thought to happen now, Alternatively, the catalytic polypeptide could contain a separate binding site for malonyl-CoA, but on solubilization of the enzyme a conformation change can occur,

which results in a lowered affinity for malonyl-CoA at this regulatory site (Nic a'Bhaird and Ramsay, 1992). From these observations of the inhibition of *in situ* peroxisomal COT by malonyl-CoA, which resemble those of CPT1, Nic a'Bhaird & Ramsay suggested that parallel regulation of the overt COT in peroxisomes and of CPT1 in mitochondria might be necessary for the control of cellular fatty acid metabolism.

1.7.4.2 Malonyl-CoA inhibition of purified COT

Further work on the malonyl-CoA sensitivity of COT in rat suggested that two non-catalytic site histidines were essential for the malonyl-CoA binding at high affinity and inhibition in peroxisomal membranes (Morillas et al., 2000). Cloned mutants of rat COT in yeast peroxisomal membranes were 57% inhibited by 200 μM malonyl-CoA only if the conserved residues His131 and His340 were present. This was similar to the competitive inhibition observed in purified bovine COT, where a Ki value of 106 uM for malonyl-CoA was determined (Ramsay and Bhaird, 1992). Alignment of the known sequences of COT (see chapter 6) showed that human and bovine COT both lack His340 in contrast to rat and mouse. Bovine, rat and human COT proteins heterologously expressed in either *E. coli* or *P. pastoris* were purified and characterised. In all cases, the inhibition by malonyl-CoA was poor and competitive with substrate. The rat COT gave a Ki for malonyl-CoA of 147 μM and the activity of the human and rat COT dropped in parallel at a fixed substrate concentration. Thus H340 does not participate in the binding of malonyl-CoA to COT (Sitheswaran et al, in preparation)

1.8 Carnitine acyltransferases as pharmaceutical targets

These enzymes are important targets for pharmacological intervention in cases of impaired lipid metabolism (Anderson, 1998), so it is important to establish similarities and differences between the various enzymes in order to facilitate the design of selective inhibitors (Nic a'Bhaird et al., 1998). In 1998, before any structural information was available, Nic a' Bhaird *et al* demonstrated some differences between the active sites of beef liver COT and CPT2, using chemical reactivity of active site groups. Both enzymes were treated with diethyl pyrocarbonate (DEPC), a histidine selective reagent.

The pattern of inhibition of CPT2 was simple linear pseudo-first-order, whereas the inhibition of COT was biphasic with an initial rapid loss of activity followed by a slower loss of activity (Nic a'Bhaird et al., 1998). The results of these experiments provide strong evidence for the presence of a single reactive and catalytically essential histidine at the active site of CPT2 (Nic a'Bhaird et al., 1998). This conclusion is consistent with site-directed mutagenesis results showing that H372 of rat liver CPT2 is essential for activity (Brown et al., 1994). Likewise, site directed mutagenesis of the histidine residue H327A in COT abolished the enzyme activity (Morillas et al., 2000). This conserved histidine is the catalytic residue first noted by (Chase and Tubbs, 1969) as the residue modified by the inactivator, bromoacetylcarnitine . In the structure of CrAT, the equivalent His 343 is clearly seen in a position to activate either CoA or carnitine by removal of a proton (Jogl and Tong, 2003).

The biphasic plots resulted from the treatment of COT with DEPC suggest that more than one residue is modified by DEPC and that the modification of the residue

reacting in the faster phase does not lead to complete inactivation of COT (Nic a'Bhaird et al., 1998). In order to identify the residues reacting with DEPC, Nic a' Bhaird *et al*, accompanied the inactivation of COT by DEPC with the changes in the absorbance spectrum of COT and did substrate protection studies. The results provide strong evidence that the residue reacting in the faster phase of inhibition by DEPC is not a histidine but possible a serine (Nic a'Bhaird et al., 1998). When this residue is modified there is only partial loss of activity, which suggests that it might not play a direct role in catalysis.

One of the residues that might be modified by DEPC in the slow phase of inhibition of COT was a lysine (Nic a'Bhaird et al., 1998). In order to verify this, Nic a' Bhaird *et al* examined the effect of fluorodinitrobenzene (FDNB), a lysine selective reagent, on the activity of COT. The resulting linear pseudo-order kinetics indicate that the loss of activity observed on treatment of COT with FDNB is the result of one residue present at or near the active site of the enzyme, probably a lysine. From sequence alignments and the structure of CrAT it is probable that the lysine modified was Lys354 in bovine COT. The equivalent Lys325 in mouse CrAT lies close to the active site histidine (as seen in the structure deposited as 1NDF in the Protein Data Bank).

The other catalytic site difference between COT and CPT2 is the presence of a thiol group (cysteine), which was thought to play a role in substrate binding of CAT (Colucci and Gandour, 1988). COT, but not CPT2, is slowly inactivated by thiol reagents (Ramsay, 1988). Although no cysteine was apparent amongst the groups required for carnitine or CoA binding in the crystal structures (Jogl and Tong, 2003), there is a cysteine residue (Cys 325) in all COT sequences that is absent from CrAT.

The reactivity of a lysine, cysteine and serine residues possibly present in the active site of COT but not of CPT2 provides the first indication of structural differences that could be very important in the design of selective inhibitors (Nic a'Bhaird et al., 1998). COT and CPT2 differ kinetically and they differ in their sensitivity to conformationally constrained inhibitors, which permits development of inhibitors that inhibit mitochondrial β-oxidation with minimal effects on peroxisomal β-oxidation and other acyl-CoA dependent reactions (Ramsay and Gandour, 1999).

AIMS

Stress is thought to increase energy needs in fish. The first aim of this project was to investigate trout liver under vaccine stress to see whether fatty acid oxidation increased to provide the extra energy required to mount an immune response. We also looked at short-term food deprivation for comparison with mammalian systems

Although mitochondria have been investigated for their role in fatty acid oxidation in fish and the presence of CPT1 confirmed, investigation of the detail of the regulation of CPT1 in response to higher energy demand had only just begun. The role of the mitochondrial contact sites in the regulation of CPT1 properties was investigated in trout liver mitochondria.

Even less was known about peroxisomal oxidation and about COT, the enzyme important for the transfer of chain-shortened products to the mitochondria. This work aimed to isolate and purify COT from trout liver to characterise its functional properties, and, by cloning the cDNA, obtain its sequence for evolutionary comparison.

CHAPTER 2

METHODS AND MATERIALS

2.1 GENERAL METHODS

2.1.1 PROTEIN ASSAY

The quantity of protein in samples was measured using the Peterson-Lowry micro-assay, a modified Lowry assay which detects small quantities of protein (Petersen, 1977). A series of BSA standards (0-150μg) were used. To 100μL of each standard solution was added 0.4mL of H_2O and 50μL of 0.5% deoxycholate. After 5 min on ice, 75μL of TCA 55% w/v were added and mixed well. The samples were incubated on ice for 15 minutes then centrifuged at 10,000g for 10 minutes at 4°C. The supernatant was removed and 0.5mL of 1M NaOH was added to redissolve the pellet. 0.5mL of Lowry reagent A (copper tartrate carbonate (CTC): 10% SDS: 0.8M NaOH: H_2O) was added, the samples were mixed and left at room temperature for 10 minutes. 0.25mL of Lowry reagent B (1 mL of Folin-Ciocalteau and 5 mL H_2O) was added; the samples were mixed and developed in the dark for 30 minutes. The absorbance was read at 750nm.

2.1.2 MEASUREMENT OF MARKER ENZYME ACTIVITIES

Three separate marker enzymes were assayed to determine the content of subcellular fractions. Catalase was used as a marker for peroxisomes, cytochrome *c* oxidase for mitochondria and NADPH-cytochrome *c* reductase for microsomes.

2.1.2.1. Catalase assay

The first step in the peroxisomal β-oxidation pathway, catalysed by acyl-CoA oxidase, is characterised by the formation of H_2O_2. Catalase present in peroxisomes, catalyses the decomposition of H_2O_2 to give H_2O and O_2 (Bergmeyer, 1974). For this assay, catalase activity was measured spectrophotometrically by following the decomposition of H_2O_2. A mixture of the reagents shown in table 2.1 was made up, sufficient for the number of assays to be performed.

A stock solution of 1.25M hydrogen peroxide was made by diluting 1.42 mL of concentrated H_2O_2 (30%) to 10 mL using 20mM phosphate buffer pH 7.5. The mixture was brought to and maintained at 30°C. Reaction mixture (1 mL) was pipetted into a 1.5mL quartz cuvette and placed in the spectrophotometer sample compartment thermostatted at 30°C. The reaction was started by the addition of 10μL sample of enzyme and followed at 240nm for two minutes using the kinetic programme on the Shimatzu spectrophotometer. The extinction coefficient used was 40000 $M^{-1}.cm^{-1}$.

Table 2.1. Catalase assay components.

Reagent	Stock conc. (mM)	Final conc. (mM)	Vol. per assay (μL)
KPi, pH 7.5	20	19.8	990
H_2O_2	1250	12.5	10

2.1.2.2 Cytochrome *c* oxidase assay

Cytochrome *c* oxidase is a membrane-bound respiratory enzyme which catalyses both the reduction of O_2 to water and proton pumping in the electron transfer chain which

is specific to the mitochondrial β-oxidation pathway. The components of this assay are shown in table 2.2.

The assay was performed as described for the catalase assay except the absorption due to the appearance of reduced cytochrome *c* was followed at 550nm (extinction coefficient 19100 $M^{-1}.cm^{-1}$).

Table 2.2. Components of the cytochrome *c* oxidase assay.

Reagent	Stock conc. (mM)	Final conc. (mM)	Vol. per assay (μL)
KPi, pH 7.5	20	19	950
Cytochrome *c*	0.82	0.04	50

2.1.2.3 NADPH-CYTOCHROME *C* REDUCTASE ASSAY

The endoplasmic reticulum, isolated from mammalian liver as a microsomal fraction, is characterised by an NADPH-dependent electron transport system. The NADPH-dependent lipid peroxidation reaction catalysed by this system is dependent on the activity of NADPH-cytochrome *c* reductase. For this assay, the reduction of cytochrome *c* was measured spectrophotometrically by following the increase in absorbance at 550nm, which has an extinction coefficient of 19100 $M^{-1}.cm^{-1}$.

A mixture of the first three reagents listed in table 2.3 was prepared, suitable for the number of assays to be carried out. The mixture (990 μl) warmed to 30°C was placed in a quartz cuvette, followed by 10 μl of enzyme. After mixing, the reaction was started by the addition of 10μL of 10mM NADPH. The absorbance change was

measured for two minutes. All samples were diluted with 50mM KH_2PO_4/KOH, pH 7.5, containing 0.01% Triton X-100 before assay.

Table 2.3. Components of the NADPH-cytochrome *c* reductase assay.

Reagent	Stock conc. (mM)	Final conc. (mM)	Vol. per assay (µL)
KPi, pH 7.5	300	279	930
Cytochrome *c*	1.5	0.075	50
KCN	100	1	10
NADPH	10	0.1	10

2.1.3 Carnitine acyltransferase assays

Carnitine acetyltransferase (CAT) and carnitine decanoyltransferase (CDT) are found in microsomes, mitochondria and peroxisomes (Farrell et al., 1984; Markwell et al., 1973b) and their activity in these fractions can be measured spectrophotometrically by reaction of the free CoA released with a thiol reagent, 4,4-dipyridine disulphide (PDS). The method used was based on (Ramsay, 1975).

All acyl-CoA solutions were made in 5 mM potassium phosphate, pH 6.5, to minimise hydrolysis. L-Carnitine hydrochloride was dissolved in 20 mM potassium phosphate, pH 7.5, and neutralised by the addition of one equivalent of 6M KOH. The stock solutions of these substrates were standardised using the commercial pigeon

breast CrAT and limiting concentration of one substrate in the presence of excess of the other. For long chain acyl-CoA stocks, beef liver COT was used in the standardisation assay.

2.1.3.1 Carnitine acetyltransferase assay

The constituents of the assay are shown in table 2.4. PDS buffer was prepared fresh every two hours by mixing 20 mM KPi, pH 7.5, and 125μM PDS (4,4'dithiobispyridine). A PDS stock solution (125 mM in ethanol) was stored frozen at –20°C for up to 4 weeks.

The buffer was placed in a quartz cuvette maintained at 30°C using a thermostatted sample compartment. A final concentration of 100μM acetyl-CoA was added to the buffer followed by 1μL of sample. The assay components were mixed and left to incubate for 10 minutes. Any hydrolase activity present could be detected during this time. The reaction was started by the addition of 2mM carnitine (final concentration) and was followed at 324nm for 10 minutes using the Shimadzu spectrophotometer. The extinction coefficient for the dithiopyridone product is 19800 $M^{-1}.cm^{-1}$. Samples of 2, 4 and 8μL were also assayed to ensure that the CrAT activity was linear with amount of enzyme. Samples of intact organelles were diluted as necessary using sucrose buffer that contained 0.3M-sucrose, 10 mM-Tris/HCl, 1mM EDTA, pH 7.4.

2.1.3.2 Carnitine decanoyltransferase assay

Carnitine decanoyltransferase was assayed by the same method described for CrAT with minor modifications as shown in table 2.5.

Table 2.4. Acetyl-CoA assay components

Reagent	Stock conc. (mM)	Final conc. (mM)	Vol. per assay (µL)
PDS buffer	20	18.8	940
Acetyl-CoA	2	0.1	50
L-carnitine	200	2	10

Table 2.5. Decanoyl-CoA assay components.

Reagent	Stock conc. (mM)	Final conc. (mM)	Vol. per assay (µL)
PDS buffer	20	19	950
Decanoyl-CoA	1	0.04	40
L-carnitine	200	2	10

2.1.3.3 CPT1 and CPT2 assays

As described above, the assays contained 20mM potassium phosphate buffer, pH 7.5, 125µM PDS, 50µM decanoyl-CoA from standardised stock, 4mM neutralised L-carnitine in 20mM phosphate buffer pH 7.5, and 75µL-200µL of mitochondrial sample.

The rate was recorded to measure the total activity, then malonyl-CoA (100µM) was added to inhibit CPT I activity. The individual enzyme activities were calculated by difference.

2.2. PREPARATION OF SUBCELLULAR FRACTIONS FROM TROUT LIVER

2.2.1 FISH

Adult female rainbow trout (College Mill Trout Farm, Almondbank, Perthshire, U.K.), weighing 400–500g, were maintained in flow-through freshwater tanks at ambient temperature and fed daily with an amount of Dynamic Red M trout pellets (Ewos, Bathgate, West Lothian, U.K.) equivalent to 1% (w/w) of their body weight. Pellet composition consisted of 42% protein and 28% fat.

2.2.2 PREPARATION OF TROUT LIVER HOMOGENATES

The fish were killed by an overdose of the anaesthetic MS222 (dosage 3g) and severing the spinal cord, according to the Home Office schedule 1 protocol. The livers (approximately 10g) were removed and placed in isolation buffer (300mM sucrose, 5mM Tris-HCl, 1mM EDTA, pH 7.4 at 4°C) for transport to the laboratory. The livers were weighed, finely chopped and rinsed, and homogenised using a Potter-Elvejem homogeniser to 10% (w/v) in ice-cold sucrose solution containing 0.3M sucrose, 10mM Tris/HCl and 1mM EDTA, pH 7.4. A total of four passes were applied and the resulting homogenate was filtered through four layers of muslin.

Mitochondria and peroxisomal fractions were then prepared from crude homogenate by differential centrifugation followed by gradient separation.

2.2.3 Separation of mitochondria and peroxisomes by differential centrifugation

The method used for the isolation of organelle fractions is shown in fig. 2.1. The low speed spin at 500g removed unbroken cells and the pellet was discarded. A second low speed spin at 4000g separated the nuclear-mitochondrial fraction (pellet 1, **P1**) from the mitochondrial-peroxisomal-microsomal fraction (supernatant 1). A third spin

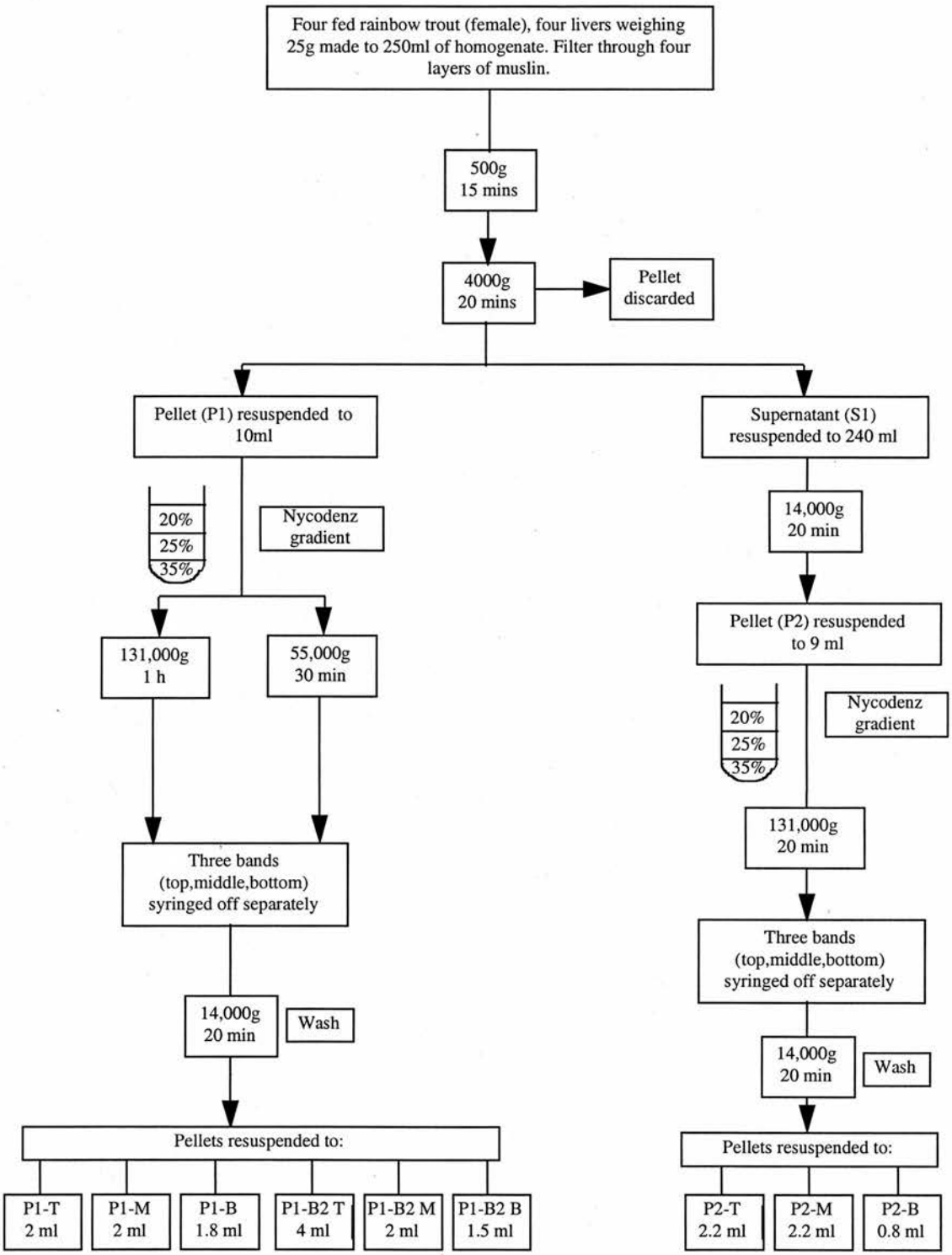

Fig 2.1 Flow diagram for the preparation of mitochondrial and peroxisomal enriched fractions.

at 14000g yielded the mitochondrial-peroxisomal fraction (**P2**). Attempts to obtain better separation of the mitochondria and peroxisomes by differential centrifugation gave no improvement

2.2.4 GRADIENT SEPARATION OF THE MITOCHONDRIAL FRACTION

Mitochondria and peroxisomal fractions were prepared from crude homogenate by differential centrifugation followed by gradient separation using Nycodenz iso-osmotic solution. Nycodenz is the trademark name for the density gradient medium, Iohexol. It has a molecular weight of 821 and its density measures 2.1g/mL in the powdered form. The chemical properties of Nycodenz are explained by its structure (fig 2.2). The high density of Nycodenz derives from the presence of a substituted triiodobenzene ring which is linked to a number of hydrophilic groups responsible for its high water solubility (Rickwood et al., 1982).

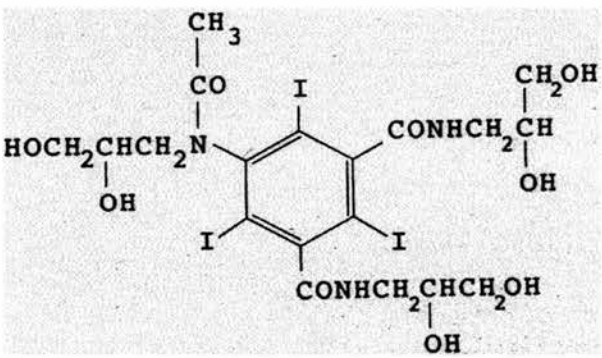

Fig 2.2. The molecular structure of Nycodenz

The **P1** pellet was resuspended to 10 mL using a glass rod and homogenized with two passes. Nycodenz gradients were prepared as follows. Nycodenz in the powder form was dissolved to make a 50% (wt/vol) solution using a buffer of 300mM sucrose, 10mM HEPES and 1mM EDTA. The 35%, 25% and 20% gradient solutions were diluted from the 50 % solution using the same buffer. Discontinuous gradients were set up in Beckman polycarbonate tubes. Starting at the bottom, 3 mL of 35% Nycodenz was overlayered by 5 mL of 25% solution using a pasteur pipette to ensure

the bands did not mix then 6 mL of 20% Nycodenz layered on top of the 25% solution using the same method. Sample (2 mL of 30mg/mL) was loaded onto each gradient tube to give a total of 16 tubes. Eight tubes (batch 1) were centrifuged at 131,000g for 1 hour. The other eight tubes (batch 2) were centrifuged at a lower speed (55,000*g*) for a shorter time (30 min). The bands were removed separately using a syringe and washed by dilution and centrifugation to remove Nycodenz. The volumes of the resuspended pellets are shown in figure 2.1. All operations were performed at 4°C and the buffer used throughout was 300mM sucrose, 1mM-EDTA and 10mM-Tris/HCl, pH 7.4 unless otherwise stated. The activities of the marker enzymes for mitochondria, peroxisomes and microsomes were measured as described in paragraph 2.1.2 to define the quality of the separation.

2.2.5 Gradient separation of the peroxisomal fraction

Protein concentration of P2 was determined using the quick biuret assay. Samples were diluted to 12mg/mL using sucrose buffer (300mM sucrose, 10mM HEPES and 1mM EDTA). Samples (8 x 2mL) were applied to the top of the Nycodenz gradients prepared as described above (paragraph 2.2.3), except that only 5 mL of the 25% solution was used. The tubes were centrifuged at 130,000*g* for 1 hr in the 50.2 rotor, using the acceleration program 5 and deceleration program 5 in the Beckman L8-M ultracentrifuge. The three resulting bands were removed separately using a syringe. The bands were then washed to remove Nycodenz and the pellets resuspended in sucrose medium to the volumes shown in figure 2.1. The activities of the marker enzymes for mitochondria, peroxisomes and microsomes were measured as described in paragraph 2.1.2 to define the quality of the separation.

2.3 MEASUREMENT OF β-OXIDATION

2.3.1 OXYGEN ELECTRODE ASSAY FOR TOTAL β-OXIDATION

The study of oxygen consumption in whole homogenates with intact organelles has the advantage of pathway activity where mitochondria and peroxisomes maintain their normal matrix environment. Respiration rates were determined polarographically, using a Clark-type oxygen electrode (Rank Bros., Bottisham, Cambridge, U.K.). All assays were conducted at 25°C. Although some workers use lower temperatures (Henderson and Sargent, 1985b), we obtained very slow rates at low temperatures. Confirming earlier observations at limited temperature ranges (such as (St-Pierre et al., 1998), Froyland et al. (Froyland et al., 2000) showed that oxidation rates increased with temperature up to at least 30°C.

Air-saturated buffer (1.3mL) containing 80mM KCl, 20mM Tris base, 3.3mM potassium phosphate, and 3.3mM MgCl, pH 7.5 was pipetted into the sample chamber thermostatted at 25°C. This was followed by 300 μL of sample. An adjustable stopper was used to seal the chamber and prevent room air dissolving during the experiments. Using a microlitre syringe, 10 μL of 100mM L-carnitine was added to the chamber through the small hole in the centre of the stopper. The reaction was started by the addition of 15 μL of 10 mM palmitoyl-CoA (final concentration 100μM). The rate of oxygen consumption per minute was measured using a chart recorder attached to the oxygen electrode. To measure peroxisomal oxidation, 10μL of 100mM potassium cyanide was added to inhibit the mitochondrial respiratory chain before initiating the reaction with palmitoyl-CoA.

2.3.2 RADIOCHEMICAL ASSAY OF β-OXIDATION

The conversion of acid insoluble [1-^{14}C]palmitate to acid soluble [^{14}C]acetate was measured using liquid scintillation counting. In the presence of KCN peroxisomal rates were measured. The assay was adapted to measure mitochondrial β-oxidation rates by the addition of L-carnitine and omission of KCN. [1-^{14}C]palmitate was purchased from Amersham Corporation.

An ice-cold mixture of the reagents in table 2.6 was prepared, suitable for the number of assays to be carried out. Aliquots (300 μL) of reaction mixture were placed in 1.5 mL plastic microcentrifuge tubes in an ice-water bath. The remaining components (table 2.7) of the assay were added to the tubes, which were then capped and mixed.

The reaction was started by transferring the tubes to a 37°C water bath. After 21 minutes (there was a one minute lag for warming), the reaction was stopped by the addition of 250μL of 6% perchloric acid and left on ice for one hour. The tubes were then spun for two minutes in a microcentrifuge to remove the perchloric acid precipitate of protein and unreacted long chain fatty acid. Aliqouts of 500μL of the supernatant was transferred to scintillation vials containing 5mL of scintillation liquid. The vials were mixed and placed in a scintillation counter and the counts measured for two minutes. Two control tubes without enzyme were similarly treated to determine the acid-soluble radioactivity present in the substrate.

Table 2.6. Components of reaction mixture

	Stock conc. (mM)	Final conc. (mM)	Vol. per assay (µL)
Tris/HCl, pH 7.5	50	17.38	173.8
ATP	50	10	100
FAD	1	0.01	5
NAD	20	0.2	5
L-carn. **OR** KCN	100	1	5
CoA	10	0.1	5
BSA	15mg/mL	0.075mg/mL	2.5
Palmitate	5	0.02	2
DTT	330	0.99	1.5
[^{14}C]Palmitate	3.5	14×10^{-2}	0.2

Table 2.7. Microcentrifuge tube setup

Tube	Sample	Buffer (µL)	Other additions	Reaction mixture (µL)	Sample (µL)
1	Mitochondria	0	L-carnitine	300	200
2	Mitochondria	0	L-carnitine	300	200
3	Pre-gradient peroxisomes	0	cyanide	300	200
4	Pre-gradient peroxisomes	0	cyanide	300	200
5	Peroxisomes	100	cyanide	300	100
6	Peroxisomes	100	cyanide	300	100

2.3.3 Spectrophotometric assay of peroxisomal β-oxidation

In the presence of palmitoyl-CoA, the third reaction of the peroxisomal β-oxidation pathway was measured spectrophotometrically. The reduction of NAD to NADH measures overall β-oxidation spiral activity because we start with the substrate of the first reaction, measure the third reaction, and the overall pathway is not exergonic without the fourth reaction to pull it (Lazarow, 1981). This method was optimised for fish liver based on the procedure developed by Lazarow (1981) for rat liver peroxisomes.

A sufficient mixture of the first eight ingredients (table 2.8) was prepared for the assays to be carried out. This mixture was brought to, and maintained at 30°C in a water bath. Reaction mixture (960μL) was added to the cuvette thermostatted at 30°C and mixed with 20μL of undiluted sample. The reaction was started by the addition of 10μL of palmitoyl-CoA and observed for 10 minutes at 340nm using the kinetics programme on the Shimatzu spectrophotometer.

Table 2.8. Components of reaction mix for spectrophotometric assay.

Reagent	Stock conc. (mM)	Final conc, (mM)	Vol. per assay (μL)
Tris-HCl pH 8	50	46.35	927
NAD	40	0.4	10
DTT	330	0.99	3
BSA	15mg/mL	0.075	5
Triton X-100	20mg/mL	0.1mg/mL	5
FAD	1	0.01	10
KCN	100	1	10
Palmitoyl-CoA	20	0.2	10

2.4 SUBFRACTIONATION OF MITOCHONDRIA AND ISOLATION OF MITOCHONDRIAL MEMBRANES

2.4.1 Preparation of mitochondria purified by a Percoll gradient

Fed female rainbow trout (2-4 fish) were killed according to the Home Office Schedule1 as described above. The livers (approximately 10g) were removed and placed in isolation buffer (300mM sucrose, 5mM Tris-HCl, 1mM EDTA, pH 7.4 at 4°C). After finely chopping and rinsing, the livers were homgenised and diluted to 20% with isolation buffer. After filtering through 4 layers of muslin the sample was centrifuged at 500g for 15 minutes. The supernatant was removed and centrifuged for a further 15mins at 1900g. The pellet was re-suspended in 10 mL of isolation buffer and centrifuged for 10 minutes at 500g. This supernatant was removed and centrifuged at 1900g for 15 minutes. The two pellets were pooled and in 2 mL aliquots applied to tubes containing 18 mL 40% Percoll solution (40% Percoll solution : 40% Percoll, 25% 1M sucrose, 20% 50mM MOPS/Kpi, pH 7.4, 1% 100mM EDTA, 14% H_2O) with a 2 mL 65% sucrose cushion. After ultracentrifugation at 50,000g for 30 min, the mitochondrial layer was harvested, diluted to approximately 30 mL and centrifuged at 7,700g for 15 minutes to remove the Percoll.

2.4.2 Fractionation of mitochondria

The final mitochondrial pellet after the removal of Percoll was resuspended in a hypotonic solution using 10mM potassium phosphate buffer to give a total volume of approximately 2.14 mL. The suspension was incubated on ice for 10min, followed by the addition of 60% (w/v) sucrose to give a final 17% sucrose solution. After a further

20 min incubation the suspension was sonicated 3 times for 30 seconds with cooling at 0°C. The sonicated suspension was centrifuged at 3000g for 10 min.

The supernatant was divided into 0.65 mL aliquots and layered on top of a continous sucrose gradient (density 1.113-1.227g/mL) prepared in 10mM potassium phospate buffer (pH 7.4) in 14mL centrifuge tubes. Separation of the different fractions was achieved by centrifugation in the SW40 rotor at 105,000g for 20 hours at 4°C. The subfractionated mitochondria were harvested by displacement using 2.26 M sucrose and 0.5 mL fractions were collected from the top of the tube. The absorbance of each fraction was measured at 280nm to determine the relative quantity of protein contained in each sample. Marker assays (as in section 2.1.2 except that 0.5μg/mL Antimycin A was added to inhibit the respiratory chain) were used to identify the membranes in each fraction. NADPH/NADH cytochrome *c* oxidoreductase was used to identify the outer membrane. Cytochrome oxidase assay was used to locate the inner membrane fractions.

CPT1 and CPT2 were assayed with 50 μM decanoyl-CoA and 4mM L-carnitine and 75μL-200μL of mitochondrial sample. The rate was recorded to measure the total activity, then malonyl-CoA (100μM) was added to inhibit CPT1 activity. The individual enzyme activities were calculated by difference.

After the marker enzymes had been determined, the fractions were pooled. Fractions containing the highest rates of NADPH-cytochrome *c* oxidoreductase activity and highest absorbance at 280nm were pooled as the outer membrane. Those containing the highest rate of cytochrome *c* oxidase activity and high absorbance at 280nm were also pooled as the inner membrane. The middle fractions contained both high

NADPH-cytochrome *c* oxidoreductase and high cytochrome *c* oxidase activity and were designated as the contact sites. The pooled fractions were then concentrated using Centricon concentrators to produce samples of approximately 1-1.5mL.

2.4.3 Composition of the submitochondrial fractions by SDS gel electrophoresis

The proteins present in the submitochondrial fractions (5-20 μg protein) were separated on 10% SDS-polyacryamide gels according to standard protocols (Bollag et al., 1996). The same technique was used to show the progress of the purification of COT (see below). Wet blotting to PVDF membranes was used to prepare samples for N-terminal sequencing (Bollag et al., 1996).

2.5 Solubilization and purification of COT

Isolation of COT from frozen rainbow trout liver was based on the method for beef liver (Ramsay et al., 1987). Four livers (22g) were almost thawed and blended vigorously with two volumes of cold ultra pure water for 2 minutes. The homogenate was sonicated on ice for bursts of 30 seconds repeated seven times using the large probe. After centrifuging at 20,000g for 20 minutes, COT activity was precipitated with 35% saturated $(NH_4)_2SO_4$, added slowly with stirring and stirred for a further 20 min on ice. The pellet after centrifugation at 20,000g for 20 minutes was resuspended and dialyzed against tap water for 6 hours, then overnight against 10mM potassium phosphate, pH 7.5. A precipitate formed, but it contained no COT activity and was removed by centrifugation at 20,000g for 20 minutes.

The supernatant was applied to a DEAE-cellulose column (20cm x 6.5cm), which was washed with 10mM potassium phosphate until no further protein was eluted and then

with 40mM potassium phosphate pH 7.5. The active fractions were applied directly to a column (25cm x 3.5cm) of Blue Sepharose CL-6B (Sigma) equilibrated with 20mM potassium phosphate, pH 7.5. The column was washed with 20mM potassium phosphate buffer containing 50mM potassium chloride (about 100mL) until the absorbance at 280nm of the eluate returned to the baseline. The COT activity was eluted with a gradient of 50-300mM KCL in 20mM potassium phosphate. The concentrated dialysed active pool was applied to a small column of Blue Sepharose CL-6B, washed with 20mM potassium phosphate-50mM potassium chloride, pH 7.5, and the COT eluted with 20mM potassium phosphate-50mM potassium chloride containing 10mg/100mL octanoyl-CoA. The pooled fractions were concentrated by ultrafiltration (Amicon YM10) with gentle stirring and dialyzed overnight against 20mM potassium phosphate, pH 7.5.

2.6 Cloning rainbow trout COT

2.6.1 Basic techniques

Basic molecular biology techniques were learned in the Hannah Research Institute under the supervision of Dr. Nigel T. Price. The sequences of the cDNAs were downloaded from the GeneBank™ database. Location of restriction enzyme cleavage sited and development of cloning strategies were performed with the aid of Lasergen MapDraw software (DNAstar).

2.6.2 Primer design

Oligonucleotide primers obtained from MWG-Biotech were designed with the help of Lasergene Primer Select software (DNAstar). Primer design strategies are more fully described in 6.3.

2.6.3 Polymerase chain reaction

The PCRs were performed using a Progene (Techne) thermal cycler. The reagents were dNTPs (Pharmacia), oligonucleotide primers from MWG-Biotech designed with the help of the PrimerSelect software, *Taq* DNA polymerase (New England Biolabs, 2.5u/μL) or *Pfu* TURBO DNA polymerase (Stratagene) and respective 10X buffer. In some cases, addition of DMSO (Sigma), which acts to reduce DNA secondary structure, was necessary to achieve successful amplification. A trout cDNA library cloned into phage Lambda or trout oligo(dT) primed cDNA were used as template. After the PCR (typically 35 cycles) was completed, the reaction solution was run in an agarose gel (2.6.4) to check the results and allow purification of the products, or if considered unnecessary, PCR products were purified directly using a Wizard® Plus PCR purification Kit (Promega). Desired PCR products were cloned into pGEM-T vector (Promega).

2.6.3.1 Control PCR amplification

Control PCR experiments were performed to ensure that the known region of the target sequence was present in the cDNA pool being used as template. Primers were designed based on partial sequence derived from trout COT expressed sequence tags (ESTs) (see chapter 6). PCRs were performed using a Progene (Teche) machine and with the reagents as described before (2.6.3). Components and quantities of a typical control PCR set up are shown in table 2.9. Cycle times and conditions are shown in table 2.10.

2.6.3.2 PCR amplification of rainbow trout head kidney lambda DNA.

PCR was performed on an aliquout of rainbow trout head kidney lambda cDNA, using primers described in table 6.1. Components and quantities of the PCR set up were as described in table 2.9, except 1μL Pfu TURBO polymerase was used and the volume of water adjusted accordingly. Cycle times and conditions were as before (table 2.10).

2.6.4 Agarose gel electrophoresis

Samples were analysed in 1% (w/v) agarose (Boehringer Mannheim) gels containing 0.5μg/mL ethidium bromide (Sigma) prepared in TAE buffer (40mM Tris base, 0.1% (v/v) glacial acetic acid, 1mM EDTA, pH 7.2). Samples were mixed with sample buffer (10mM Tris-HCl, pH 7.5, 50mM EDTA, 10% Ficoll®, 0.25% bromophenol blue, 0.4% Orange G) and electrophoresed alongside DNA size markers (New England Biolabs 2-Log or 100bp DNA ladder) in a horizontal gel electrophoresis apparatus (Hybaid, Bio-Rad) typically at 100V for 1h. Images of ethidium bromide stained gels were recorded using a UV transilluminator and gel imaging system (Herolab E.A.S.Y. store). The extraction and purification of plasmid DNA from agarose gel slices was done using a Wizard® Plus DNA Gel Extraction Kit (Promega).

Table 2.9 Components and quantities in a PCR set up using DMSO[1]

Components[2]	Quantities (μL)	
	0% DMSO	5% DMSO
Water	40.5	38
10X polymerase buffer	5	5
10mM dNTP	1	1
50μM sense primer	1	1
50μM antisense primer	1	1
DMSO	0	2.5
template[3]	1	1
Pfu TURBO Polymerase	0.5	0.5
Final volume	50	50

(1) DMSO (Sigma) reduces DNA secondary structure; (2) The components were assembled in the order shown; (3) A Lambda cDNA library or cDNA was used as template.

Table 2.10. PCR program using the Progene (Teche) machine

Stage	Temperature (°C)	Time (min:sec)	Number of cycles
1	95[1]	05:00[1]	1
2	95	01:00	35
	59.8[2]	01:00	
	72	02:30[3]	
3	72[4]	10:00[4]	1

(1) Denaturation of DNA; (2) Optimal annealing temperature, depending on the primer pair used (as suggested by primer design software); (3) The amplification time is dependent on the length of the PCR product: 1min per 1kbp; (4) PCR product extension.

2.6.5 TA Cloning

The pGEM-T vector is specially designed for cloning of PCR products generated by certain thermostable polymerases, such as *Taq* polymerase. *Taq* polymerase adds a single deoxyadenosine (A) to the 3'-ends of the amplified fragments, so the vector is supplied already linear with added thymidine (T) to both ends. For cloning of blunt ended products generated with *Pfu* polymerase, a 30 min incubation of the purified products with Taq polymerase and 0.2 mM dATP was performed to allow cloning by the same method (table 2.11). This tailing reaction was also performed with *Taq* polymerase products in order to increase the efficiency of the cloning step. The ligation set up of the tailed PCR product to the pGEM-T vector is shown in table 2.11. After the ligation incubation, the ligase was heat-inactivated at 65°C for 15min and the DNA was transformed into bacterial cells (chapter 2.6.6). After transformation and bacterial growth, the plasmid DNA was extracted, purified and digested with the restriction enzyme *Eco*R I to detect clones containing the insert.

Table 2.11 Cloning of PCR products into pGEM-T vector.

PCR product tailing		**pGEM-T ligation**	
Components	Volume (µL)	Components	Volume (µL)
PCR product	7[1]	2X T4 DNA ligase buffer	5
10X *Taq* polym. Buffer	1	pGEM-T vector	1
2mM dATP	1	Tailed PCR product	2
Taq polymerase (5u/µL)[2]	1	Sterile distilled water	1
		T4 DNA ligase (3u/µL)[3]	1
Final volume	10	Final volume	10
Incubation conditions	70°C, 15-30min	Incubation conditions	4°C, overnight

(1) Usually 1-7µL, depending on concentration of DNA. (2) One unit of *Taq* polymerase, u, is defined as the amount of required to catalyse the incorporation of 10 nanomoles of dNTPs into acid insoluble material in 30min at 74°C. (3) 0.01 Weiss unit of T4 DNA ligase is defined as the amount of enzyme required to catalyse the ligation greater than 95% of the *Hind* III fragments of 1µg of Lambda DNA at 16°C in 20min.

2.6.6 Bacterial transformation and subsequent growth

Transformation of cells of *E. coli* XLI-Blue (Stratagene) was performed by electroporation (BioRad *E. coli* pulser, Equibio Easyject Plus and 0.2cm gap cuvettes) using approximately 10ng of plasmid DNA and a voltage of 2.5 kV. Bacteria containing the plasmids pGEM-T (promega) were grown in LB (10g/L NaCL, 10g/L tryptone, 5g/L yeast extract) liquid medium or LB agar (LB plus 15g/L agar) containing 0.1g/mL carbenicillin (Melford). For blue/white screening of PCR products cloned into pGEM-T, the agar plates also contained 0.1mM IPTG (Melford) and 40ug/mL X-Gal (Melford). To perform the transformation, 1.2μL of the TA ligation was mixed with ice-thawed 40μL of competent cells and kept on ice. The bacterial cells *E. coli* XLI Blue were made competent as follows: the bacteria were grown overnight in 5mL LB liquid medium containing 0.05g/mL tetracycline, 37°C with shaking at 200rpm. A dilution of 1/100 in 100mL of the same medium was shaken at 200rpm and 37°C until the absorbance at 600nm reached 0.6 (3-4h). The culture was cooled down in ice and then centrifuged at 5000rpm, 4°C. The pellet was resuspended in 15mL of filter-sterile TFB1 (30mM potassium acetate, pH 5.8, 10mM $CaCl_2$, 50mM $MnCl_2$, 100mM RbCl, 15% glycerol) and kept in ice for about 10min. The cells were centrifuged again and the pellet resuspended in 2mL of filter-sterile TFB2 (100mM MOPS, pH 6.5, 75mM $CaCl_2$, 10mM RbCl, 15% glycerol). Aliquots of 40μL were transferred into 0.5mL tubes and then frozen in dry-ice and stored at –70°C. After electroporation, 0.5 mL of pre-warmed (37°C) SOC medium (0.5g/L NaCL, 20g/L tryptone, 5g/L yeast extract, 10mM $MgCl_2$, 20mM glucose) was added and the culture shaken at 200rpm, 37°C for 1h. The 0.5 mL cultures with PCR products were plated out in LSLB-agar (LSLB plus 15g/L agar) with 0.1μg/mL

carbenicillin and incubated at 37°C overnight. Single colonies of the PCR product transformants were chosen to incubate in 5mL of LSLB with 0.1μg/mL carbenicillin and the cultures were grown overnight in a 37°C shaker. The DNA was extracted and checked as described in 2.6.7 and 2.6.8.

2.6.7 Plasmid DNA extraction and purification

Plasmid DNA was purified from 5mL of overnight bacterial cell culture using a Gene Elute miniprep DNA purification system (Sigma). DNA was eluted in 100uL of TE buffer (10mM Tris-HCl, pH 8.0, 1mM EDTA) or nuclease-free water.

2.6.8 Digests with restriction enzymes

Inserts were detected by *Eco*R I digestion. Table 2.12 lists *Eco*R I along with its specifications and supplier. Digests were done in a reaction volume of 20μL (table 2.13). Digests were incubated at the optimum temperature for at least 1 hour. Following digestion, DNA samples were analysed by agarose gel electrophoresis and desired fragments were excised from the gel and purified (2.6.4). Plasmid containing inserts detected by *Eco*R I digestion were sent to MWG-Biotech for sequencing with T7 promoter or SP6 vector primers.

Table 2.12. Restriction enzymes used, specifications and suppliers[1]

Enzyme	Stock conc. (u/μL)[2]	Cleavage site	Reaction temperature (°C)	Supplier
*Eco*R I	10	G∨AATTC	37	Promega

(1) The buffers were supplied along with the respective enzymes in a 10X concentration to be used in the digest. (2) u is activity unit defined as the amount of enzyme required to digest 1μg of DNA in 1 hour at the reaction temperature in a total volume of 50μL.

Table 2.13 Restriction enzymes reaction mixture in digestions

Reaction components	Digest
Sterile distilled water	6μL
Restriction enzyme 10X buffer	2μL
100X BSA, acetylated (Promega)	1μL
DNA sample	10μL (0.8-1.6μg)
Restriction enzyme	1μL (2-5u)[1]
Final volume	20μL

(1) u is defined in table 2.12

CHAPTER 3

FATTY ACID OXIDATION IN TROUT LIVER

3.1 Background

Fatty acids are a major energy source in mammalian systems and the metabolic alterations required to facilitate their use in the absence of ingested food have been well characterised (Robinson and Williamson, 1977). In teleost fish, fuel use is more constant, with lipids and proteins both providing metabolic fuel for sustained swimming (Bastrop et al., 1992; Weber and Haman, 1996).

Unlike mammals, teleosts do not produce ketone bodies from fatty acids during starvation (Zammit and Newsholme, 1979). This suggests that the flux of β-oxidation in mitochondria may not be regulated in the same way as in mammals. Experiments in this chapter measure fatty acid oxidation in trout liver as the basis for examination of regulation of β-oxidation in the teleost, both in the peroxisomes and in the mitochondria. A study of peroxisomal fatty acid oxidation indicated that peroxisomal oxidation rate was NOT related to the polyunsaturated fatty acids (PUFA) in the trout diet (Moyes et al., 1991) and different marine oils gave no induction of peroxisomal oxidation in salmon (Henderson et al., 1982). These observations suggest that the flux and specificity of β-oxidation in fish peroxisomes will also differ from mammalian systems.

In mammals, mitochondrial β-oxidation has evolved for optimum oxidation of C_{16}-C_{18} fatty acids and very long chain fatty acids (VLCFA) are poorly oxidised (Singh et al., 1987). In elasmobranches, mitochondria also oxidise much longer fatty acids but trout muscle mitochondria gave optimum oxidation with C_{14}-C_{16} and the rate with C_{18} fatty acids, including PUFA, was close to that for C_{16} (Moyes et al., 1991). The

essential fatty acids, linoleic and linolenic were oxidised at a slower rate (Kiessling and Kiessling, 1993). A study of chain length specificity of peroxisomal and mitochondrial oxidation in trout liver also showed the wide specificity of mitochondria for C_{12}-$C_{22:6}$ (Henderson and Sargent, 1985b) but the trout liver peroxisome oxidised C_{12}-C_{16} best. This is in contrast to mammals where peroxisomes oxidise the very long chain fatty acids (VLCFA) that are poorly oxidised by mammalian mitochondria. In this chapter, samples enriched in mitochondria and peroxisomes were isolated and characterised to provide material to examine the molecular basis of the specificity in fish.

3.2 Separation of trout liver peroxisomes and mitochondria by differential centrifugation

Differential centrifugation of the homogenate from mammalian liver produces fractions enriched in mitochondria and peroxisomes suitable for measuring fatty acid oxidation (Osmundsen et al., 1991; Singh et al., 1993).

The method should be simple, repeatable and provide peroxisomes and mitochondria from the same sample. Characterisation of the fractions using well-established marker enzyme activities is essential to verify the success of the separation. Many studies on fatty acid oxidation in fish tissues simply used the post nuclear homogenate, a valid choice because it retains all the activities and mitochondrial/peroxisomal oxidation can be distinguished functionally, but this crude sample is less suitable for the further investigation of regulatory properties intended here. The first results have characterised the differential centrifugal separation of mitochondria and peroxisome from trout liver.

Tables 3.1 (enrichment values) and 3.2 (full data) show the marker enzyme levels for the separation in two experiments. The P1 fraction obtained by centrifugation of the post-nuclear homogenate at 4000 g for 20 min is generally considered the predominantly mitochondrial fraction and the P2 fraction obtained by centrifugation of the post-mitochondrial supernatant at 14000 g for 20 min should contain few mitochondria, most of the peroxisomes, and very little of the endoplasmic reticulum. The data in Table 3.1 show clearly that, for trout liver, the separation is not good. In Table 3.1 peroxisomal and mitochondrial markers are almost equally enriched in both P1 and P2. In Table 3.2 the recovery values show that the P1 mitochondria fraction has less than 20% of the catalase so may be considered enriched in mitochondria. However, the P2 peroxisomal fraction still has considerable mitochondria present. As in earlier studies, these fractions can be used for oxidation measurements (see below) but are not as suitable for specificity and regulation studies.

Sample	**Mitochondria (Cyt *c* oxidase)**	**PEROXISOMES (Catalase)**	**ER (NADPH-Cyt *c*)**
HOMOGENATE	1	1	1
P1	12.1	9.7	3.6
P2	7.3	7.4	1.9

TABLE 3.1 RELATIVE ENRICHMENT OF CRUDE FRACTION AGAINST HOMOGENATE: The activity of the homogenate is set at unity, and the other values as relative values. The primary data is given in Table 3.2.

Table 3.2. Marker enzyme distribution in crude mitochondrial and peroxisomal fractions from fish liver.

	Total units/g liver			Specific activity/mg protein?			Recovery			Enrichment		
Fraction	Catalase	Cyt *c* Ox	NADPH Cyt *c*	Catalase	Cyt c Ox	NADPH Cyt c	Catalase	Cyt c Ox	NADPH Cyt c	Catalase	Cyt c Ox	NADPH Cyt c
Homog	3848 ± 4712.2	6102.5 ± 5540.2	427 ± 414.4	41.5 ± 12.0	105.05 ± 49.6	6.8 ± 2.5	100	100	100			
P1	1629.9 ± 1728.5	4051.1 ± 2961.3	80.2 ± 65.8	381.2 ± 42.7	1366.2 ± 861.5	24.95 ± 12.7	59.3 ± 27.7	75.5 ± 20.0	21.3 ± 5.2	9.71 ± 3.8	12.45 ± 2.3	3.55 ± 0.5
S1	911 ± 1020.6	1075.6 ± 711.6	171.5 ±163.4	15.85 ±1.6	30.2 ± 20.1	3.65 ± 0.9	29.7 ± 9.8	21.0 ± 7.4	40.9 ± 1.3	0.39 ± 0.1	0.275 ± 0.1	0.55 ± 0.1
P2	602.8 ± 457.3	1439.5 ± 800.6	48.4 ± 56.7	267.5 ± 200.1	775.5 ± 710.6	12.1 ± 0.1	33.5 ± 29.1	30.1 ± 14.1	9.1 ± 4.1	7.41 ± 6.9	7.3 ± 2.5	1.9 ± 0.7
S2	501.4 ± 593.6	356.2 ± 383.5	174.4 ± 191.3	19.5 ± 27.6	16.6 ± 13.3	8.15 ± 6.9	24.9 ± 17.1	5.1 ± 1.6	36.1 ± 9.8	1.04 ± 0.4	0.21 ± 0.2	1.49 ± 1.6

Incubation conditions for each marker enzyme are described in Materials and Methods 2.1.2. Fraction details and incubation centrifugation are also described in Materials and Methods 2.1 (fig 2.2). The results are expressed as total units/g liver, specific activity/mg of protein, relative recovery and enrichment when compared to the homogenate sample. Activities are given as means $\pm^{S.D.}$ ($n = 2$).

3.3 Gradient centrifugation to improve separation of trout liver mitochondria and peroxisomes

The differential centrifugation results described in section 3.2 suggested that the density of mitochondria and peroxisomes in trout liver are closer than those for mammalian mitochondria and peroxisomes. However, sucrose density gradient centrifugation has successfully separated trout liver mitochondria and peroxisomes (Henderson and Sargent, 1985b), so we tried the rapid Percoll and Nycodenz methods developed for convenient isolation of purified mitochondria and peroxisomes from rat liver (Derrick and Ramsay, 1989).

3.3.1 Nycodenz discontinuous gradients

Table 3.3 shows the conditions used for Nycodenz separation of the organelles in the fractions P1 and P2 and the band pattern obtained. The bands were clearer after 60 min than after 30 min at 131,000g. The catalase distribution for P1-b (T,M,B) shown in Table 3.4 clearly indicates that 30 min at 55.000g is not sufficient to allow sedimentation of peroxisome from the other bands. However, this lower force with shorter time was the only condition where a band (P1-bB) enriched in catalase, the peroxisomal marker, was obtained without significant contamination by mitochondria (0.23 enrichment compared to the homogenate). The one-hour gradient of the P2 fraction did not enrich the catalase marker as successfully. The mitochondria band from P1 after 30 min (P1-bM) was strongly contaminated with catalase, but after 1 hour (P1-M) gave good enrichment of cytochrome *c* oxidase (23.6 fold) with low catalase contamination (2 fold). Thus, two different conditions could yield fractions of adequate purity. However, the poor recovery of activity at 60 minutes was disappointing, suggesting that gradient separation is not really suitable for metabolic

studies. In general, such a poor yield made it impractical to purify the organelles without starting with large numbers of fish.

Gradient-purified fraction	Purified from:	*g* x t (min)	Band Pattern
P1-M P1-B	P1 P1	131,000 x 60	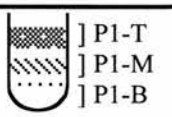
P1-bB	P1	55,000 x 30	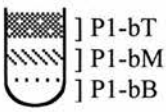
P2-M P2-B	P2 P2	131,000 x 60	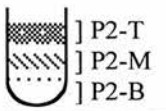

Table 3.3 Purification of fish liver fractions in a discontinuous Nycodenz gradient: Discontinuous gradients were set up in Beckman polycarbonate tubes. 3ml of 35% Nycodenz was over layered by 5ml of 25% solution using a Pasteur pipette to ensure the bands did not mix. The final addition of 5ml of 20% Nycodenz over layered the 25% solution using the same method. Samples (8 x 2ml) were applied to the top of the Nycodenz gradients.

Table 3.4 Marker enzyme distribution in gradient-purified preparations of peroxisomal and mitochondrial fractions from trout liver.

	Total units/g liver			Specific activity/mg liver			Recovery			Enrichment		
Fraction	Catalase	Cyt *c* Ox	NADPH Cyt *c*	Catalase	Cyt c Ox	NADPH Cyt c	Catalase	Cyt c Ox	NADPH Cyt c	Catalase	Cyt c Ox	NADPH Cyt c
P1-T	909	13235	329	71.3	1038	25.8	1.3	4.5	1.8	2.2	7.4	3
P1-M	775	39719	118	64.6	3310	9.8	1.1	13.5	0.66	2	23.6	1.1
P1-B	1374	6046	60	203.5	895.7	8.9	1.8	1.8	0.3	6.2	6.4	1
P1-bT	2712	7551	395	271.2	755.1	39.5	4.3	2.8	2.4	8.2	5.4	4.6
P1-bM	4103	18700	65	482.7	2200	7.6	6.5	7	0.4	14.6	15.7	0.88
P1-bB	4707	155	25	990.9	32.6	5.3	6.1	0.05	0.12	30	0.23	0.62
P2-T	787	19333	600	75	1841	57.1	2.3	13	6.6	2.3	13	6.6
P2-M	1412	19733	53	209.2	2923.4	7.8	2	6.7	0.29	6.3	20.9	0.91
P2-B	1475	962	16	310.5	202.5	3.4	1.6	0.24	0.07	9.4	1.4	0.4

Marker enzymes were measured as described in Materials and Methods 2.1.2. Fraction details and centrifugation conditions are as described in Materials and Methods 2.1 (fig 2.2). Activities per g of liver and specific activities were measured at 30°C throughout. Presented data results from one experiment (starting material: 4 fish, total liver weight: 25g)

3.3.2 Discussion of centrifugal gradient separation of trout mitochondria and peroxisomes

Overall, the recovery of the purified mitochondria and peroxisomes was not substantial as shown in Table 3.4. Several reasons may explain why the recovery was so low. Firstly the isolation medium may be at fault. An important attribute of any gradient medium is its ability to resolve the major subcellular organelles from liver samples (Graham et al., 1994). Nycodenz, an isopycnic medium was used to separate the organelles by their cell density. This medium was developed as a replacement for sucrose density gradients. Sucrose had several disadvantages that include a high osmolarity, which causes membrane-bound, osmotically-sensitive particles to lose water and shrink. This could alter their buoyant density leading to co-banding of organelles. Although not conclusive, it could be suggested from the data in Tables 3.1. and 3.4. that co-banding of mitochondria and peroxisomes has occurred. This could mean that fish organelles are more osmotically sensitive than those from rat liver. The osmotic activity of the medium is an important consideration and the viscosity of the medium helps determine the rate at which the particles sediment (Ford et al., 1994). Percoll, another isolation medium that has been used successfully to purify mitochondria in rat liver (Derrick and Ramsay, 1989) was used earlier in this study to isolate mitochondria from trout liver. The experiment was not successful. A diffuse band was removed from the gradient that was largely contaminated with microsomes. It could be hypothesised that Nycodenz and Percoll are too viscous and hyperosmotic for trout liver fractions leading to slow sedimentation rates for small particles and loss of water from subcellular organelles. The density of mitochondria and peroxisomes in rat liver is 1.1 g/cm (3) and 1.22-1.24 g/cm (3) respectively. No

data exist as to the exact densities of mitochondria and peroxisomes in fish. It may be that their densities are less different, making separation by density gradient centrifugation difficult. The fish organelles may have contacts in the cell as found for mitochondria to the endoplasmic reticulum that could also causing difficulties in separation.

Another explanation for poor recovery may be the centrifugation times and speeds to which the gradient suspensions were subjected. It can be seen from Table 3.2 that the recovery of peroxisomes is greater at the lower speed (P1-bB) than it is for the higher speed, suggesting that peroxisomes in fish liver are more sensitive to higher centrifuging speeds than rats and that the processes may be damaging the structure of the organelle. (Henderson and Sargent, 1985b) reported cross contamination of density-gradient-purified organelles when centrifuging speeds were increased. Isolation of organelles in fish differs between species. For example, (Crockett and Sidell, 1993c) successfully isolated mitochondria and peroxisomes from dogfish, a bottom dwelling fish using a Percoll continuous gradient scheme. However when the same method was applied to rainbow trout during the course of this work, the same separation was not obtained suggesting that the heterogeneous nature of fish may complicate the isolation procedure.

Density gradient centrifugation remains one of the most widely used techniques for the purification of subcellular organelles, but other methods do exist. For example, immune free flow electrophoresis (IFFE) separates the organelles in an electric field with the high selectivity of an immune reaction. It has already been used in rat liver to isolate subpopulations of peroxisomes (Volkl et al., 1999). This procedure could be used for isolating mitochondria and peroxisomes from fish liver.

3.4 Carnitine acetyltransferase and carnitine decanoyltransferase activities in trout liver

Inhibition of the overt mitochondrial carnitine palmitoyltransferase by malonyl-CoA is important in the regulation of fatty acid oxidation in mammals. Studies of the subcellular distribution of carnitine palmitoyltransferase indicated that most of the activity in mammalian liver cells is mitochondrial (Clarke and Bieber, 1981). However, carnitine acetyltransferase activity has also been reported in microsomes (Markwell et al., 1973a) and in peroxisomes (Farrell et al., 1984). The aim of this experiment was to evaluate quantitatively the distribution of carnitine acetyltransferase (CAT) and carnitine decanoyltransferase (CDT) activities within crude organelle fractions from trout liver. The data should be examined in the light of the marker enzyme profiles in Table 3.2.

It can be seen from Table 3.5 that CAT is divided almost equally between S1 (which still contains some mitochondria and peroxisomes as well as microsomes) and P1 (enriched in mitochondria and peroxisomes). The same is also true for CDT, although the recovery is decreased. In fact, recovery of CDT and CAT is poor in all samples shown in Table 3.5 so further work is needed, including analysis of profiles after gradient separation of the organelles. Enrichment of CAT is greatest in P1 (the mitochondrial fraction) as would be expected. This correlates with mitochondrial marker assay in Table 3.2 where cytochrome *c* oxidase enrichment was highest in P1 fraction.

Fraction	Specific activity (μmol/min/mg)		Recovery (%)		Enrichment	
	CAT	CDT	CAT	CDT	CAT	CDT
homogenate	1.03	1.24	100	100	1	1
P1	6.3	1.36	34.6	6.22	6.1	1.1
S1	0.5	0.14	33.1	7.8	0.49	0.11
P2	1.6	1.52	7.9	6.31	1.6	1.23

Table 3.5 Carnitine acetyltransferase and carnitine decanoyltransferase activities in trout liver fractions. Assay conditions were as described in Materials and Methods. 2.1.3. For fraction details and centrifugation conditions see Materials and Methods section 2.2.3 (Fig. 2.2). The data presented are results from one experiment, starting from 34.1g of liver.

3.5.1 Fatty acid oxidation: methods for measurement of fatty acid oxidation in rainbow trout liver fractions, and their reliability.

Three methods for the measurement of the rate of breakdown of palmitate (C_{16}) were tested. All have been used to compare mitochondrial and peroxisomal fatty acid oxidation rates in mammalian homogenates. The results from radiochemical assays, oxygen consumption, and a spectrophotometric assay for peroxisomal oxidation were applied to trout liver extracts and compared.

3.5.1 Radiochemical measurement of β-oxidation

The release of soluble [^{14}C]acetyl-CoA from [^{14}C]palmitate is the most sensitive of the methods for measuring the rate of β-oxidation in crude samples. However,

mitochondrial β-oxidation also releases $^{14}CO_2$ after metabolising the acetyl-CoA in the TCA cycle so trapping must be used if this is to be measured. For peroxisomal oxidation, [^{14}C]acetyl-CoA is a final product. Using KCN to inhibit mitochondrial respiration, this assay has been shown to measure peroxisomal β-oxidation (Lazarow, 1981).

Table 3.6 shows that the rates observed for peroxisomal β-oxidation in fractions from fish liver are very low. A control was carried out using the same procedure but using rat liver organelle fractions instead of fish to detect any fault in the procedure. A good rate was achieved suggesting that the rate in fish liver was indeed too low to be detected. The rate in the rat liver was not as high as previously published data (1μmol/min/g liver) (Lazarow, 1981), suggests that there may still have been a problem with the application of the radiochemical method. For example quenching, which results in a reduction of the scintillation count rate, chemiluminescence or photoluminescence. Also, palmitate was used as the substrate here whereas for the published rat data, palmitoyl-CoA was used.

3.5.2 β-oxidation rates using the O_2 electrode

Oxygen consumption (recorded using the O_2 electrode) measures all the oxidation processes in the sample. However, the rates in cell fractions are dependent on the added substrate. Palmitoyl-CoA induces an increase in the rate of O_2 consumption due to both peroxisomal acyl-CoA oxidase (ACO) and mitochondrial electron transport chain oxygen use. Peroxisomal oxidation rates were below detection level. The rate observed using gradient purified mitochondria (0.73 nmol/min/mg, shown in Table 3.6) was comparable to the rate (0.74 nmol/min/mg) obtained by (Henderson and Sargent, 1985a).

Assay	Substrate	KCN	Fraction	Organelle	Rate (μmol/min/mg)	Rate (μmol/min/mg)
Radiochemical	Palmitate	+	P2	Peroxisomes	9×10^{-9}	0.37×10^{-6}
	Palmitate	-	P2-B	Peroxisomes	33×10^{-9}	0.06×10^{-6}
Spectrophotometric	Palmitoyl-CoA	+	P1	Peroxisomes	0.93×10^{-3}	9.5
O_2 electrode	Pamlitoyl-CoA	-	P2	Peroxisomes and mitochondria	0.04	2.05
	Palmitoyl-CoA	-	P1-M	mitochondria	0.73×10^{-3}	0.012

Table 3.6. Fatty acid oxidation rates in trout liver fractions. The incubation conditions for each assay (column 1 of table) were as described in Materials and Methods 2.6. Fractions used are as displayed in column 4 of the table. Fraction details and centrifugation conditions are described in Materials and Methods 2.1 (fig 2.2). Specific activities (μmol/min/mg protein) were measured at 30°C throughout. Presented data results from one experiment.

3.5.3 Spectrophotometric measurement of peroxisomal β-oxidation

This assay measured the reduction of NAD-NADH in the third reaction of the peroxisomal β-oxidation spiral. This gives total peroxisomal rates and is more sensitive than the O_2 electrode method. The rate in fish liver (0.93 nmol/min/g liver) was lower than the rate for rat found by Lazarow (1μmol/min/g liver). The author quotes the rates from purified peroxisomes so it is not directly comparable to the numbers in Table 3.6. Fraction P1 is enriched in peroxisomes but is not highly purified. To decide which is the best assay to measure β-oxidation, highly purified fractions should be used in future assays as done in other literature.

3.5.4 Discussion of the fatty acid oxidation rates in trout liver fractions

The rates of trout liver fatty acid oxidation as shown in Table 3.5 are in several cases much lower than was anticipated. It was expected that optimal rates would be achieved in the radiochemical assay, as this is the most sensitive method. This did not occur and it was concluded that the application of the method might have been at fault. There are other reasons, which may explain why the rates from these experiments were not uniform. Firstly, (Love, 1970) observed an increase in liver fatty acids and triglycerides during later maturation of female fish. The rainbow trout used in these experiments were approximately one year old, too young to have laid down large reserves of fatty acids. Secondly, spawning enhances a fish's capacity for fatty acid oxidation (Kiessling et al., 1995b). Both spawning and non-spawning fish were used in these experiments, introducing a source of variability. Thirdly, the isolation procedure may have damaged the integrity of the organelles, as mentioned previously. This could result in a poor or non-functioning β-oxidation system,

particularly for the mitochondria. And, finally liver disease was reported in some of the fish. Although, it is unclear if the trout used in these experiments were affected. At this stage, the spectrophotometric assay is the most convenient and reliable and is suitable for future peroxisomal studies and therefore the spectrophotometric protocols used for measurement of mammalian peroxisomal fatty acid oxidation can be successfully applied to rainbow trout.

3.6 Effect of mounting an immune response on fat acid oxidation *ex vivo*

Fish are animals that are sensitive to stressors such as handling, injecting, transportation and thermal changes. These bring about physiological and chemical changes that have been studied extensively in the laboratory. One such change is the mobilisation of lipids from the muscle to the liver. A study carried out on *Oncorhyncus gorbuscha* which were stressed by tagging and being confined saw liver lipid increase from 5.9% in the controls to 10.4% in the tagged specimens, accompanied by a diminution in total muscle weight and an increase in liver weight (Saddler and Cardwell, 1971)

At present no data exist as to the metabolic consequence stress may bring in particular the partitioning of fatty acid oxidation rates between the mitochondria and peroxisomes. The need to produce protein for an immune response increase should the energy demand for which fat oxidation is a possible source. The aim of this particular study, therefore, was to examine the rates of mitochondrial and peroxisomal fatty acid oxidation in control and stressed to see if any differences could be observed.

Rainbow trout were stressed by an injection that elicited an immune response. The control specimens were also injected with an adjuvant so that any changes observed were a direct result of the vaccination and the response mounted to it, but not to the handling or injection stress.

3.6.1 Fatty acid oxidation in mitochondria and peroxisomes before and during an immune response

Livers from fish sacrificed immediately after the injection either of adjuvant or vaccine were pooled as the control sample for 0 days. In these livers, the mitochondria contributed about 54% of the total fatty acid oxidation (Table 3.7). After two days, there is a dramatic increase in the mitochondrial oxidation rates in both the control (over 5-fold) and immune-stressed (almost 10-fold) groups. In the control group, the peroxisomal rate was unchanged but in the immune-stressed group it increased although only by 2-fold. The increase in the total fatty acid oxidation rate had disappeared in the control group by five days, but persisted in the immune-stressed group (3-fold higher than the total day 0 rate). By day 8, both groups showed fatty acid oxidation rates well below the starting values. The reason for these low rates is not clear. It could be an artefact of changing conditions in the tank or an overshoot response to the increase at day 2.

The conclusion from this study is that there may be elevated fatty acid oxidation as part of the cost of mounting an immune response. It would be worth repeating the study in conjunction with a physiological assessment of calories used from fat, protein, and carbohydrate. The response in the control group suggests that even the transient stress of handling and injection can perturb the rates measured for the liver

samples *ex vivo*. Given the variable conditions of life in a tank in shared space, such a response could add to biological variability.

Days	Liver weight (g)		Fatty acid oxidation activity (nmol/min/g liver)			
	Control	Stress	Control (adjuvant)		Stress (vaccine)	
			Mito	Perox	Mito	Perox
0	5.32	5.32	8	6.7	8	6.7
2	4.75	4.02	44	6.8	79	16
5	7.43	3.30	2.2	2.8	42	3.0
8	5.07	7	0.4	1.5	1.8	0.6

Table 3.7 Hepatic fatty acid oxidation rates in sham-injected (control) and immune-stressed rainbow trout. Activities were measured at 30°C in P1 fractions throughout. P1 was fractionated as described in section 2.2 (Fig 2.2). Presented data results from one experiment. Mitochondrial oxidation rates were measured polarographically using the oxygen electrode as described in 2.3.1. Peroxisomal rates were determined spectrophotometrically as described in 2.3.3. Abbreviations: Mito: mitochondria Perox: peroxisomes

3.7 Food withdrawal stress

Fish undergo periods of starvation during various points in the life cycle. General metabolic rates have been studied but there is a lack of data distinguishing mitochondria fatty acid oxidation from peroxisomal and any changes that may be observed in the balance between them during fasting. The aim of the following study was to measure mitochondrial and peroxisomal fatty acid rates and see if there was any difference after 7 days of food withdrawal and then in a longer study up to 14 days. Due to Home Office regulations for the immunology project, the fish could not

have food withheld for more than fourteen days. Therefore, even although a fish in the wild can survive for a prolonged period without feeding, we were not able to examine the metabolic changes for more than two weeks. However, we hoped that adaptation might begin in the first two weeks and that is why we chose to carry out this study.

3.7.1 Fatty acid oxidation after food-withdrawal: First study

Mitochondrial and peroxisomal fatty acid oxidation rates were measured by the oxygen consumption of the P1 fraction in the absence and presence of cyanide to inhibit the mitochondrial oxidation. Table 3.8 shows that the observed peroxisomal rate left after the mitochondrial contribution was inhibited declined slightly from the control value, which was gratifyingly, similar to the control value obtained in the earlier immune-stress experiment. Despite the variability that plagued these experiments, the control values were repeatable. The mitochondrial fatty acid oxidation rate had increased relative to the peroxisomal rate at day 4; from 54% to 76% of the total oxidation rate but is was only at day 7 that the rate increased greatly (3-fold). Clearly, unlike in the immune-stress experiment, there was not an immediate response of the mitochondrial rate to food withdrawal and this study would have to be run over a longer period.

Days	Liver weight (g)	Activity/ g liver (nmol/min/g liver)	
		Mitochondria	Peroxisomes*
0	5.3	8.1	6.7
4	7.5	9.8	2.9 (4.1)
7	4.9	28	3.7 (1.5)

Table 3.8 Mitochondrial and peroxisomal fatty acid rates in rainbow trout liver: comparison between fed and unfed fish. Activities were measured at 30°C in P1 fractions throughout, or P2 where indicated (* Values in parenthesis are for the P2 fraction). P1 and P2 were fractionated as described in section 2.2 (Fig 2.2). Presented data results from one experiment. Mitochondrial oxidation rates were measured polarographically using the oxygen electrode as described in 2.3.1. Peroxisomal rates were determined spectrophotometrically as described in 2.3.3.

3.7.2 Fatty acid oxidation after food-withdrawal: Second study

The aim of the second study was to measure mitochondrial and peroxisomal fatty acid rates in a longer study up to 14 days. For this experiment, the homogenisation to release organelles from the tissue had been improved to see whether the lower rates seen previously had been the result of poor extraction or if indeed that fatty acid oxidation rates in fish remains markedly lower than in the mammalian system. A further change in the protocol was that gradient purified samples of the organelles were used in order to get more reliable rate determinations. The rates obtained were then referred back to the starting weight of liver to allow calculation of the relative contribution of the mitochondrial and peroxisomal pathways. For the zero time only, marker enzymes were determined, so for that time point only, correction for the recovery of cytochrome oxidase and catalase in the purified mitochondria and P1 was possible.

The results are shown in Table 3.9. Table 3.9a lists the rates for mitochondrial fatty acid oxidation and Table 3.8b the rates for peroxisomal oxidation. For the zero time point, recovery of catalase in the purified mitochondrial fraction was 12% and of cytochrome oxidase was 38% but overall recovery of cytochrome oxidase was 200% so the data cannot be used to make conclusions. Compared to the P1 fraction, the purified mitochondria contained 65% of the catalase and 44% of the cytochrome oxidase. After modulation for this difference, the rate measured by the spectrophotometric assay would be expected to give a rate of 1.2 $\mu mol.min^{-1}.mg^{-1}$ in the mitochondrial fraction, in good agreement with the 1.42 $\mu mol.min^{-1}.mg^{-1}$ obtained in the oxygen electrode. Since marker data were not done for the other time points, the relative contribution of the peroxisomes to the total oxidation was calculated for the mitochondrial fraction based on the recovery of the markers in the zero time point sample. They are thus merely an estimate at this point. A complete study needs to be done.

The estimated relative contributions of each organelle to the overall rate are given in Table 3.9a on the far right. It is quite clear that no trend of change is seen over this two-week period but there is considerable variability. Again the control values at the start of the experiment are satisfactorily similar to previous values at 9.2 nmol/min/g liver for mitochondrial oxidation and 4.9 nmol/min/g liver for peroxisomal oxidation. The variability between the days of this experiment then becomes puzzling. The lack of the increase observed at day 7 in the first experiment could mean that the first experiment was wrong or could be due to food dropped into the tank by passers-by despite the labels. Given the inexplicable variability, we decided that it was not economical to do the experiment again without better control over the conditions

under which the fish were held and without permission for a much more extended fasting period.

3.7.3 Discussion of the lack of change in fatty acid oxidation after food withdrawal

In starvation, fish use both lipids and protein from both liver and muscle tissue. For example, after five weeks without food, rainbow trout mosaic muscle lost 4% of its lipid and dark muscle lost 31%. However, the fatty acid level in plasma showed little rise in early starvation (before about 100 days). The loss of lipid from muscle at 5 weeks does suggest considerable use of fat stores even in the early stages of starvation, so we looked for increase in fatty acid oxidation rates in mitochondria and peroxisomes over two weeks. This time frame allowed for new protein synthesis if up-regulation of beta-oxidation enzymes took place.

In our experiments, liver weight did not decrease over the two-week period suggesting that little mobilisation of the lipid stores had occurred. Neither of the two experiments (Tables 3.9a and 3.9b) showed significant change in the rates of fatty acid oxidation in either mitochondria or peroxisomes. This suggests that the fuel use in this period did not require up regulation of the beta-oxidation pathways.

(a)

Sample (days)	Weight of liver (g)	Specific activity (nmol/mg/mg protein)		Total activity (nmol/min/)		Activity/g liver (nmol/g liver)		Marker corrected % Total oxidation	
		Mito	Perox	Mito	Perox	Mito	Perox	Mito	Perox
0	12.7	7.35	1.42	14.7	2.84	9.16	1.77	64	36
1	15.3	3.50	1.00	13.3	3.80	4.45	1.27	54	46
4	13.1	5.26	0.48	10.5	0.96	8.67	0.79	79	21
7	12.8	1.90	0.60	6.84	2.16	2.41	0.76	51	49
14	12.3	3.44	0.76	10.3	2.28	5.27	1.17	60	40

(b)

Sample (days)	Activity (nmol/min/ml)	Specific activity (nmol/min/mg/ protein)	Total activity (nmol/mg protein)	Activity/g liver (nmol/min/g liver)
0	61.8	1.77	3.54	4.88
1	58.9	1.53	4.94	3.84
4	42.9	1.17	2.34	3.27
7	50.8	1.73	6.23	3.97
14	66.4	1.74	5.22	5.41

Table 3.9 Mitochondrial and peroxisomal fatty acid rates in rainbow trout liver: comparison between fed and unfed fish

(a) Mitochondrial oxidation rates were measured polarographically using the oxygen electrode as described in section 2.3.1. Activities were measured at 30°C using gradient purified mitochondria (with some residual peroxisomal contamination). Mitochondria were purified from P1 by percoll gradient as described in section 2.2.4. **(b)** Peroxisomal β-oxidation rates were determined using the spectrophotometric assay. Assay conditions are as described in section 2.3.3. Activities were measured at 30°C using the P1 fraction (fractionated as described in 2.4). The data is the result of one experiment, with two livers in each group.

Chapter 4

Contact sites and CPT1 in trout liver mitochondria

4.1 Introduction

Hackenbrock first identified the contact site of the mitochondria in 1968. Contact sites are areas within the mitochondria where the outer membrane and inner membrane are so close that physical force cannot separate them (Hackenbrock, 1968). At these sites a pore is formed, the mitochondrial permeability transition pore (mPTP). The pore has been shown to be involved in the transport of various metabolites and ions, and has been suggested to play a role in apoptosis (Crompton, 1999).

The transport of fatty acids across the mitochondrial membranes involves two enzymes, carnitine palmitoyltransferase 1 (CPT1) and carnitine palmitoyltransferase 2 (CPT2). CPT 1 is sensitive to malonyl-CoA and has been suggested to control fatty acid oxidation across the mitochondrial membranes. Previous research has identified that CPT 1 and CPT 2 are located in the contact sites (Fraser and Zammit, 1998).

The aim of this chapter therefore is to develop methods from mammalian studies to subfractionate the mitochondrial membranes from rainbow trout liver. Marker enzymes will be used to identify the outer and inner membranes and contact sites. Another aim is to identify the location of CPT1. The location of CPT1 may relate to the unique microenvironment of the contact site. Contact sites contain relatively high levels of cardiolipin which greatly increase the sensitivity of malonyl-CoA, (Mynatt et al., 1994) and therefore provides further evidence for the role of CPT 1 in the control of fatty acid oxidation.

Moreover, in mammalian liver tissue, it has been observed that under starvation conditions contacts between the inner and outer mitochondrial membranes are increased. (Blok et al., 1971) This event has not been studied in fish. Fish undergo periods of fasting at various life stages and require an enhanced flux of fatty acids to meet metabolic needs which the contact site may facilitate. Therefore we undertook these experiments to investigate the distribution of CPT in submitochondrial fractions from fed and fasted rainbow trout livers.

4.2 Contact sites from trout liver mitochondria

4.2.1 Isolation and subfractionation of mitochondria

The initial aim of this project was to subfractionate mitochondria from rainbow trout liver. This was attempted through a process of homogenization and centrifugation as detailed in Chapter 2.4.

After centrifugation through Percoll the initial pellet was fractionated into three layers. The middle layer was enriched with mitochondria with some cross contamination from microsomes and peroxisomes. This layer was extracted and washed. The isolated mitochondria were re-suspended in a hypotonic solution and subjected to a series of freezing, thawing and sonication to separate the mitochondria into its outer and inner membranes. The fraction was then centrifuged at 105,000g for 20 hours in a sucrose density gradient to allow identification of these membranes.

After centrifugation, the sucrose density gradient contained a distinct white band approximately two-thirds down the gradient. This white band indicates that the fractionated mitochondria have passed through the sucrose gradient.

4.2.2 Marker enzymes and protein content

The distributions of NADPH cytochrome *c* oxidoreductase (outer membrane marker) and of cytochrome *c* oxidase (inner membrane marker) (fig 4.1) demonstrate that two individual enzyme profiles are present. Both the outer membrane, represented by NADPH cytochrome *c* oxidoreductase and the inner membrane represented by cytochrome *c* oxidase are distinguishable as individual peaks in the early fractions (1-5) and the later fractions (15-18) respectively. There is also a peak from fractions 8-14 in which both the NADPH cytochrome *c* oxidoreductase and cytochrome *c* oxidase are present in relatively high proportions, which may represent the contact sites. The absorbance at 280 nm (figure 4.1b) shows that the protein content of the fractions is highest in fractions 0-4 and 15-19 reflecting the increased enzyme activity in these fractions.

4.2.3 CPT Activity

Figure 4.2 shows the distribution of CPT activity and when compared to the marker enzymes, (fig 4.1) demonstrates that CPT activity is highest in the outer membrane and the presumed contact site fraction. Although the CPT activity does decline across the fractions there is a small increase in activity in the peak inner membrane fractions 20-23.

Determination of the distribution of malonyl-CoA sensitive CPT activity in submitochondrial fractions was attempted but because of low activity rates, the assays were abandoned in favour of measuring the activity in the pooled samples.

(a)

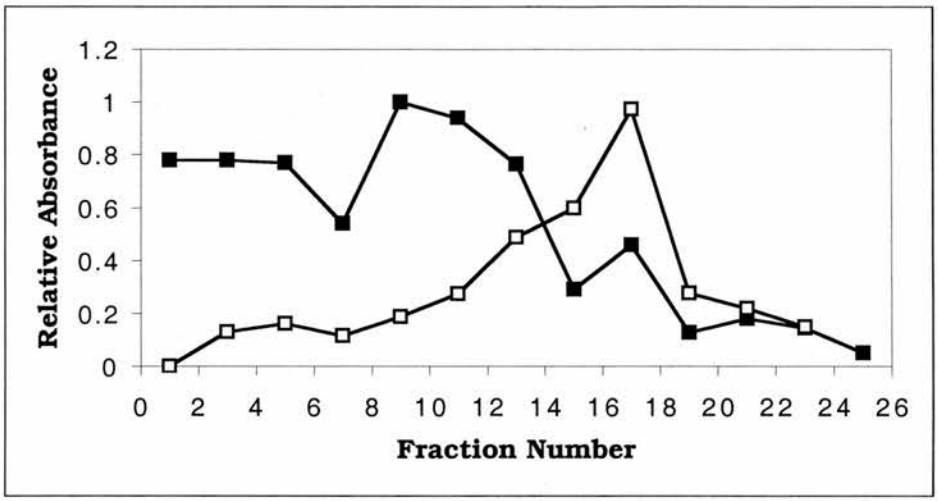

(b)

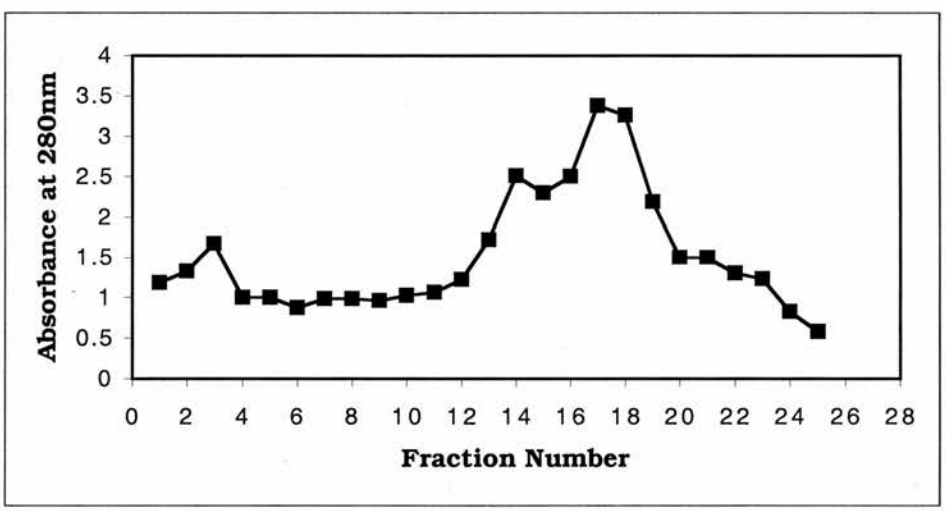

Figure 4.1a Distribution of (a) outer and inner membrane marker enzymes and (b) membrane protein in submitochondrial fractions obtained from rainbow trout liver mitochondria after 1st sucrose gradient. Mitochondrial outer and inner membranes and contact sites were prepared and separated on continuous sucrose gradient as described in 2.4.2. (**a**) Activities of marker enzymes for outer membrane (■) and inner membrane (□) are shown. In (a) the activity of each enzyme in the fraction in which it was most abundant is set at unity and the other values are expressed as relative values (**b**). The estimation of amount of membrane protein (measured at A_{280}) in each fraction is given (■).

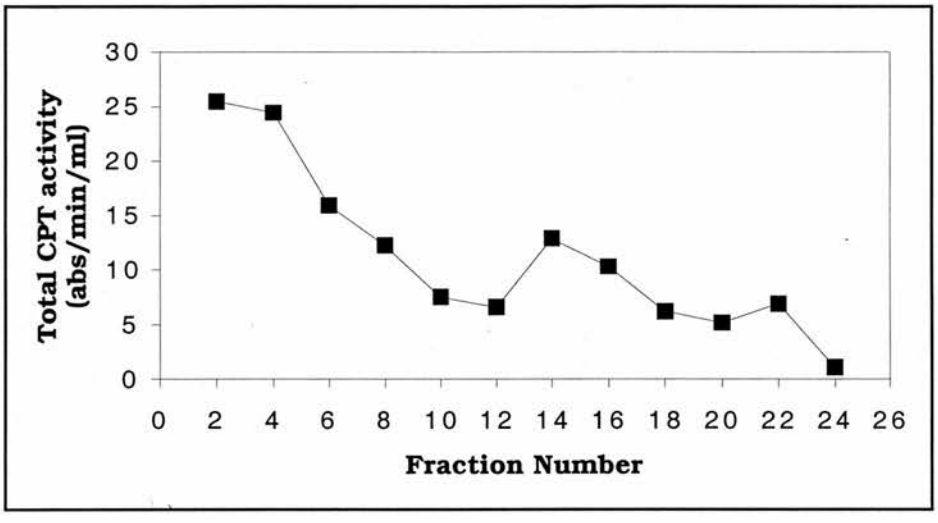

Figure 4.2. The distribution of total CPT activity after 1st sucrose gradient. Enzyme activity was assayed as described in 2.1.3.3

4.2.4 Second continuous sucrose density gradient

The marker distribution pattern shown in figure 4.1a is typical, although contamination of inner membrane within the outer membrane fraction is somewhat higher than expected. To improve on the separation in the first continuous sucrose density gradient, it was decided to repeat the procedure to see if it would help further separate the mitochondrial membranes and remove cross contamination. From the original gradient (see figure 4.1a), fractions were pooled and categorized into four groups: A, B, C and D composing of fractions 1-7, 8-15, 16-19 and 19-25 respectively.

Group A was considered predominantly outer membrane and was not subjected to further sucrose density gradient centrifugation. Similarly group D was considered predominantly unbroken mitochondria and was also not subjected to further fractionation. Both groups were concentrated using a 10 mL concentrator (Centricon) and were aliquoted to 0.5mL fractions and stored at –20°C until required.

Group B and C fractions were pooled and concentrated by ultrafiltration through an YM10 membrane (Amicon). Aliquots (0.9mL) of group B and C were applied to continuous sucrose gradients as previously described (see 2.4.2).

Marker enzyme distribution and protein profiles for B and C after subjection to sucrose density gradient centrifugation are shown in figures 4.3 and 4.4 respectively. Group B fractions 4 -7 and 8 -14 were pooled to give contact site 1 (CS1) and contact site 2 (CS2) respectively. Group C fractions 14 -17 were pooled and concentrated to give contact site 3 (CS3). Group C fractions 18-24 were pooled and concentrated to give he inner membrane sample.

After measurement of marker enzymes in these concentrated fractions, it was decided to pool CS1 and CS2 because their profiles were very similar (data not shown). Marker enzyme and CPT1 specific activities of this final contact site fraction and the inner membrane sample are displayed in table 4.1.

(a)

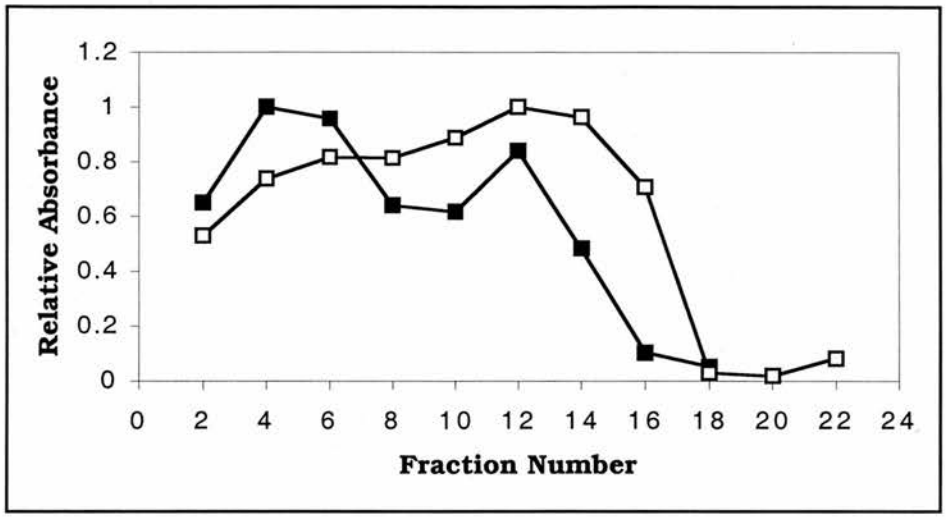

(b)

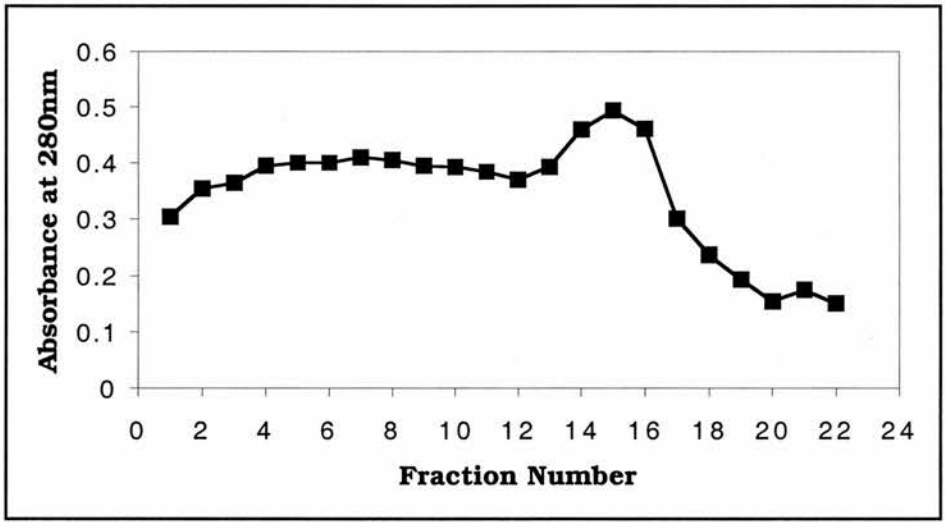

Figure 4.3a Distribution of (a) outer and inner membrane marker enzymes and (b) membrane protein in submitochondrial fractions obtained from rainbow trout liver mitochondria 'B' fraction after 2nd sucrose gradient. Mitochondrial outer and inner membranes and contact sites were prepared and separated on continuous sucrose gradient as described in 2.4.2 **(a)** Activities of marker enzymes for outer membrane (■) and inner membrane (□) are shown. In (a) the activity of each enzyme in the fraction in which it was most abundant is set at unity and the other values are expressed as relative values. **(b)** The estimation of amount of membrane protein (measured at A_{280}) in each fraction is given (■).

(a)

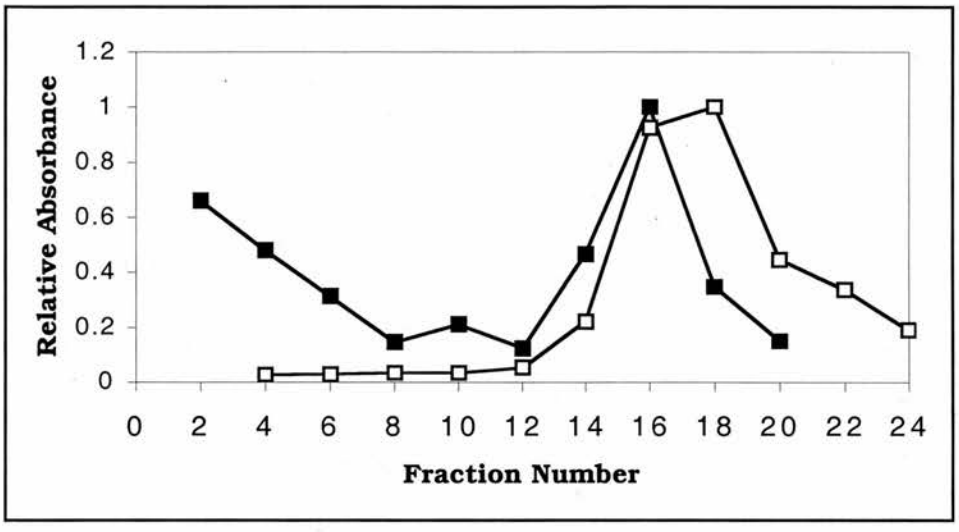

(b)

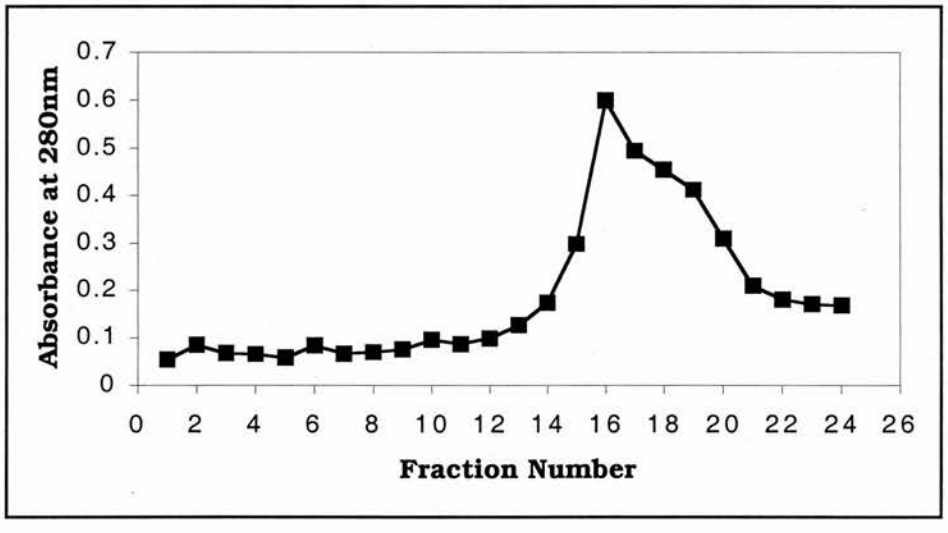

Figure 4.4a Distribution of (a) outer and inner membrane marker enzymes and (b) membrane protein in submitochondrial fractions obtained from rainbow trout liver mitochondria 'C' fraction after 2nd sucrose gradient. Mitochondrial outer and inner membranes and contact sites were prepared and separated on continuous sucrose gradient as described in 2.4.2. **(a)** Activities of marker enzymes for outer membrane (■) and inner membrane (□) are shown. In (a) the activity of each enzyme in the fraction in which it was most abundant is set at unity and the other values are expressed as relative values. **(b)** The estimation of amount of membrane protein (measured at A_{280}) in each fraction is given (■).

4.2.5 Enzyme activities in the pooled fractions

The overall specific enzyme activities show that the outer and inner membrane samples represent two distinctly different proportions of the mitochondria. One sample has relatively high levels of NADPH cytochrome *c* oxidoreductase and low cytochrome *c* oxidase and the other has low levels of NADPH cytochrome *c* oxidoeductase and high levels of cytochrome *c* oxidase. Table 4.1 demonstrates that CPT1 is present in the contact site but is not enriched. The outer membrane has some CPT1 activity, whilst the inner membrane has little CPT1 activity. It should be noted that the malonyl-CoA sensitivity assay might underestimate CPT1 activity. Malonyl-CoA sensitivity can be lost during subfractionation of mitochondria, as found by Zammit (1990) and malonyl-CoA sensitivity differs between outer membrane and contact site CPT1.

4.2.6 Analysis of the proteins in each pooled sample

These concentrated fractions were subjected to 10% SDS-PAGE to analyse the proteins of the outer membrane, contact site and inner membrane. This revealed specific protein patterns that differ between the samples (fig 4.5).

4.2.7 Protein sequencing of bands in outer membrane

In a separate experiment the outer membrane fractions were again subjected to a 10% SDS gel which was then followed by transfer of the separated proteins to a polyvinylidene diflouronide (PVDF) transfer protein membrane for N-terminal sequencing of the bands at 88 and 32 kDa, considered to be the CPT and VDAC protein respectively (figure 4.6). Two unknown proteins identified with molecular weights of 47 and 115 kDa were also sequenced. An automated protein sequencer

(Applied Biosystems) was used to sequence N-terminus amino acids of the protein. One band was N-terminally blocked; another gave a partial sequence that gave no putative matches when searched on the BLAST database. The other band that was assumed to be CPT1 was not present in suitable quantity to achieve an accurate determination of the sequence (table 4.2). No further work was done regarding this approach.

	Outer membrane	Contact Site	Inner membrane
Protein (mg)	146	105	31.5
Specific activities (μmol/min/mg)			
NADPH cyt *c* oxidoreductase	21.1	23.2	11.9
Cyt *c* oxidase	432	924	2816
CPT I activity (nmol/min/mg)	**6.0**	**8.5**	**2.25**

Table 4.1 Distribution of marker enzymes in samples from the sub-fractionation of mitochondria prepared from control trout liver. The weight of a control trout liver was 10g. The sucrose gradient fractionation of hypotonically–shocked Percoll purified mitochondria is shown in Fig. 4.1. The outer membrane sample came from fractions 1-7. The contact site and inner membrane sample was the result of refractionation of fractions 8-15 and 19-25 from the first gradient onto a second sucrose gradient as described in 4.2.4.

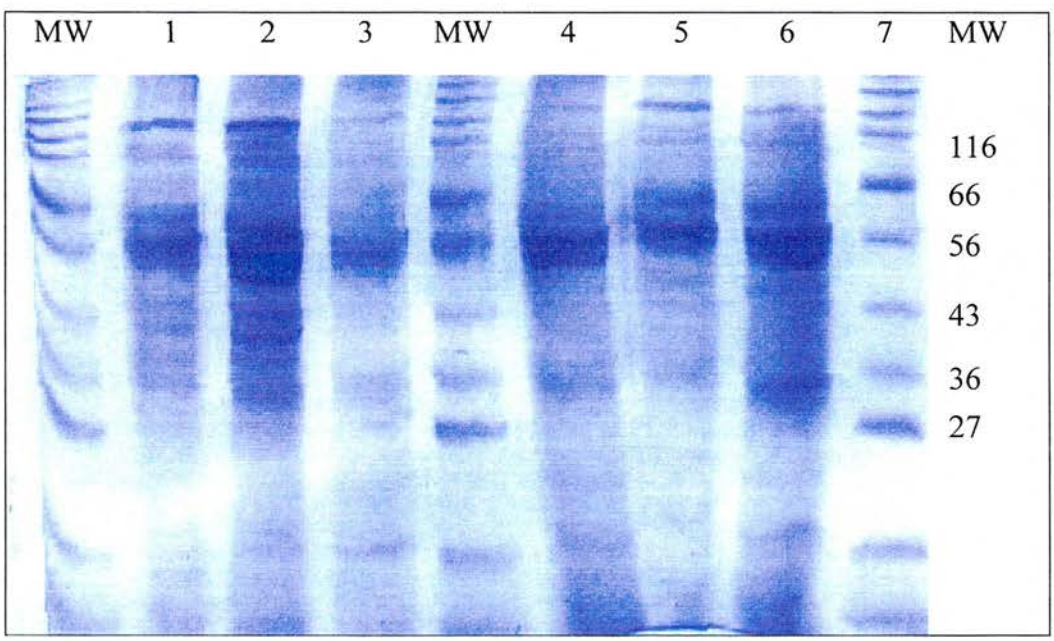

Figure 4.5 Gel electrophoresis of submitochondrial fractions stained with Coomassie blue. MW: molecular weight standards (kDa). Lane 2 and 3: 5 and 10μg respectively, outer membrane; lane 4 and 5: 5μg, contact site; lane 6 and 7: 5 and 10μg respectively, inner membrane.

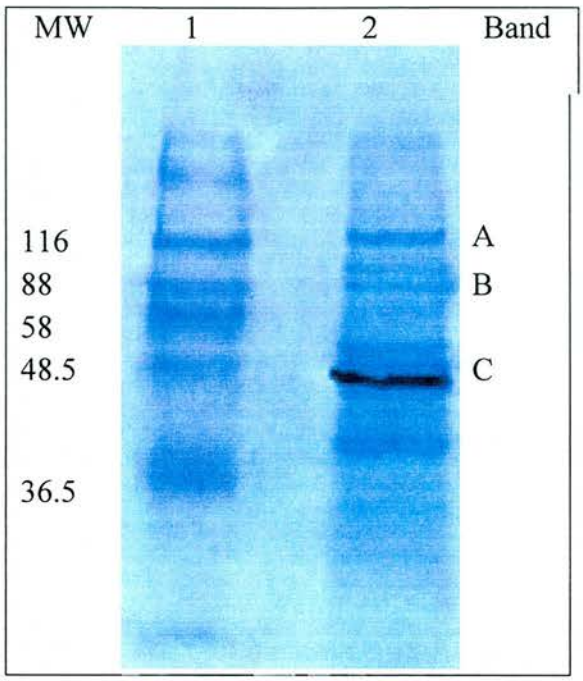

Figure 4.6 Electroblot using PVDF from 1-D polyacrylamide gel electrophoresis of rainbow trout liver mitochondrial outer membrane stained with amido black. MW: molecular weight standards (kDa). Lane one, molecular weight standards (Sigma Chemical Co.); lane two: 20µg trout liver mitochondrial outer membrane. Bands A-C were removed from PVDF membrane and taken for sequencing (results shown in table 4.2).

Band	*Molecular wt (kDa)*	*Location*	*Partial Sequence*	*Identification*
A	*115,000*	*Outer membrane*	*QHNSPQTLEY*	*No matches*
B	*88,000*	*Outer membrane*	*Unsuccessful attempt*	*CPT-I?*
C	*47,000*	*Outer membrane*	*N-terminal blocked*	*unknown*

Table 4.2 **Band identification and sequence data**. Identification of bands extracted from PVDF membrane (fig 4.6).

The identification of VDAC and ANT, known components of the contact sites, was attempted through the use of western blotting of the 1 dimensional SDS electrophoresis gel. The western blots using commercial antibodies raised in rabbits and shown to be cross-reactive for humans, mice and rats failed to identify the location of VDAC and ANT and in fish. A second attempt to identify trout liver mitochondrial VDAC was made using an anti-peptide antibody (a gift from Professor Vito de Pinto, University of Catania) and this antibody did react with one band of the correct molecular weight for VDAC and is comparable to the band isolated from rat liver mitochondrial outer membrane (figure 4.7). However, lack of sample prevented us from investigating the distribution of porin across the mitochondrial membranes.

4.3 Distribution of CPT in fed and fasted rainbow trout submitochondrial fractions

Fasted fish had feed withheld for a maximum (according to Home Office regulations) of two weeks. Fed fish were kept on a diet of commercial pellets until ready for sacrifice. The isolation of mitochondria from liver and subfractionation of mitochondrial membranes from fed and fasted fish was as described in Chapter 2.4.2. Activities of marker enzymes were assayed to assess the distribution of mitochondrial membranes and are shown in 4.8 and 4.9.

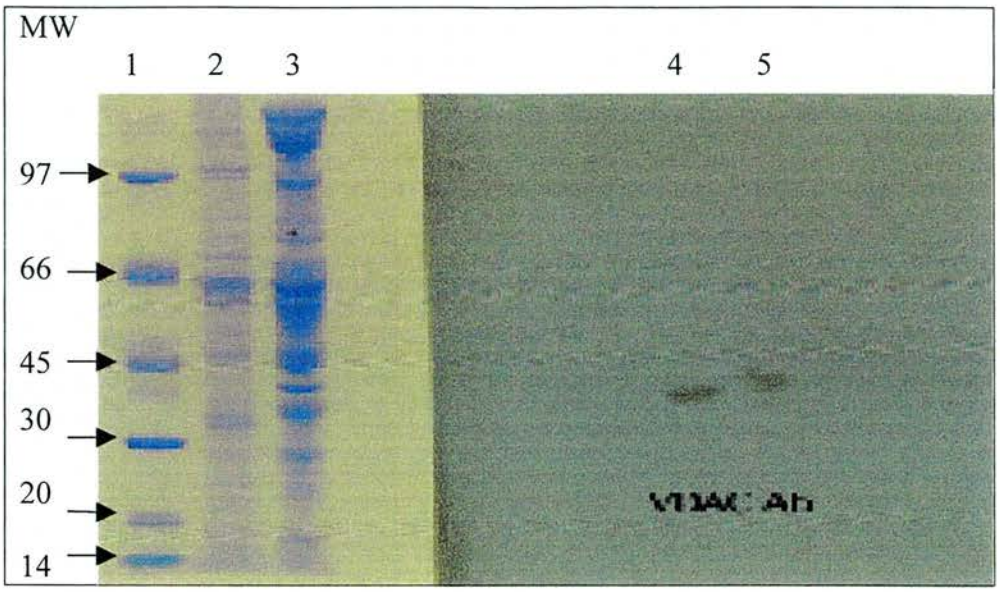

Figure 4.7 Identification of VDAC in rainbow trout outer membrane fraction using immuno blotting. Lane 1: molecular markers (KDa) (Amersham). 15μg trout liver mitochondria (lane 2) and 30μg rat liver mitochondria outer membrane (lane 3) components were isolated using SDS polyacrylamide gel electrophoresis, stained with Coomassie blue. Western blotting was performed after SDS PAGE using an anti-peptide antibody. Anti-porin antibody was obtained against purified porin isoform 1 from bovine heart mitochondria. Primary and secondary antibodies were used at 1:5000 dilution. VDAC proteins from trout liver mitochondria (lane 4) and rat mitochondrial outer membrane (lane 5) were detected by enhanced chemiluminescence (ECL) staining. Abbreviations: MW-molecular weight.

4.3.1 Enzyme distribution in fed fish

The distribution of NADPH cytochrome *c* oxidoreductase and of cytochrome *c* oxidase (fig 4.8a) demonstrates that two individual enzyme profiles are present. NADPH cytochrome *c* oxidoreductase activity (outer membrane marker) is located mainly in the top fractions (1-5) and decreases thereafter.

Cytochrome *c* oxidase activity shows a peak in activity at fractions 12-15 which is where the distribution of inner membrane is expected. Another considerable peak in cytochrome c oxidase activity in fraction 4 suggests that the inner membrane is not solely located in the lower fractions.

The absorbance at 280nm (fig 4.8b) shows that the protein content is highest in fractions 2-5 reflecting the increased enzyme activity in these fractions. There is a slight shoulder in the general trend around fractions 8-12 reflecting the peak of cytochrome *c* oxidase activity observed in these fractions.

Due to the high levels of NADPH cytochrome *c* oxidoreductase activity and increased absorbance at 280 nm, fractions 1-3 were pooled and concentrated to give the mitochondrial outer membrane. The peak in outer membrane marker activity was actually observed in fraction 4 but due to significant contamination of cytochrome *c* oxidase activity, this fraction was excluded from the pooled outer membrane fraction.

Fractions 12-15 were pooled and concentrated to give the inner membrane fraction. These fractions displayed a peak of cytochrome *c* oxidase activity which was relatively free of outer membrane cross contamination.

A third set of fractions (5-8) were also pooled and concentrated. These fractions were considered to be where contact sites are localized as they represent an area between the peak outer and inner membrane fractions.

4.3.2 Marker enzyme distribution in fasted fish

The distribution of NADPH cytochrome *c* oxidoreductase and of cytochrome *c* oxidase demonstrates that the enzyme profiles displayed here (4.9a) are similar to those observed in fig 4.8a. A peak in activity of the outer membrane marker is observed in fraction 1-3 which is reflected in the protein content (fig 4.9b). Another peak in activity at fraction 12 suggests cross contamination with the inner membrane. Activity of the inner membrane marker enzyme displays a peak of activity in fraction 13-15, representing the inner membrane and another peak in fraction 4. The presence of the outer membrane enzyme in this fraction is much less than was observed in 4.8a. The absorbance at 280nm (fig 4.9a) shows that the protein content is highest in fractions 2-5 and 12-14 reflecting the increased enzyme activity in these fractions.

(a)

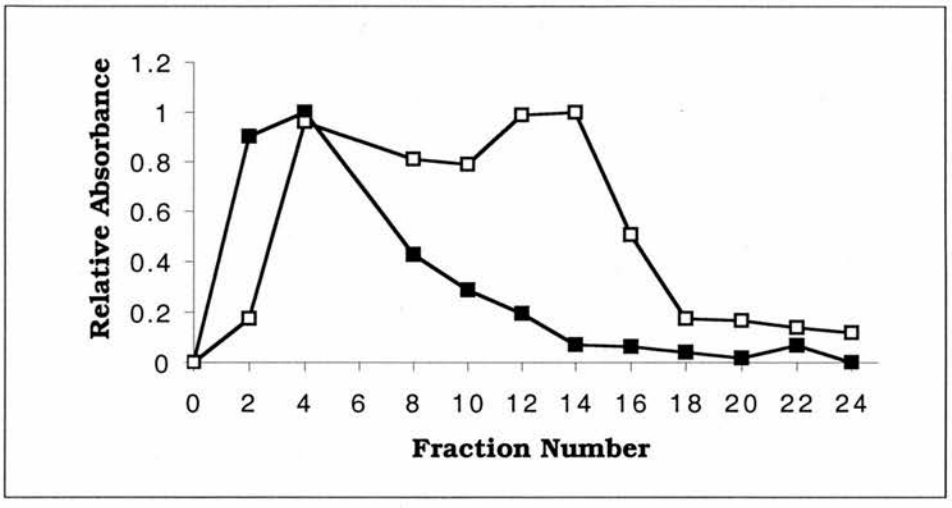

(b)

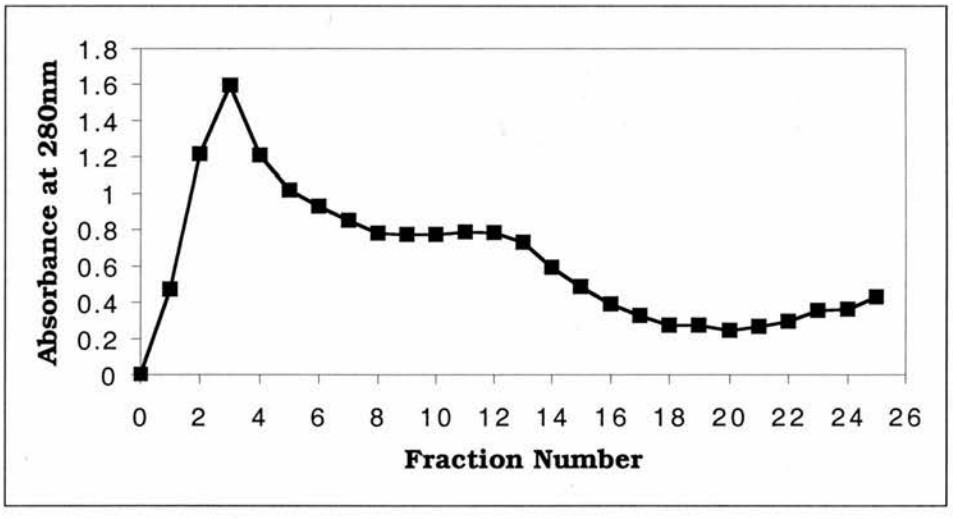

Figure 4.8a Distribution of (a) outer and inner membrane marker enzymes and (b) membrane protein in submitochondrial fractions obtained from fed rainbow trout liver mitochondria after sucrose gradient. Mitochondrial outer and inner membranes and contact sites were prepared and separated on continuous sucrose gradient as described in 2.4.2 (a) Activities of marker enzymes for outer membrane (■) and inner membrane (□) are shown. In (a) the activity of each enzyme in the fraction in which it was most abundant is set at unity and the other values are expressed as relative values. (b) The estimation of amount of membrane protein (measured at A_{280}) in each fraction is given (■).

(a)

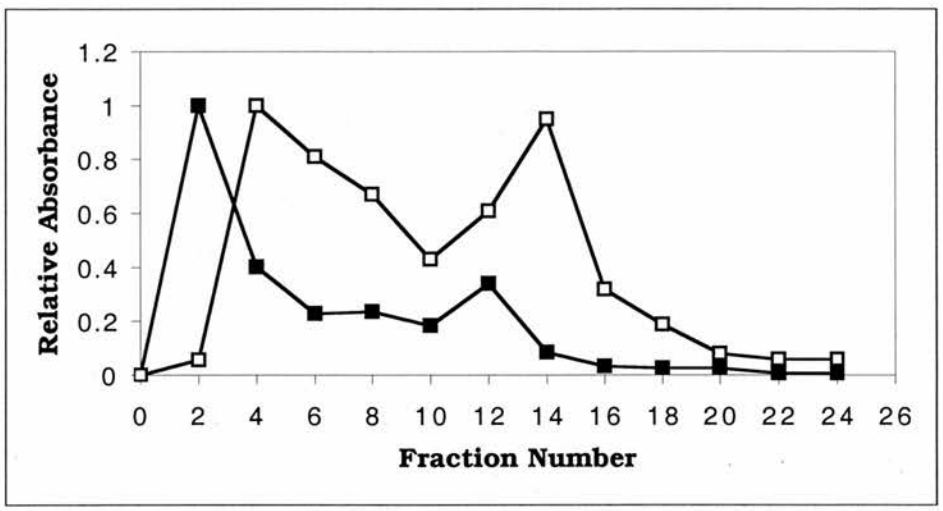

(b)

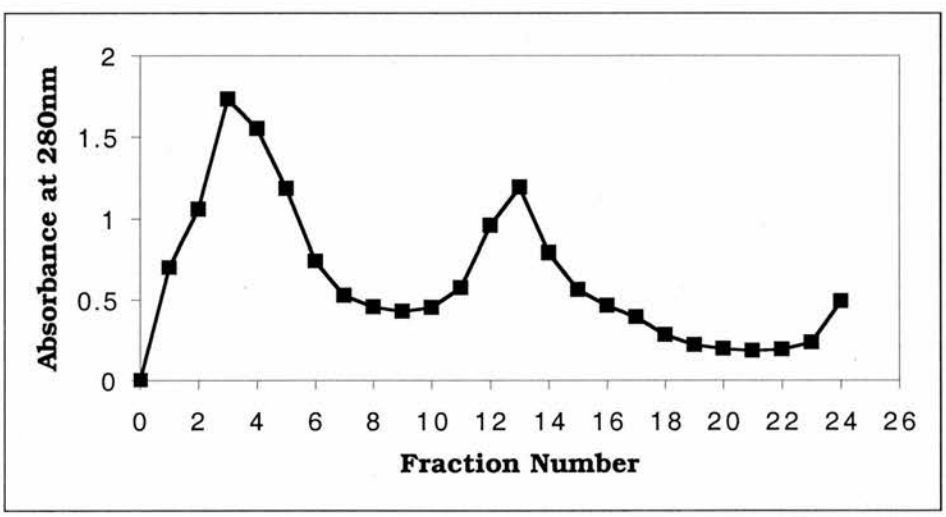

Figure 4.9a Distribution of (a) outer and inner membrane marker enzymes and (b) membrane protein in submitochondrial fractions obtained from fasted rainbow trout liver mitochondria after sucrose gradient. Mitochondrial outer and inner membranes and contact sites were prepared and separated on continuous sucrose gradient as described in 2.4.2 **(a)** Activities of marker enzymes for outer membrane (■) and inner membrane (□) are shown. In (a) the activity of each enzyme in the fraction in which it was most abundant is set at unity and the other values are expressed as relative values. **(b)** The estimation of amount of membrane protein (measured at A_{280}) in each fraction is given (■).

Fractions 1-3 and 12-15 were pooled and concentrated to give the outer and inner membrane fractions. Fractions 5-8 were pooled to give the crude contact site fraction and also to allow for a direct comparison with the contact site fraction in fed fish (4.3.1).

4.3.3 Marker enzyme and CPT distribution

Table 4.3 shows that NADPH cytochrome *c* oxidoreductase activity is highest in the outer membrane and lowest in the inner membrane as would be expected. Cytochrome *c* oxidase is enriched in the inner membrane in both fed and fasted but cross contamination is observed in the outer membrane in both fed and fasted samples.

Distribution of CPT in gradient fractions was not determined but rather its activity and its inhibition by malonyl-CoA was measured in the pooled fractions. CPT1 in fed samples was excluded from analysis (table 4.3) as rates were measured later than the other samples after several months in the freezer and appeared to show no malonyl-CoA sensitivity so the rates measured did not reflect the expected values.

Table 4.4 demonstrates that the specific activity of total CPT and CPT1 is highest in the outer membrane fraction. Its presence in the contact sites is not greater than the outer membrane marker so there is no enrichment there. Malonyl-CoA sensitivity was similar in all fractions, surprisingly even in the inner membrane. It is clear from the activity of the outer membrane marker in the inner membrane fraction that some contamination remains there, perhaps enough to explain this effect of malonyl-CoA on the CPT activity.

	Outer Membrane		Contact site		Inner Membrane	
	fed	**fasted**	**fed**	**fasted**	**fed**	**fasted**
Liver weight (g)						
Protein (mg)	1.84	4.44	1.73	9.58	0.63	1.721
Specific activities (μmol/min/mg)						
NADPH-cyt *c* oxidoreductase	7.69	9	3.54	4.42	3.07	2.30
Cyt *c* oxidase	138	203	251	258	379	610
Specific activities (nmol/min/mg)						
Total CPT	66.10	53.81	11.94	26.2	4.66	5.67
CPT I	-	**35.7**	-	**12.3**	-	**2.82**

Table 4.3 Characteristics of submitochondrial fractions. The total protein in each sample has no relevant meaning since each fraction was pooled for optimum purity rather than recovery. The OM sample was fractions 1-3 from Fig. 4.8a and 4.9a, the CS sample was fractions 5-8 from Fig. 4.8a and 4.9a, and the IM sample was fractions 12-15 from Fig. 4.8a and 4.9a.

SOURCE MATERIAL AND ACTIVITY	Outer membrane	Contact sites	Inner membrane
Rat liver CPT1	1	1.49	0.02
Control trout liver CPT1	1	1.29	0.67
Fasted Trout liver CPT1	1	0.70	0.31
Fasted Trout liver total CPT	1	0.99	0.41

Table 4.4. Comparison of the specific activities of CPT1 in the sub-mitochondrial fractions relative to the outer membrane marker, NADPH-cytochrome *c* reductase. The specific activity of CPT1 was divided by the specific activity of the OM marker for each sample so that changes in the contact site ratio (enrichment of CPT1) could be compared in different preparations. For ease of interpretation, the ratio in the OM is taken as 1 and the other samples expressed relative to that ratio.

Thus, in contrast to the situation in rat (Fraser et al., 2001; Fraser and Zammit, 1998), there is no evidence for the sequestration of CPT1 in the contact sites, nor for a change in malonyl-CoA sensitivity there.

4.4 Discussion

Kolodziej and Zammit (Kolodziej and Zammit, 1990) described a method to isolate rat mitochondria, and subfractionate them into outer membrane, contact site, and inner membrane. Previously it was not known whether this method could be adapted to fish mitochondria and allow the investigation into the location of specific proteins and enzymes contained within the fish mitochondria. The results of this chapter establish that a sub-mitochondrial fraction of fish liver mitochondria have components similar to mammalian mitochondria.

4.4.1 Isolation and subfractionation of mitochondria

After centrifugation through Percoll it was shown that the fish mitochondria could be separated from other cell organelles. With sonication and hypotonic shock the isolated mitochondria could then be subfractionated into outer membrane, contact sites, and inner membrane (fig 4.1). The varying concentrations of NADPH cytochrome *c* oxidoreductase and cytochrome *c* reductase identify both the outer and inner mitochondrial membranes (table 4.1). Mid-fractions of the gradient show a significant presence of both NADPH cytochome *c* oxidoreductase and cytochrome *c* oxidase identifying parts of the mitochondrial membranes that cannot be separated through sonication and hypotonic shock. These fractions indicate that mitochondrial contact sites may be present in rainbow trout. The method used by Kolodziej and Zammit

(Kolodziej and Zammit, 1990) for rat mitochondria can therefore be developed to subfractionate the outer membrane, contact sites and inner membrane of rainbow trout mitochondria.

4.4.2 Analysis of the proteins in each fraction

SDS gel electrophoresis revealed that the pooled outer and inner membrane fractions contain proteins of different molecular weights, reflecting the different membrane proteins and confirming that the fish mitochondria can be fractionated and their membranes separated (fig 4.5). Western blotting (fig 4.7) confirmed the presence of VDAC, a 31.5 kDa molecular weight protein in a mitochondrial fraction. VDAC has been shown in the mammalian system to be located in the outer membrane and enriched in the contact site (Fraser and Zammit, 1998). Western blots could not be performed on the contact site fractions due to lack of sample, therefore it is not possible to conclude that VDAC is exclusively found in the outer membrane or enriched in the contact site.

4.4.3 CPT activity

Overall CPT activity was shown to decrease across the fractions (figure 4.2). There is however, a slight increase in CPT activity in fractions 14-16, which may correspond to the contact site. The CPT I activity was shown to have decreased over these fractions therefore suggesting that this increase in activity could be due to CPT2 activity. CPT1 was shown to be present in all three pooled fractions but not enriched within the contact site (table 4.3) as has been seen in the mammal.

4.4.4 Contact sites

Zammit's group previously showed that the CPT is enriched in the contact sites in the mammalian system and that malonyl-CoA inhibition of CPT in the contact site is competitive allowing long chain acyl-CoAs to overcome malonyl-CoA inhibition and permitting channelling of activated fatty acids into β-oxidation (Fraser et al., 2001). They also demonstrated that CPT is very sensitive to its membrane environment, which may account for the different kinetics. Contact sites in rat also increase during starvation in parallel with the increase in the delivery of activated fatty acids to the mitochondrial matrix in the rat (Blok et al., 1971). If this were also the case in fish then we would have expected to see an enrichment of CPT in contact sites. However in fish this was not observed. We show no enrichment of CPT1 or CPT (malonyl-CoA sensitivity can be lost in fractionation) in the contact sites in fasted fish. Residual contamination after the separation of mitochondrial membranes may have obscured minor change. However, fish are capable of surviving prolonged periods of fasting and we did not find an increase of fatty acid oxidation in response to food withdrawal so perhaps the appropriate conditions for CPT1 enrichment in fish mitochondrial contact sites have not been found.

It may be that upregulation of CPT activity in fish mitochondria does not occur because ketone bodies are not required as extra fuel. Perhaps the competitive inhibition of CPT in rat contact sites is present to allow the rapid fat oxidation required for ketone bodies to be made. Trout do not produce ketone bodies as a source of fuel. In carp, the enzymes to make ketone bodies are present and the only minimally enhanced ketone body production was attributed to the low rates of β-oxidation (Segner et al., 1997). The low rates of oxidation also found in trout liver perhaps means that there is no need for enhanced CPT activity in contact sites.

These results dispute the importance of contact sites in control of flux of fatty acids in the fasted fish metabolising system perhaps signifying that their significance is only in mammals were ketogenesis is upregulated in the fasting state.

4.4.5 Further work

Due to constraints of materials the CPT activity assays were run for only one sucrose density gradient. These assays would need to be repeated to show that the locations of CPT1 and CPT 2 were statistically significant. The location of CPT1 and CPT2 could also be confirmed through the use of more specific antibodies than were available. The association of VDAC and ANT in contact sites also needs to be confirmed for fish and the development of antibodies for these fish proteins would significantly aid this process.

In further investigations of fatty acid metabolism and control within fish, the location of long-chain fatty acyl-CoA (LCAS) and carnitine: acylcarnitine translocator (CACT) should be completed. It has shown in rats that LCAS is enriched within the contact site, but CACT is enriched in the contact site to a much lesser degree (Hoppel et al., 2001). Once research into the location of these two enzymes has been completed a more reliable model could be produced for the control of fatty acid transport across the mitochondria.

For the elucidation of the mPTP structure, further assays could be completed to identify the location of other enzymes such as monoamine oxidase, creatine kinase and hexokinase. 2-Dimensional gels could also be completed for all three samples, (outer membrane, contact site, and inner membrane). Comparisons of these gels

would identify specific proteins that are only present in one or two of the samples. The gels should also be completed over the full pH range to ensure significant proteins are not missed.

In the long term, further investigations could be completed into the role of mitochondria in apoptosis and the role of fatty metabolism may play in apoptosis. Previous work (reviewed by (Tatton and Olanow, 1999) has shown that different proteins are present when the pore is closed compared to when it is open.

4.4.6 Conclusions

It has been possible using methods developed for rats to isolate and subfractionate rainbow trout mitochondria into outer membrane, contact sites and inner membrane (albeit with some cross contamination). It is concluded malonyl-CoA sensitive CPT activity (CPT1) is not enriched within the contact sites of mitochondria in trout. The location of CPT1 may be because of the unique microenvironment found in the contact site. Previous research has shown that the contact site is rich in the phospholipid cardiolipin and that cardiolipin dramatically increases malonyl-CoA sensitivity (Mynatt et al., 1994). The composition of phospholipids in the contact site may help maintain the positioning of the N-terminal domain of CPT1 that is critical in malonyl-CoA inhibition. With further research into the location of other enzymes involved in the fatty acid oxidation a detailed model of the control of fatty acid oxidation across the mitochondrial membrane in fish could be elucidated.

Chapter 5

PURIFICATION AND PROPERTIES OF CARNITINE OCTANOYLTRANSFERASE FROM RAINBOW TROUT LIVER

5.1 Introduction and aims

Carnitine acyltransferases represent a group of enzymes that are important in the regulation of fatty acid oxidation. Carnitine octanoyltransferase (COT) is found in peroxisomes and has been purified and characterised from mammalian systems (Farrell et al., 1984; Miyazawa et al., 1983; Ramsay, 1988). Several mammalian COT were cloned, sequenced, and heterologously expressed (Choi et al., 1995; Cronin, 1997a; Ferdinandusse et al., 1999). A major role of peroxisomal fatty acid oxidation is to chain shorten longer chain fatty acids that are poor substrates for the mitochondrial oxidising system. The role of COT is to transfer the chain shortened acyl-CoA product to carnitine for export to mitochondria. There is no data available for this enzyme in fish and yet the marine diet is rich in long chain fatty acids so the enzyme may have a more significant role in fish than its mammalian counterpart.

The aim of this chapter is to purify and characterise COT from rainbow trout liver with a view to understanding its significance in the fish metabolic system.

5.2 Results

5.2.1 Purification of COT

COT was released from frozen rainbow trout liver by water extraction. The ease of its release is consistent with the peroxisomal matrix location established in beef (Ramsay

et al., 1987) and it remained quite stable during the purification at 4°C. Several purification methods were attempted (data not shown) in order to optimise the yield of COT. The purification procedure and subsequent data given in this chapter resulted in the purest COT preparation that was achieved from several methods attempted.

Rainbow trout liver was vigorously homogenized and sonicated and the proteins fractionated by ammonium sulphate precipitation. The fraction that contained COT activity was collected and then applied to a DEAE-cellulose column. Figure 5.1a shows the chromatographic profile. The fractions containing COT were pooled and dialyzed, then subjected to a Blue Sepharose CL-6B column (Fig 5.1b). The active fractions eluted by the salt gradient were collected, dialysed, and further purified by a small Blue Sepharose CL-6B column. After washing with 20 mM potassium phosphate containing 50 mM KCl, purified COT was affinity-eluted using octanoyl-CoA (10 mg/100ml, Fig 5.1c).

The results of purification procedures are presented in table 5.1. By comparing the specific activities of the impure supernatant fraction and pure enzyme, it can be shown that a 3180-fold purification was achieved. The enzyme had no impurities detectable by SDS/polyacrylamide-gel electrophoresis (Fig 5.2, lane 1 and 2). A single band was identified with a molecular weight of approximately 66 KDa similar to the molecular weight of COT found in mammalian species (Miyazawa et al., 1983)

A

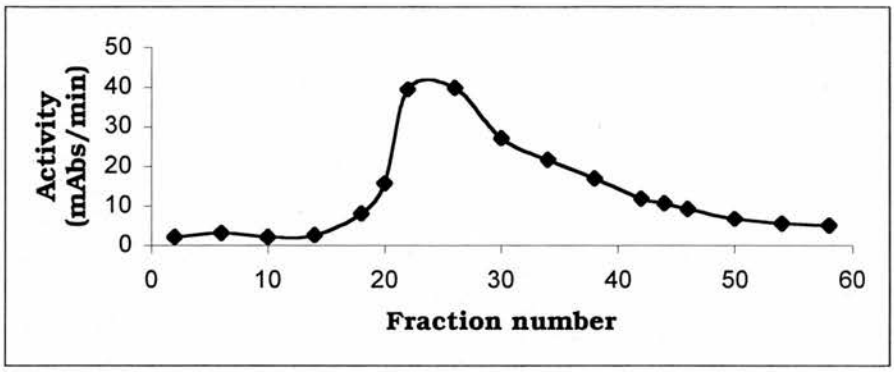

B

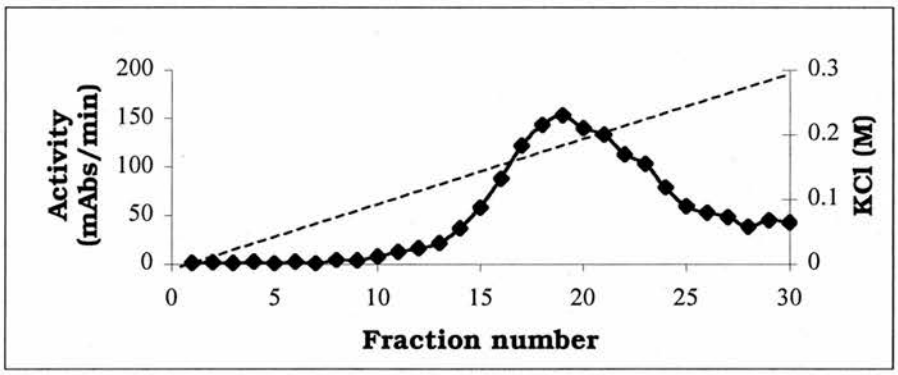

C

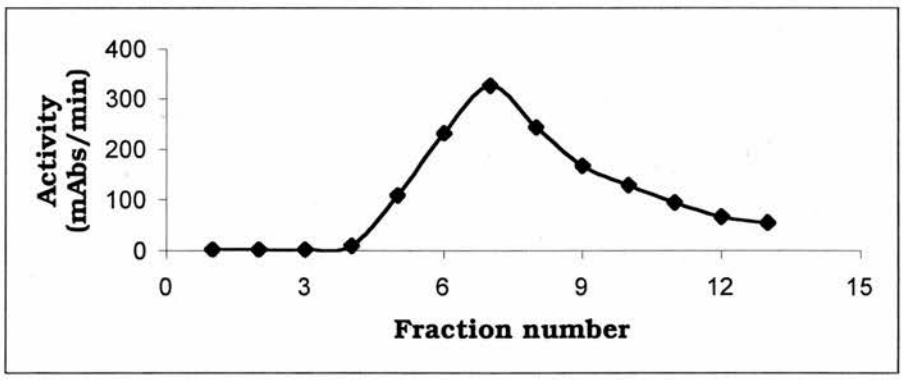

Figure 5.1. Elution profiles for chromatographic purification of COT from rainbow trout liver. The detailed experimental procedures are described in Materials and Methods 2.5. The liver was homogenized and the proteins were fractionated by ammonium sulphate precipitation. The fraction containing COT was applied to a DEAE cellulose column (**A**). Fractions containing COT activity were pooled and subjected to a Blue Sepharose CL-6B column and eluted with the salt gradient (profile shown as a dashed line, right hand y-axis) (**B**). The active fractions were collected and applied to a small blue CL-6B column. Pure COT was affinity eluted with octanoyl-CoA (**C**).

Table 5.1 Purification of COT from rainbow trout liver

Step	Protein (mg)	Total Activity (units)	Specific Activity (units/mg)	Yield (%)
Acid supernatant	1700	3600	0.002	100
Dialysed after AS cut	702	3771	0.005	104
DEAE-cellulose	13.6	3567	0.263	99
Large Blue Sepharose	4.2	4312	1.02	119
Affinity elution	0.1	692	6.36	19

The purification was performed as described in chapter 2.5. The starting material was 22g of liver. The protein was measured by the Peterson-Lowry method. The definition of activity unit (U) is μmol (product)/min using decanoyl CoA transferase as substrate measured at 324nm. Abbreviations: AS- Ammonium sulphate.

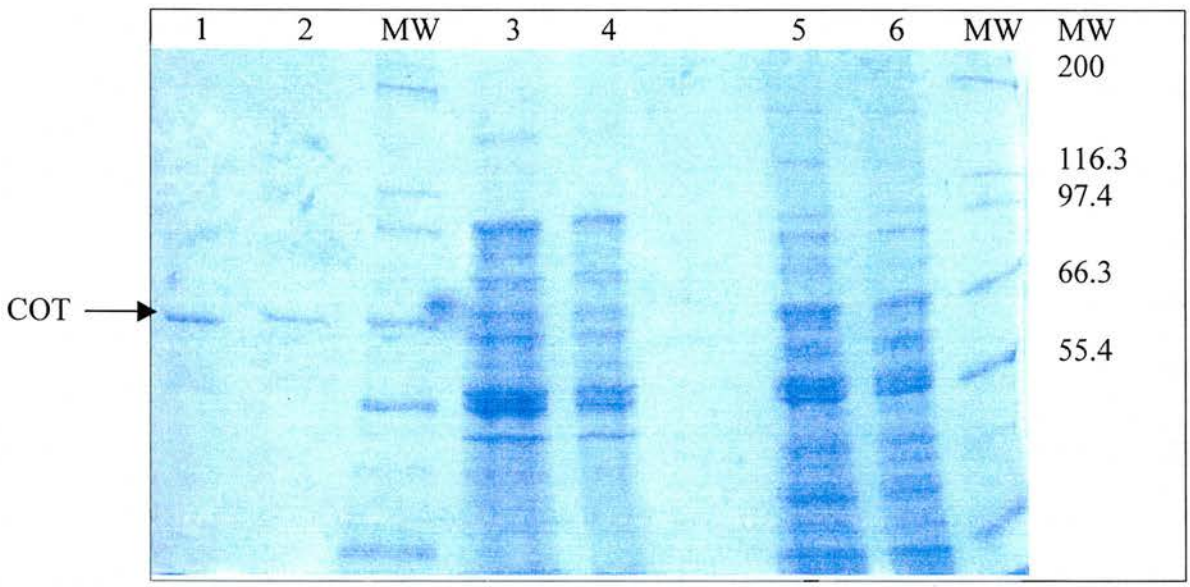

Fig 5.2 SDS/polyacrylamide-gel electrophoresis of COT during and after its purification from rainbow trout liver. MW – protein markers; track 1and 2: 1.8 and 1μg of purified enzyme after affinity elution; tracks 3 and 4: 5 and 2μg of pooled fractions after salt elution from the large Blue Sepharose column; tracks 5 and 6: 4 and 2μg of pooled fractions after DEAE-cellulose step.

5.2.1.1 Protein sequencing of purified COT

The band obtained on SDS-PAGE appeared as a doublet when run again for submission for mass spectrometric analysis. The upper band shared eight peptides in common with bovine COT by MALDI mass fingerprinting, the lower only six. High scoring hits for the lower band included (after COT) several matches with glutaminyl-tRNA synthase (61,700 daltons) from Salmo and *E. coli* but with only three peptide matches. This band is not further considered.

The upper band resulted in matches with COT from cow, rat, human and mouse. MALDI gave two peptides identical with bovine COT and MS/MS confirmed these. One is in the sequence obtained for trout COT in Chapter 6 and one in the part for which the sequence has not yet been deduced. Three other peptides give good MS/MS data and the remaining three reasonable data, so we can make deductions from these peptides with reasonable confidence. The peptides, detailed in Table 5.2, confirm the identity of the trout protein analysed as a COT as expected from its activity, confirm part of the sequence obtained by cDNA sequencing, and give some of the sequence lacking from the molecular biology approach.

Both MALDI and MS/MS suggest that peptide 6 corresponding to 228-247 of the bovine sequence is identical to the bovine peptide. Another two peptides (no. 7 and no.8 in Table 5.2) were also identified as the same as the bovine peptides but these differ from the deduced sequence for trout as obtained in Chapter 6. Further analysis would be required to resolve these differences.

In the section for which a deduced sequence is not available, the peptide 1 corresponding to 13-34 of the bovine sequence indicates that the trout COT is not truncated, but is likely to be of similar length to bovine COT as is the deduced sequence for pufferfish COT. Peptides 1-5 in Table 5.2 cover 34% of the missing part of the trout sequence.

The mass spectral data for the isolated trout COT protein confirm the identification of the trout activity with the sequence obtained by cloning. Further work with new primers is now required to complete the sequence (see Chapter 6).

Table 5.2. Sequence data from MS analysis of trout COT protein

Peptide	Bovine residues	Sequence from trout COT *(deduced in red)*
1	13-34	TFQ YQDSL PSLPV PSLEE SLKK
2	50-69	NTEAI VQKFQ NGIGE KLQQK
3	118-141	EGT QLERG SISLW HNLNY WQLLR K
4	149-160	VG NTPLD MNQFR
5	174-181	DS IINYF R
5b	182-197	TE SEGHS PSHLA VLCR
6	228-247	CHS EPDGP GVAAL TTEER TR *GVAAL TSEER TR*
6b	254-282	YLISL NPENL TILEK IQSSL LVFCL DDDS *YLIGI DPANK TILET IQSSL FVVSL DDAK*
7	359-375	VR DIPVD EELVF TVDEK *VR PMPLP EELVF TVDDR*
8	481-489	HMMLE AFAK *KALLL AFNK*

5.2.2 Kinetic characterisation

The kinetics of the trout liver COT activity with respect to its substrates, carnitine and acyl-CoA were determined with the use of purified and partially purified COT. The enzyme obeyed Michaelis-Menton kinetics in the forward reaction and representative data is shown in figure 5.3.

5.2.2.1 Substrate specificity

Apparent Michaelis constants of the enzyme for several substrates (C_4-C_{18} acyl-CoA) are summarised in table 5.3 and figure 5.4. The pattern of the apparent constants is similar to those of the beef liver enzyme (Derrick and Ramsay, 1989). The lowest K_m occurs at a long chain length (C_{16}). The K_m values for all the acyl-CoA derivatives are low, indicating that all chain lengths from C_4 up will compete for the enzyme. It would be interesting to see if this trend continued but unfortunately time restraints prevented these experiments from being carried out. Clearly this enzyme is not an octanoyltransferase as found in mouse.

It is difficult to measure the rates in the assays with low acyl-CoA concentrations (below 5 μM). Since the K_m for most of the acyl-CoAs is so low, the total absorbance change for these concentrations is very small. Only a linear and short range of absorbance change with the time graph (<10% of total change) at the beginning of the reaction should be used to determine the reaction rate. These errors in low acyl-CoA concentration assays can be verified by observation of the $V_{max\ (app)}$ values (fig 5.3a). For palmitoyl-CoA concentration at 2.5μM, the $V_{max\ (app)}$ value is somewhat less than the value for the remaining assays. There is some variability in the K_m for L-carnitine

(table 5.3) which again is similar to bovine COT (108 μM in (Nic a'Bhaird et al., 1993) but largely the K_m is unaffected by the chain length of the acyl-CoA substrate.

(a)

[Pal-CoA] (μM)	K_m (Cn) (μM)	V_{max} app (Abs/min)	[S]/V_{max}
2.5	47.11	0.007644	327.1
5	64.6	0.009912	504.4
7.5	51.9	0.009811	764.4
10	46.87	0.01009	991.1
15	47.44	0.01028	1459.1

(b)

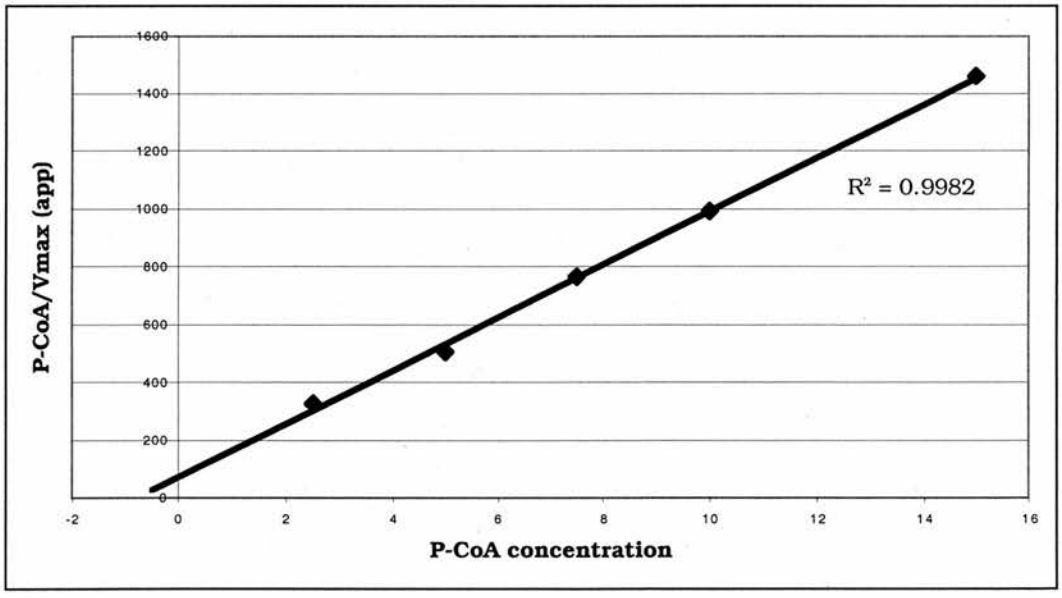

Figure 5.3 Kinetic characterisation of COT purified from trout liver (a) Kinetics parameters obtained by Shimadzu UV2401PC software using the Hanes plots. At each fixed concentrations of palmitoyl-CoA, the L-carnitine concentration was raised from 50 to 500μM **(b)** Secondary plot of [S]/$V_{max\ (app)}$ against [S] to determine the K_m of COT for palmitoyl-CoA. Assay details are described in Chapter 2.1.3.1.

Table 5.3. Apparent kinetic constants for COT assayed in the forward reaction

Carbons	Km (acyl-CoA) μM	Vmax μmol/min/mg	App Km (carnitine) μM
4	3.15	10.80	
6	3.32	10.20	
8	3.63	9.30	55.8
10	1.075	9.91	94.4
12	1.06	10.30	
14	0.68	8.82	63.2
16	0.625	8.45	54.8
18	0.65	8.24	

The assay was carried out as described in 2.1.3. The value was obtained by changing one of the substrates at a saturating fixed concentration of the other. Substrate concentrations were between 2.5-35μM for acyl-CoAs and 50-500μM for L-carnitine. Carbon chain lengths of the acyl-CoAs are expressed by C_4-C_{18}. The values for carnitine come from single experiments using various partially purified preparations.

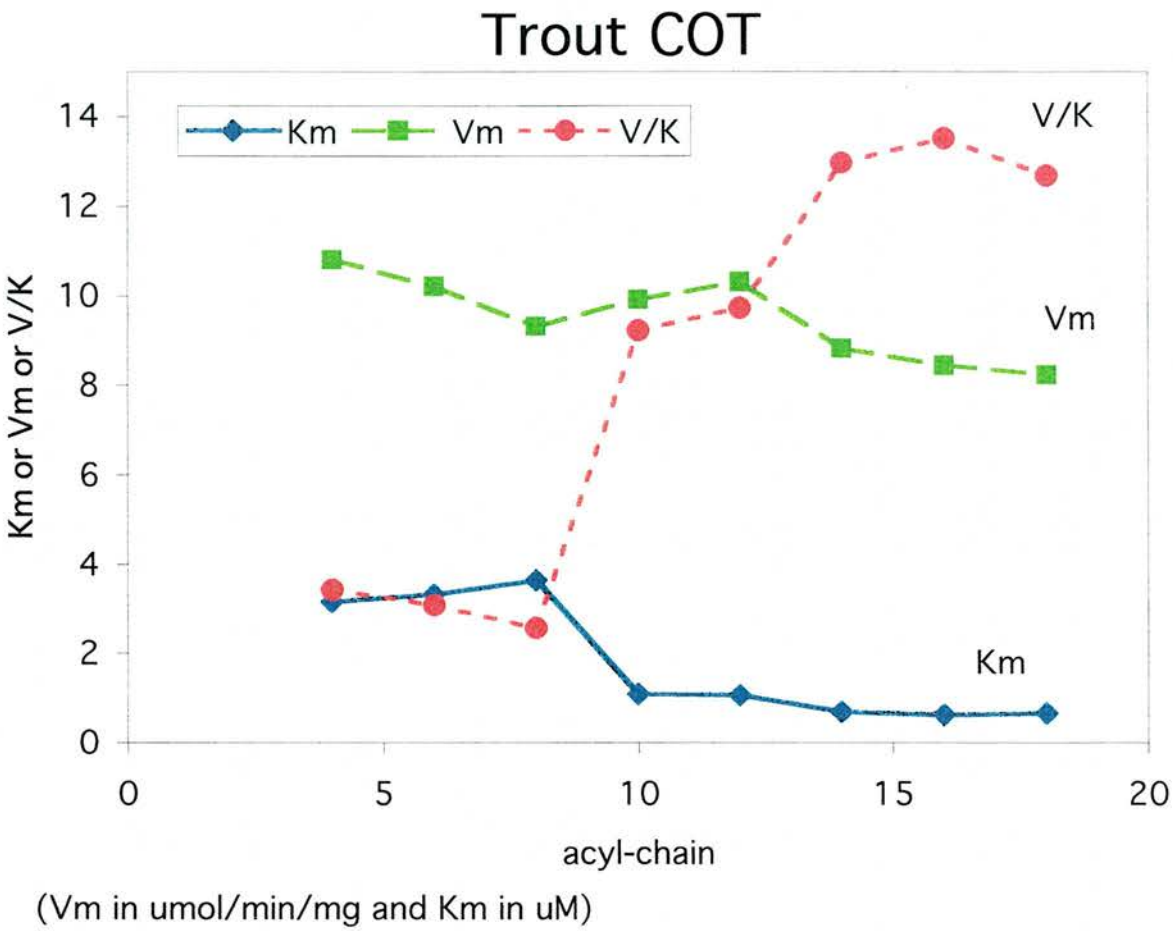

Fig 5.4 Plot of data represented in table 5.3.

5.2.2.2 Sensitivity to malonyl-CoA

The inhibition of the CPT activity by malonyl-CoA is a key mechanism for the regulation of fatty acid oxidation in mitochondria. Studies on bovine COT (Nic a'Bhaird and Ramsay, 1992) demonstrated that purified COT is subject only to competitive malonyl-CoA inhibition.

Figure 5.4 shows that rainbow trout COT was slightly inhibited by malonyl-CoA when palmitoyl-CoA (in the presence of BSA) was used as substrate. Inhibition was observed with 20μM malonyl-CoA and the maximal suppression effect was obtained with 100-200 μM. This inhibition is seen at 50 μM palmitoyl CoA (in the presence of 1.3mg/mL BSA) and 2mM L-carnitine both of which are saturating (100 times K_m and 80 times V_{max}, respectively) so the observed inhibition is not competitive with either substrate.

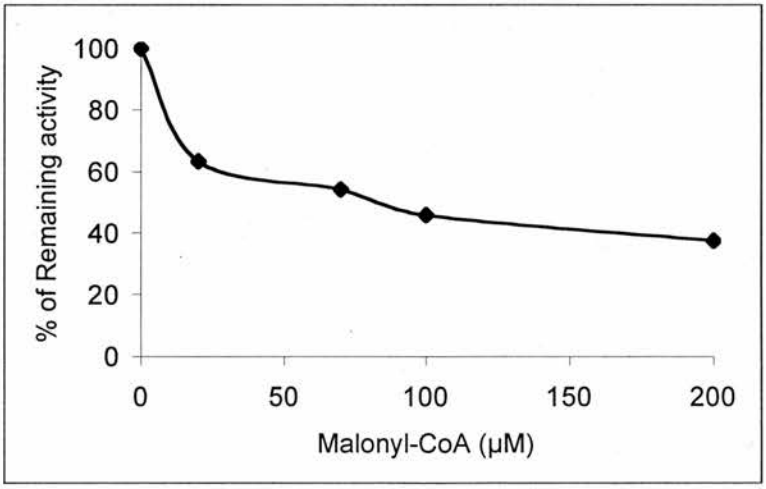

Figure 5.5. Effect of malonyl-CoA on rainbow trout liver COT. The enzyme activity was assayed in the presence of various amounts of malonyl-CoA as described in 2.1.3. The substrates were 50 μM palmitoyl-CoA (in the presence of 1.3mg/mL BSA) and 2mM L-carnitine.

5.3 Conclusions

COT has been purified from livers of several mammalian species including mouse (Farrell et al., 1984), rat (Miyazawa et al., 1983) and cow (Ramsay, 1988). The results here are the first data in the characterization of this enzyme in fish. Trout liver COT shows kinetic values comparable with those observed for beef liver COT. Inhibition of trout COT by malonyl-CoA appears to be only partial as also seen in rat COT (Morillas et al., 2000). When purified rat and human COT were investigated for malonyl-coA sensitivity, it was found (Sitheswaran et al, unpublished) that only competitive inhibition was observed as in beef liver COT (Nic a'Bhaird and Ramsay, 1992) unless bovine serum albumin was present. It is thus likely that the partial inhibition effect observed here is similarly an artefact of the assay system, so it can be concluded that trout COT is not sensitive to regulation by malonyl-CoA.

The yield of COT purified from trout liver tissue was relatively low (20%). Therefore, it would be helpful to clone, express and modify the trout COT gene in order to explore further its structure-function relationships.

CHAPTER 6

SEQUENCING COT FROM RAINBOW TROUT

6.1 Background

Carnitine octanoyltransferase (COT) belongs to a group of enzymes that catalyse the reversible transfer of fatty acyl groups from CoA to L-carnitine. COT facilitates the transport of medium chain fatty acids through the peroxisome membrane and determines the chain length at which the incompletely oxidised fatty acyl-CoA is transported to the mitochondria for further oxidation. The substrate specificity for this enzyme varies widely between the mammalian species with no apparent molecular basis. Understanding of the role of specific amino acid residues involved in substrate specificity, catalytic activity and malonyl-CoA sensitivity is hampered by the high sequence conservation observed in mammalian COT. Therefore the aim of this chapter was to sequence COT from rainbow trout cDNA to improve knowledge of this enzyme in fish and also to compare the sequence with its mammalian counterpart with the aim of finding differences in conserved residues that may be more apparent in a lower vertebrate.

6.2 Database searching for trout EST sequences

We searched for COT like sequences within the expressed sequence tag (EST) and genomic sequence data available for a number of model organisms. Bovine COT amino acid sequence data was used as a guide for obtaining cDNA sequences encoding the rainbow trout homologue. The program tblastn was utilised to search using these amino acid sequences versus nucleotide sequences.

Several trout cDNA clones with high homology were in dbEST (the EST database), and these were also catalogued in The Institute of Genome Research (TIGR) *Oncorhynchus mykiss* Gene Index (RtGI; www.tigr.org). In total, three overlapping sequences were identified, two of which originated from the opposite ends of the same clone insert. Both COT clones were derived from the same pooled tissue cDNA library. The assembled trout EST sequences are shown in fig 6.1. Assembly of the three overlapping clones was achieved with the aid of Lasergen Seqman software (DNAstar). In the case of sequence BX862965, the original trace data was kindly provided by Yann Guignen, (INRA, Rennes, France), so we could be reasonably certain of the sequence to which we subsequently designed PCR primers.

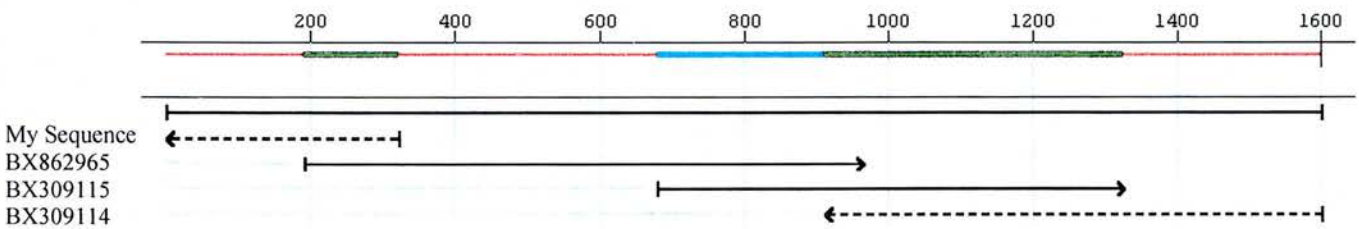

Fig 6.1 Assembly of the available trout EST sequence as (drawn to scale) together with new 5' sequence. Arrows indicate directions of sequencing. BX309114 and BX309115 correspond to the 3' and 5' sequences, respectively, from the same clone. New 5' sequence is discussed in 6.4.2.2

6.3 Design of primers

The known nucleotide sequences of the cDNA retrieved from the EST database were used to design gene specific oligonucleotide primers. Reverse primers were designed firstly to amplify COT from a trout head kidney lambda library (a gift from Aberdeen University); using forward primers based on the lambda vector arms.

Secondly, primers were designed to complement a sequencing speed-up kit obtained from Seegene, Inc. The DNA walking *SpeedUp*™ kit is directed to the method using

the DNA Walking ACP (DW-ACP) primer designed to capture unknown target sites using the optimised PCR conditions (referred to as DW ACP- PCR™ technology, fig 6.2). The DW-ACP primer system aims to obtain only genuine unknown target products up to the length (up to 2 kb) of which *Taq* polymerase is able to synthesize. This method provides a way to directly amplify unknown sequences adjacent to known sequences (fig 6.2a). We designed primers TSP1, TSP2 and TSP3 (see table 6.1 for sequence data) to complement the primers provided in the kit. We designed primers that would amplify an internal region of the original amplified product (nested PCR), which helps increase specificity and sensitivity by reducing non-specific products (fig 6.2b). All primers used are listed in table 6.1 and their position on the nucleotide sequence is shown in fig 6.6.

Step	Orientation	Sequence
1. Lambda S	Forward	GCGCGTTGGCCGATTCATTA
2. Lambda S2	Forward	AGGCACCCCAGGCTTTACACTTTATG
3. Lambda S3	Forward	ACGCCAAGCTCGAAATTAACCCTCAC
4. Om COT A1	Backward	GTTACCGCCCCCGCCACTCT
5. Om COT A2	Backward	GTACAGGGCCTCATGGTCTCAGTCC
6. Om COT A3	Backward	TACCGCCCCCGCCACTCTTG
7. Om COT TSP1	Backward	GCATAGGCCGCACCGTCTCA
8. Om COT TSP2	Backward	GAGCCCTTCCACTTGCCGTCTGTAG
9. Om COT TSP3	Backward	CGTAGGGGGCATGGTCACAA
10. Om COT TSP4	Backward	TCAGCGAAGGAGAGGGAGTTGTAGGA
11. Om COT S control	Forward	TCTACCACGGCAGGACTGAGACCAT
12. Om COT S control2	Forward	CGGGGTTGTCTCGGGGGTAGGT
13. Om COT S control3	Forward	GCGCTGACAGGAGACCCCACCAT

Table 6.1 Oligonucleotide primers used for rainbow trout COT cDNA cloning.

(a)

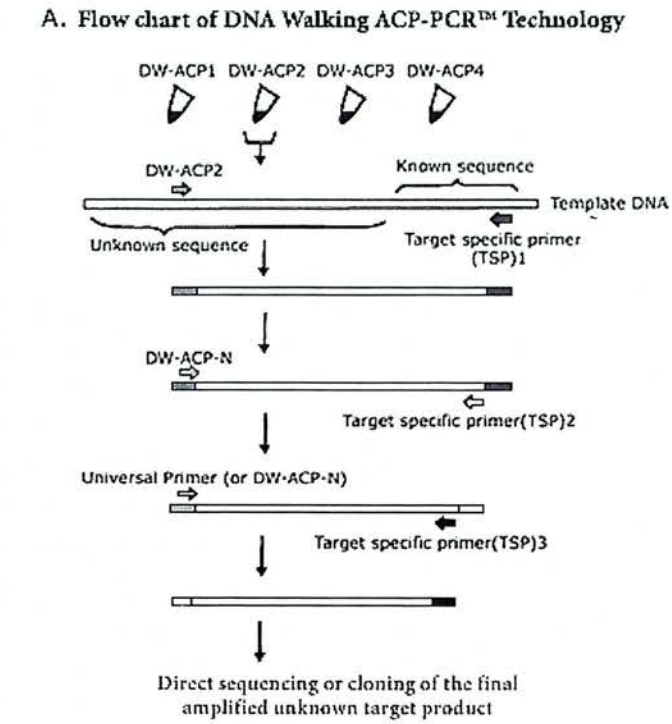

(b)

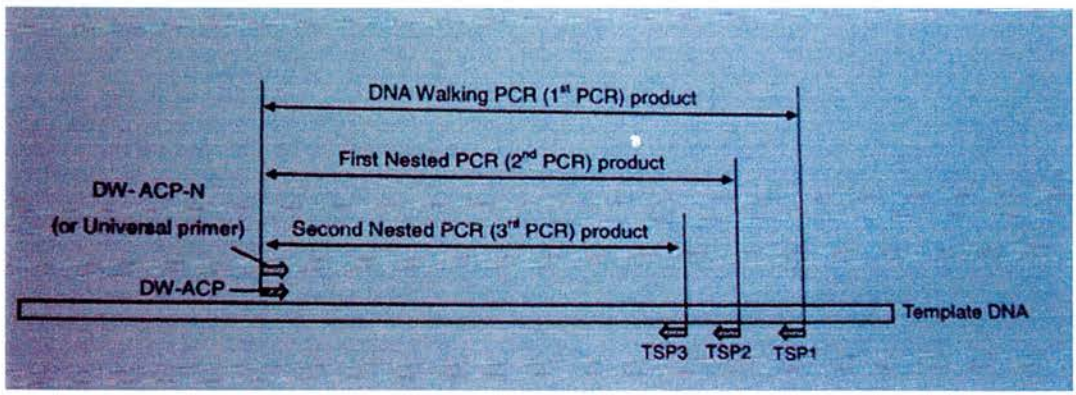

Figure 6.2 (a) Flow chart of the general DNA walking ACP-PCR™ Technology. DW-ACP and TSP denote **D**NA **W**alking-**A**nnealing **C**ontrol **P**rimer and **T**arget **S**pecific **P**rimer, respectively. **(b)**. Primer design: the spotted arrows indicate target specific primers (TSPs). Nested primers are designed to amplify an internal region of the original amplified product. The TSP2 and TSP3 indicate nested primers (Source: WWW.see-gene.com)

6.4 Cloning of rainbow trout COT

6.4.1 PCR amplification using cDNA Lambda library from a rainbow trout head kidney.

Dr Chris Good from the University of Aberdeen provided a cDNA lambda library of rainbow trout head kidney. Control experiments were performed to ensure that the target sequence could be found in the library. Control primer sets (numbers 6 and 11 from table 6.1) were designed to amplify a partial sequence of approximately 300bp and as can be seen in figure 6.3 the primers have successfully amplified a sequence of that length. Despite this, further 5' sequence was not obtained from this library. Six primer pairs were tested (primer no 1-6, where primers 1-3 were derived from the lambda vector, table 6.1) using the PCR amplification method described in 2.6.3.1. Although a rough estimate of product size was available based on COT sequences from other species, smaller products could also have yielded useful novel sequence. Only one primer set produced a product after PCR amplification. However, this product was cloned and its sequence was found to be unrelated to that of COT (data not shown), and this approach was discontinued. Although the control PCR shows at least partial COT cDNA(s) to be present in the library, here the template could have been a pool of several clones with different discrete amounts of 5' sequence upstream of the priming sites. Low abundance of clones of any one length, together with predicted lower efficiency of the primer pairs used may have explained the failure of this approach. It is also possible that the cDNAs present in this oligo (dT) primed library were 5' truncated due to premature termination of the reverse-transcriptase reaction, such that not much sequence was present upstream of the control primer region. Very short PCR products (less than approximately. 300 bp) were not characterised, as these could not possibly have provided novel sequence.

6.4.2 Rainbow trout liver and gill cDNA

Dr Stéphanie Gutières (INRA-IFREMER, Saint-Pee-Sur-Nivelle, France) very kindly provided us with cDNA from rainbow trout gill and liver. Control PCR amplification was run using primer sets 8 and 13 (as numbered in table 6.1). Primer 13 was designed to be optimal for use in subsequent cloning attempts (see below), and primer 8 was chosen to form an optimal pairing. (These primers were designed after new trout EST became available in dbEST). PCR components and conditions are as described in 2.6.3.1. It is quite apparent that one of the reasons we were not successful using the DNA lambda library is that the presence of the COT like sequence is weak when compared to the presence of COT in the rainbow trout liver and gill cDNA (fig 6.4).

6.4.2.1 PCR amplification with liver cDNA

Firstly, experiments were conducted using rainbow trout liver cDNA. Three target specific primers (TSP1, 2 and 3) were designed to amplify unknown target sequences adjacent to the known sequences (see table 6.1 for primer sequence data). The strategy of the kit is outlined in figure 6.2 and described in 6.3. The kit was followed according to the manufacturer's instructions (protocol available at www.seegene.com). The first PCR reaction was performed using DW-ACPs and TSP1 primer as described in section 5A of the protocol. In the second and third PCR reactions DW-ACP-N and TSP2, and the universal primer and TSP3 were used as described in 5B and C, respectively.

Unfortunately we were not successful in obtaining any major PCR products using trout liver cDNA. One band of potential interest (visible by agarose gel electrophoresis), which was a product of the second PCR reaction was not amplified

when tested with control primers (data not shown), and thus could not be related to COT.

6.4.2.2 PCR amplification with gill cDNA

The kit was used again in an attempt to amplify unknown sequences but trout gill cDNA was used as the template instead of trout liver cDNA. The protocol was followed in much the same way as before, with minor adjustments. Primer TSP4 was designed to optimise the specificity towards the COT nucleotide sequence. Other changes are described in the following text, which describes the three reactions involved in the protocol.

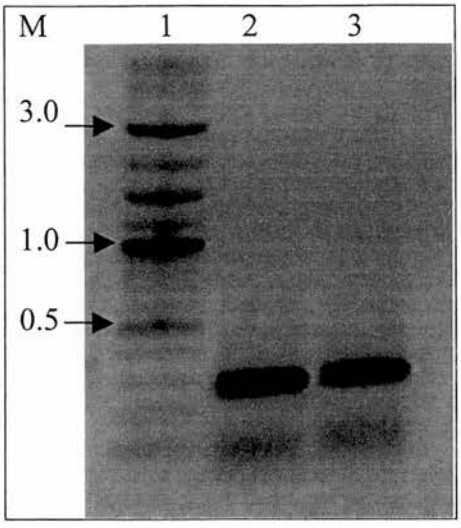

Fig 6.3 Band pattern obtained by PCR amplification using rainbow trout head kidney lambda library as template. PCR products were obtained using the primer set Om COT S control 3 and Lambda S. (see table 6.1 for details of the primers). Lane 1: molecular DNA markers (kilobases); lane 2: rainbow head kidney lambda library (-DMS0) lane 2: rainbow head kidney lambda library (+DMS0).

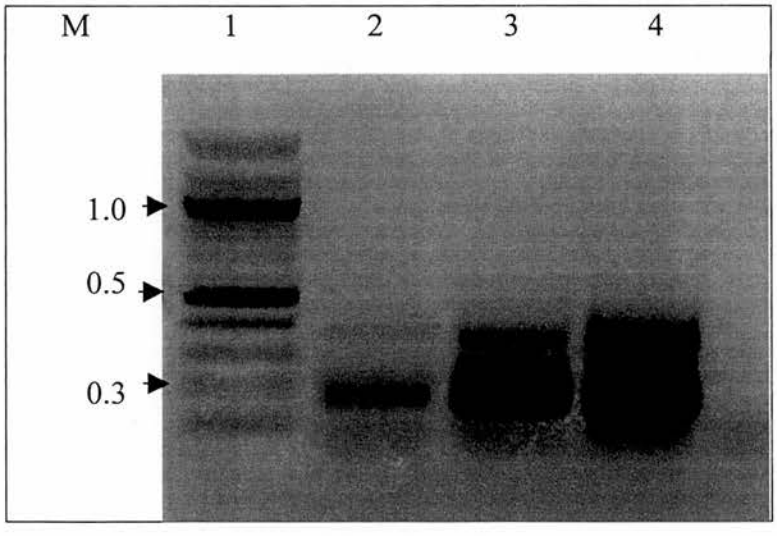

Fig 6.4. Band pattern obtained after control PCR amplification using rainbow trout cDNAs and head kidney lambda DNA as templates. PCR products were obtained using primer sets Om COT TSP2 and Om COT S control 3 (see table 6.1 for details of the primers). Lane 1: molecular DNA markers (kilobases); lane 2: trout head kidney lambda library; lane 3: rainbow trout liver cDNA; lane 4: rainbow trout gill cDNA.

6.4.2.2.1 First PCR reaction

The first PCR amplification involves four individual reactions using primers DW-ACP 1, 2, 3 and 4 (provided by the manufacturer) combined each with the primer TSP1. After the PCR reaction the four separate products were purified to remove primers using the Wizard® Plus PCR purification Kit (Promega).

6.4.2.2.2 Second PCR reaction

The second PCR amplification involved nested PCR. PCR products from the first reaction were used as the template. Four individual experiments were set up and each used primer DW-ACP-N (provided by the manufacturer) and TSP4 (designed by the experimenter). PCR products were analysed using agarose gel (1.5%) electrophoresis (fig 6.4). Two major PCR products were identified (3(A) and 4(A)). These bands were excised from the gel and purified using the Wizard® Plus DNA Gel Extraction Kit (Promega).

6.4.2.2.3 Third PCR reaction

The final PCR reaction again involved nested PCR and we used this reaction to amplify further the two products we had obtained in the second PCR reaction. 3(A) and 4(A) were used as the template and amplification was performed using the Universal primer (provided by the manufacturer) and TSP4. We achieved increased amplification for both fragments (fig 6.5); however a second band was amplified with fragment 4(A), so this fragment was not considered for cloning. Fragment 3(A) was excised, purified and subcloned into pGEM-T Easy vector (Promega) as described in 2.6.5. We were able to obtain plasmids containing 3(A), detectable after *Eco*R I

digestion (see 2.6.8 for digestion procedures). This plasmid was purified and sent for sequencing of the insert. The fragment obtained was relatively short (126 bp) however it did provide new sequence data that was aligned with the original sequence using Seqman (fig 6.6). Its position in relation to the assembled trout EST sequences is shown in fig 6.1.

6.5 Analysis of sequence

The nucleotide sequence and deduced protein sequence are shown in figure 6.7. We successfully obtained a partial sequence of 1592 bp, which predicts a primary translation of 374 amino acid residues. The number of amino acid residues in mammalian COT is 612, so approximately 238 residues are missing from the trout COT sequence in addition to the 5' untranslated region. The extreme 5' end nucleotide sequence (approx 74 nucleotides) as shown in fig 6.7 is clearly not COT derived and does not compare with any data available for COT-like sequences, therefore the sequence is more likely to be an artefact due to the methodology used by the amplification technique, although it was not the sequence of the forward primer.

(a)

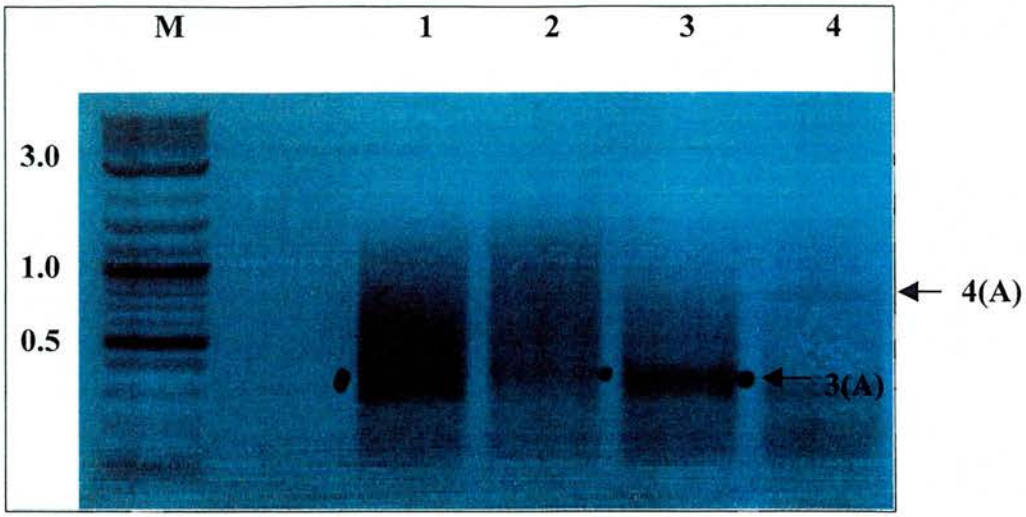

(b)

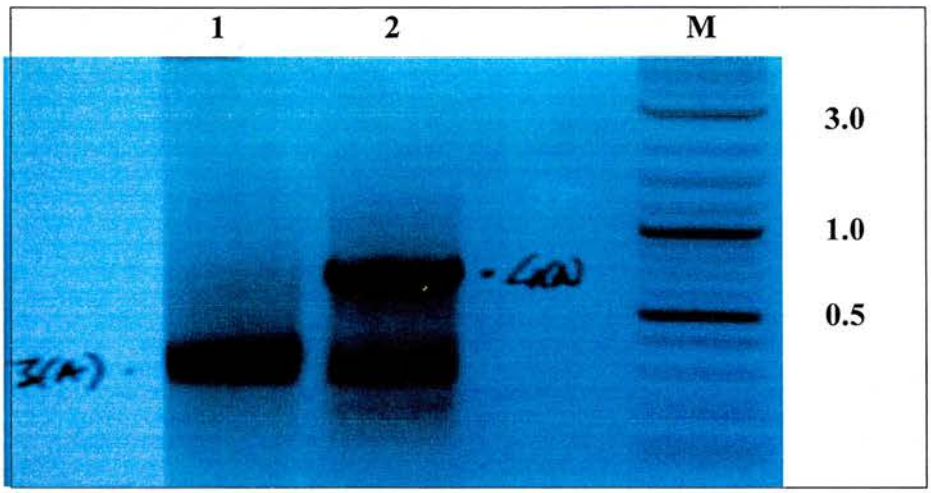

Fig 6.5 Band pattern obtained after 2nd and 3rd PCR reactions. (a) The See-gene speed up kit protocol was followed as described in 6.4.2.2.2. Templates used were the PCR products originating from the first PCR reaction (6.4.2.2.1). PCR products are highlighted with black dots. 3(A) and 4(A) (as designated in the figure) were excised and purified for use in further experiments. Lane 1-4: products originating from DW-ACP 1, 2, 3 and 4 respectively; M: molecular DNA markers (kilobases) **(b)** Products from the 2nd PCR reaction were amplified as described in 6.4.2.2.3.

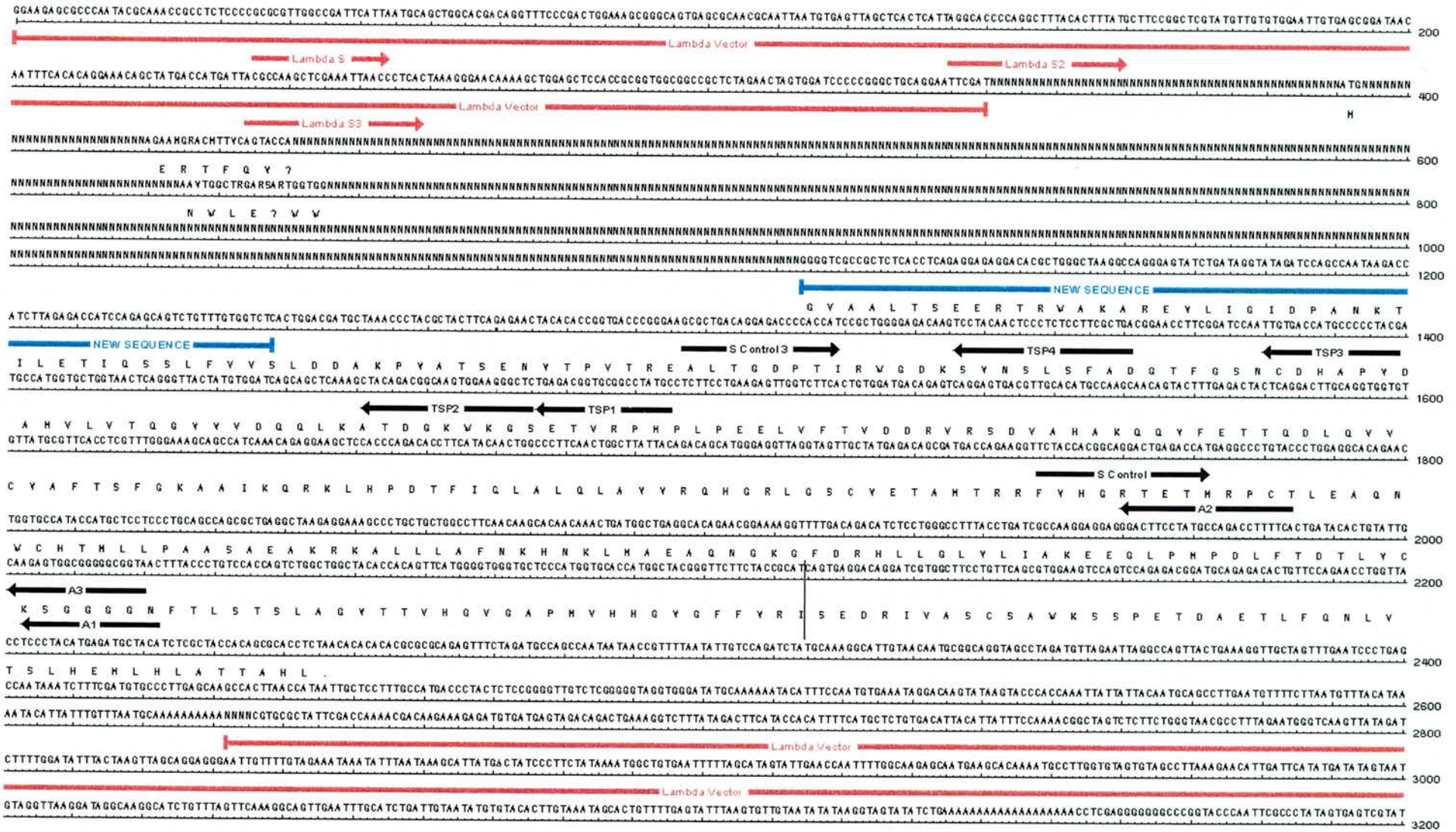

Fig 6.6 Theoretical full-length COT cDNA in lambda library. Figure shows known and unknown (represented by 'N's) trout sequence. The position of the start codon (ATG) and regions of protein sequence conserved in other COT sequences are shown, together with their reverse translations (target sequence of PCR primers (as listed in table 6.1) are highlighted with black arrows). Sizes of unknown regions are predicted from sequences of COT from other species. Part of the lambda vector sequence at the 3'- and 5'-ends is also shown. Annotations appear below the nucleotide sequence.

```
TTCAGCGAAGGAGAGGGAGTATGCCAAGCGAGGGGGGGGGGGTCATCTCATAGAAGTATGCCAAGCGAGGGGGGGGGGGTCGCCGCTCTCA 90
                                                                                    G  V  A  A  L

CCTCAGAGGAGAGGACACGCTGGGCTAAGGCCAGGGAGTATCTGATAGGTATAGATCCAGCCAATAAGACCATCTTAGAGACCATCCAGA 180
T  S  E  E  R  T  R  W  A  K  A  R  E  Y  L  I  G  I  D  P  A  N  K  T  I  L  E  T  I  Q

GCAGTCTGTTTGTGGTCTCACTGGACGATGCTAAACCCTACGCTACTTCAGAGAACTACACACCGGTGACCCGGGAAGCGCTGACAGGAG 270
S  S  L  F  V  V  S  L  D  D  A  K  P  Y  A  T  S  E  N  Y  T  P  V  T  R  E  A  L  T  G

ACCCCACCATCCGCTGGGGAGACAAGTCCTACAACTCCCTCTCCTTCGCTGACGGAACCTTCGGATCCAATTGTGACCATGCCCCCTACG 360
D  P  T  I  R  W  G  D  K  S  Y  N  S  L  S  F  A  D  G  T  F  G  S  N  C  D  H  A  P  Y

ATGCCATGGTGCTGGTAAC|TCAGGGTTACTATGTGGATCAGCAGCTCAAAGCTACAGACGGCAAGTGGAAGGGCTCTGAGACGGTGCGGC 450
D  A  M  V  L  V  T| Q  G  Y  Y  V  D  Q  Q  L  K  A  T  D  G  K  W  K  G  S  E  T  V  R

CTATGCCTCTTCCTGAAGAGTTGGTCTTCACTGTGGATGACAGAGTCAGGAGTGACGTTGCACATGCCAAGCAACAGTACTTTGAGACTA 540
P  M  P  L  P  E  E  L  V  F  T  V  D  D  R  V  R  S  D  V  A  H  A  K  Q  Q  Y  F  E  T

CTCAGGACTTGCAGGTGGTGTGTTATGCGTTCACCTCGTTTGGGAAAGCAGCCATCAAACAGAGGAAGCTCCACCCAGACACCTTCATAC 630
T  Q  D  L  Q  V  V  C  Y  A  F  T  S  F  G  K  A  A  I  K  Q  R  K  L  H  P  D  T  F  I

AACTGGCCCTTCAACTGGCTTATTACAGACAGCATGGGAGGTTAGGTAGTTGCTATGAGACAGCGATGACCAGAAGGTTCTACCACGGCA 720
Q  L  A  L  Q  L  A  Y  Y  R  Q  H  G  R  L  G  S  C  Y  E  T  A  M  T  R  R  F  Y  H  G

GGACTGAGACCATGAGGCCCTGTACCCTGGAGGCACAGAACTGGTGCCATACCATGCTCCTCCCTGCAGCCAGCGCTGAGGCTAAGAGGA 810
R  T  E  T  M  R  P  C  T  L  E  A  Q  N  W  C  H  T  M  L  L  P  A  A  S  A  E  A  K  R

AAGCCCTGCTGCTGGCCTTCAACAAGCACAACAAACTGATGGCTGAGGCACAGAACGGAAAAGGTTTTGACAGACATCTCCTGGGCCTTT 900
K  A  L  L  L  A  F  N  K  H  N  K  L  M  A  E  A  Q  N  G  K  G  F  D  R  H  L  L  G  L

ACCTGATCGCCAAGGAGGAGGGACTTCCTATGCCAGACCTTTTCACTGATACACTGTATTGCAAGAGTGGCGGGGGCGGTAACTTTACCC 990
Y  L  I  A  K  E  E  G  L  P  M  P  D  L  F  T  D  T  L  Y  C  K  S  G  G  G  G  N  F  T

TGTCCACCAGTCTGGCTGGCTACACCACAGTTCATGGGGTGGGTGCTCCCATGGTGCACCATGGCTACGGGTTCTTCTACCGCATCAGTG 1080
L  S  T  S  L  A  G  Y  T  T  V  H  G  V  G  A  P  M  V  H  H  G  Y  G  F  F  Y  R  I  S

AGGACAGGATCGTGGCTTCCTGTTCAGCGTGGAAGTCCAGTCCAGAGACGGATGCAGAGACACTGTTCCAGAACCTGGTTACCTCCCTAC 1170
E  D  R  I  V  A  S  C  S  A  W  K  S  S  P  E  T  D  A  E  T  L  F  Q  N  L  V  T  S  L

ATGAGATGCTACATCTCGCTACCACAGCGCACCTCTAACACACACACGCGCGCAGAGTTTCTAGATGCCAGCCAATAATAACCGTTTTAA 1260
H  E  M  L  H  L  A  T  T  A  H  L  .

TATTGTCCAGATCTATGCAAAGGCATTGTAACAATGCGGCAGGTAGCCTAGATGTTAGAATTAGGCCAGTTACTGAAAGGTTGCTAGTTT 1350

GAATCCCTGAGCCAATAAATCTTTCGATGTGCCCTTGAGCAAGCCACTTAACCATAATTGCTCCTTTGCCATGACCCTACTCTCCGGGGT 1440

TGTCTCGGGGGTAGGTGGGATATGCAAAAAATACATTTCCAATGTGAAATAGGACAAGTATAAGTACCCACCAAATTATTATTACAATGC 1530

AGCCTTGAATGTTTTCTTAATGTTTACATAAAATACATTATTTGTTTAATGCAAAAAAAAAA 1582
```

Figure 6.7 Nucleotide and deduced amino acid sequence of COT from rainbow trout. Nucleotide sequences are numbered on the right.

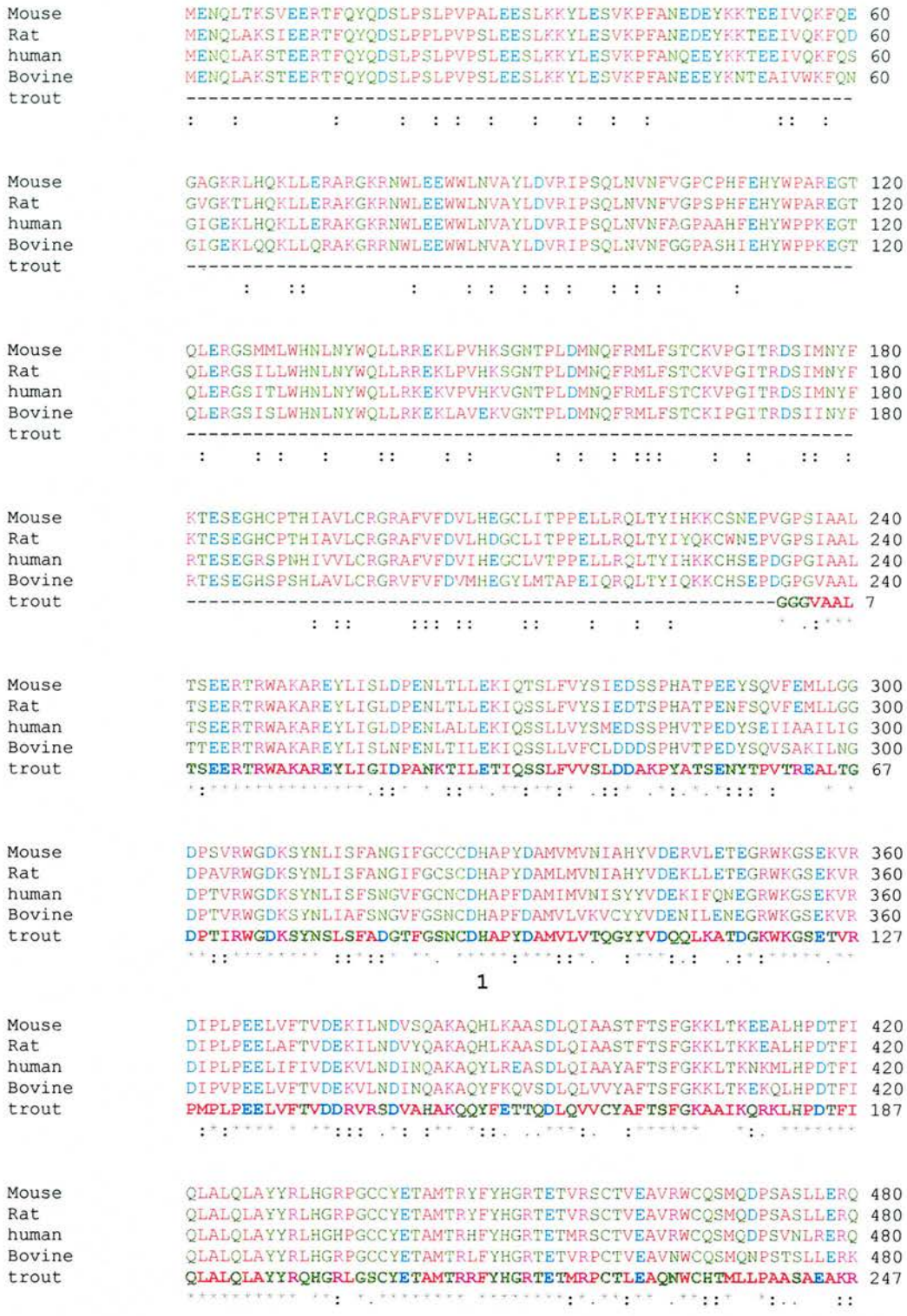

Fig 6.8 Alignment of the predicted trout COT translation with known mammalian COT genes. Identical (*) and similar (. or:) residues identified by the CLUSTAL program are indicated. Hyphens denote missing sequence. Mutations that result in loss of enzyme activity or affect carnitine binding or substrate specificity are numbered below the sequence (see table 6.2 for details).

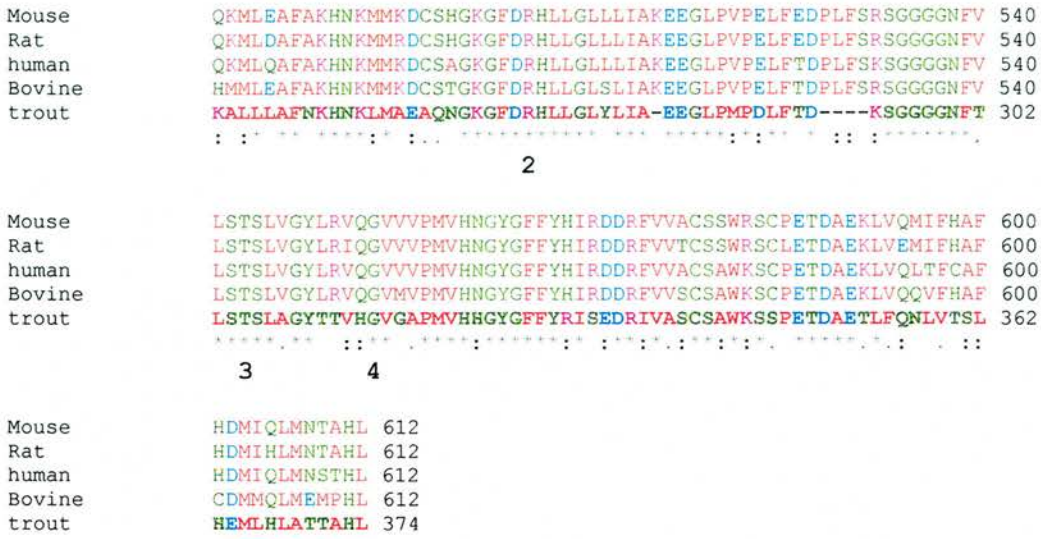

Fig 6.8 (continued)

Substitution	Enzyme	Decrease in	References
1. H327A	rat COT	activity	Morillas et al., 2000
2. R505A	bovine COT	carnitine binding	Cronin, 1997
3. S542A	bovine COT	carnitine binding	Cronin, 1997
T543A	bovine COT	carnitine binding	Cronin, 1997
S544A	bovine COT	carnitine binding increase	Cronin, 1997
4. G553M	rat COT	Acyl chain length specificity	Cordente et al., 2004

Table 6.2 Mutations in mammalian carnitine octanoyltransferase and their effect (numbering corresponds to residues in Fig 6.8). All the residues listed in this table are conserved in the rainbow trout homologue.

6.6 Sequence alignment of the trout sequence against mammalian COT

The deduced 374 amino acid sequence was compared with other sequence data in a BLAST search. The best similarity was found with sequences corresponding to members of the COT family. The peptide sequence had highest percentage identity with bovine COT (65.0%), followed by mouse (62.9%), human (62.9%) and rat (62.6%). All the regions of the trout enzyme were perfectly aligned with those of the mammalian COT. The high percentage identity in alignment of COT with other mammals suggests that the sequence has been significantly conserved throughout evolutionary changes between mammals and lower vertebrates.

6.7 Sequence alignment of the trout sequence against COT sequences from several vertebrate species.

More recently COT sequences from several other species have become available on databases including several from fish so a second sequence alignment was performed to consider the conservation of residues in these species. Protein sequences were obtained from BLAST at NCBI using the trout amino acid sequence to probe the database. Percentage (%) identity of COT amino acid sequences from mammalian and non mammalian species were assessed using the Clustal W algorithm (fig 6.9). The predicted trout COT protein sequence shared highest percentage homology with zebra fish (*Danio rerio*) (76.1%), followed by pufferfish (*Fugu: Takifugu rubripes)* (73.7%) and the freshwater pufferfish *Tetraodon nigroviridis* (70.8%). Sequence alignments revealed that the trout COT sequence is perfectly aligned with these species and the results are shown in fig 6.11.

6.8 Phylogenetic tree

The evolutionary relationship among COT sequences was investigated by the construction of a phylogenic tree (fig 6.10). Analysis of the trout nucleotide sequence showed a relatively tight grouping with other known COT genes.

Percent Identity

Divergence

	1	2	3	4	5	6	7	8	9	10	11		
1		84.6	85.5	84.8	67.0	60.9	61.8	60.0	62.6	30.6	33.8	**1**	Human
2	17.2		94.3	79.7	65.4	60.9	61.4	59.5	62.6	29.7	34.0	**2**	Rat
3	16.2	6.0		81.2	66.0	60.5	61.3	58.8	62.9	29.7	33.7	**3**	Mouse
4	17.0	23.7	21.7		67.2	63.1	63.9	61.1	65.0	31.4	33.0	**4**	Cattle
5	43.4	46.3	45.1	43.1		59.6	60.6	58.8	60.2	30.9	33.5	**5**	Chicken
6	54.6	54.6	55.6	50.5	57.3		70.4	87.4	73.7	31.9	34.8	**6**	Fugu
7	53.0	53.7	54.0	49.0	55.3	37.6		69.4	76.1	32.7	35.1	**7**	Zebrafish
8	56.6	57.6	59.0	54.3	59.0	13.8	39.2		70.8	32.2	35.6	**8**	Tetraodon
9	51.4	51.4	50.9	46.9	56.1	32.4	28.8	36.9		30.0	36.3	**9**	Trout
10	153.7	154.7	154.7	148.9	150.8	144.4	140.0	140.9	152.7		42.6	**10**	Drosphila
11	136.7	135.9	136.7	135.9	138.3	131.1	130.4	128.9	123.9	100.2		**11**	Mosquito
	1	**2**	**3**	**4**	**5**	**6**	**7**	**8**	**9**	**10**	**11**		

Fig 6.9 Homology (%) of rainbow trout COT predicted amino acid sequence with other known COT genes. Sequence divergence is shown on the left hand side of the figure.

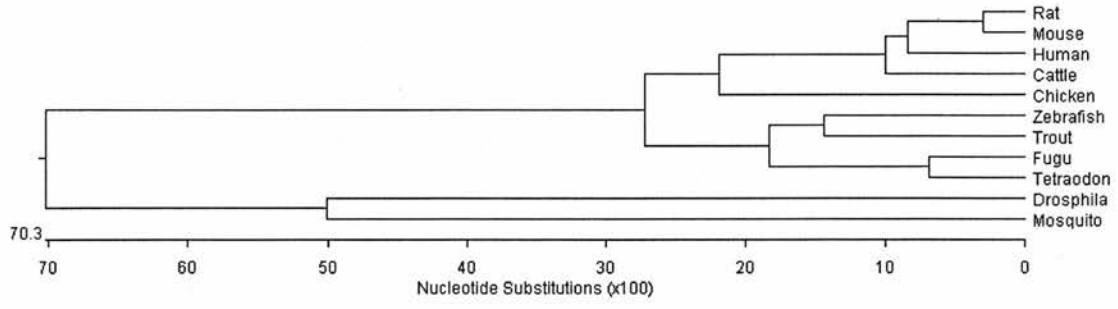

Fig 6.10 Phylogenic tree showing the relationship between the nucleotide sequence of trout COT and other known COT sequences. The tree was constructed using the CLUSTAL W algorithm and the horizontal line represents the genetic distance.

6.9 Conserved sequences

Amino acid residues involved in catalysis (H327) and substrate binding (R505, S542, T543 and S544) in mammalian species (table 6.2) were found to be conserved in rainbow trout COT (fig 6.8 and fig 6.10) and also COT sequences available from other species (fig 6.10) although the STS motif is not conserved in *Fugu*, *Tetraodon* or *Drosophila*, with the Thr residue being replaced by Ser in each case - a highly conservative substitution.

Interestingly G553 was conserved in all COT sequence studies. The mutation of G553 to the methionine results in loss of activity with any substrate longer than acetyl-CoA (Cordente et al., 2004). The recently published crystal structure of mouse COT, (Jogl et al., 2004) also highlighted the significance of G553 in defining the substrate selectivity of COT. In the same study it was proposed that the M335 residue might be important in catalysis by COT. Our sequence alignment revealed that the residue is conserved in human, rat and mouse sequences and conservatively replaced by Leu, except in insects.

Cys325 present in all mammalian COT sequences but absent from CrAT was conserved in trout COT and all other species studied except mosquito and *Drosophila*. Structural studies (Jogl et al., 2004; Jogl and Tong, 2003) reveal that this residue may be important in the substrate selectivity of COT.

(Morillas et al., 2000) suggested that H131 and H340 are essential for the malonyl-CoA binding to COT yet our studies reveal that conservation of H340 is confined to mouse and rat sequences only.

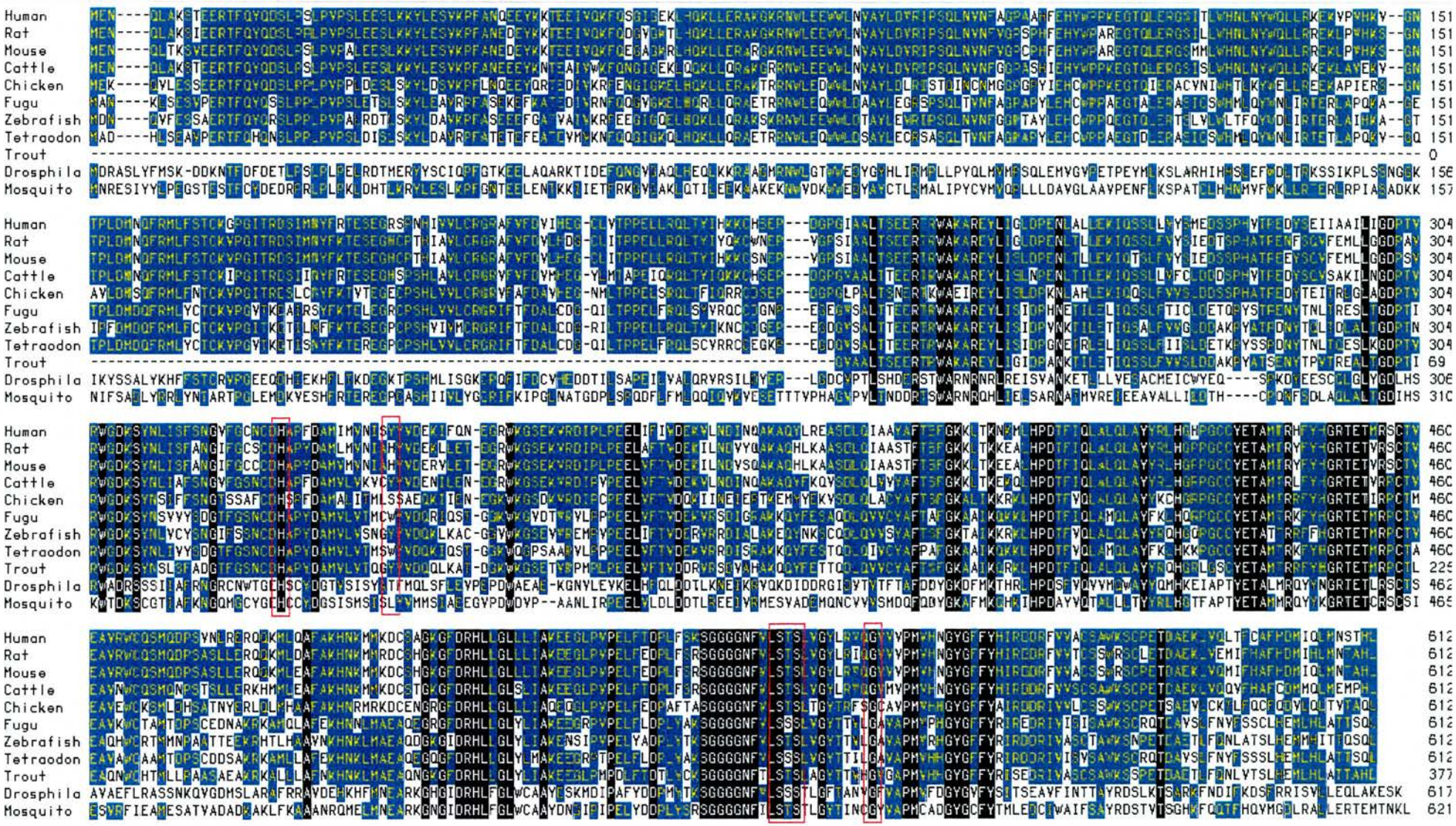

Fig 6.11 Alignment of COT amino acid sequences from different species. Amino acids shared by all the sequences are shaded back. Semi-conserved residues are shaded blue. Missing amino acids are denoted with hyphens. Residues in red boxes are significant and described in text (6.9)

6.10 Discussion

This chapter describes the cloning and partial sequencing of the COT cDNA in rainbow trout. This is the second acyltransferase to be described in rainbow trout (previously CPT1 cDNA has been cloned, Gutières *et al*, 2003).

Many genes in fish are present as two paralogous copies due to genome duplication (Venkatesh, 2003) . There is currently no evidence for a second COT gene in trout, and the almost finished *Fugu* genome appears to have a single COT gene encoding a protein with accession number AAO20903. This also seems to be the case for the zebrafish and *Tetraodon.*

The deduced amino acid sequence in the rainbow trout homologue shows highest sequence identity in mammalian species with bovine COT (65%) and in clusters with the phylogenetic tree.

The sequence compares well with COT sequences from non-mammalian species including several from fish (trout shared 76.1% identity with zebrafish) providing strong evidence that the sequence described in this chapter belongs to the COT family. In common with the mammalian COT sequences, the trout sequence shows conservation of amino acid residues involved in catalytic activity, carnitine binding and substrate selectivity. These same residues were also conserved in the non-mammalian species studied in this chapter.

The crystal structure of mouse COT revealed that G553 is important in substrate selectivity. It is interesting that this residue is conserved in all mammalian and non-mammalian species studied here. Probing the binding pocket where this residue is located may help understand the varying substrate specificity that is observed in mammalian COT kinetics studies (Ramsay, 1999).

Alignment of COT sequences also revealed that H340 (thought to be important in malonyl-CoA sensitivity) is not highly conserved in mammalian or non-mammalian species. Recent studies in the Ramsay lab have shown that none of the purified COT proteins in bovine, rat, human and trout have any sensitivity to malonyl-CoA except as a competitive inhibitor and the H340Y mutation makes no difference either (N. Sitheswaran and R.R. Ramsay, unpublished). This suggests that contrary to what (Morillas et al., 2000) reported, the residue is not significant in the binding of malonyl-CoA to COT.

6.11 Conclusions

In conclusion: 1) it is clear from our findings that COT gene expression exists in fish and the sequence is well conserved when compared to the sequence known in mammals and lower vertebrates. 2) the protocol originally used to amplify unknown regions of cDNA in mammals has been successfully applied to the study of cDNA in rainbow trout. 3) further studies are required to elucidate the full length sequence of COT in rainbow trout and could be achieved using 5'-RACE-PCR or traditional library screening techniques. Alternatively design of degenerate primers in conserved regions of COT could be attempted now that protein sequence data is available for trout COT

In gaining the full-length sequence, it would be advantageous to clone the enzyme into an expression system. Purification and subsequent kinetic studies from the recombinant enzyme would enable us to understand better the control of the carnitine acyltransferases which remain poorly understood in the lower vertebrates.

CHAPTER 7

DISCUSSION

7.1 Does stress require upregulation of fatty acid oxidation?

7.1.1 Fatty acid oxidation in mitochondria and peroxisomes from trout liver

Metabolic rates in fish are predominantly lower than in mammals (Schmidt-Nielsen, 1975). We studied fatty acid oxidation rates in the liver to compare with liver mammalian studies. Fatty acid oxidation capacities however do not dominate in fish liver. In a study by Froyland et al. fatty acid oxidation rates were highest in red muscle (Froyland et al., 2000). Inconsistencies in rates may be explained by a low capacity to metabolise fats in the liver or a failure to isolate mitochondria and peroxisomes with intact metabolising systems. We used isolation procedures that had been optimised for use in mammals and found that mitochondria and peroxisomes did not separate as easily as in mammals. Studies in fish mitochondria have shown that the size of mitochondria can vary with temperature (Johnston et al., 1998). Peroxisomal studies in fish indicate that peroxisomal size varies with temperature and age (Cancio and Cajaraville, 2000). The fish were not maintained at a constant temperature, so this may have created variations in mitochondrial size and also peroxisomal size.

Lack of success in optimising the radiochemical assay meant that the less sensitive oxygen electrode method and enriched organelle preparations rather than homogenate had to be used. However, the distribution of oxidation at approximately 40% peroxisomal and 60% mitochondrial is not greatly different from what is observed in mammals.

7.1.2 Preliminary data on changes in fatty acid oxidation as a result of the metabolic demands of stress

In the immune stress study we observed a surge in oxidation rates at 4 days. We concluded that the immune stress may occur at a metabolic cost to the animal. This study was only performed once and therefore can only be considered preliminary data. For that reason we need to repeat the experiment to confirm the findings, do a full oxidation study and probably co-ordinate these experiments with behavioural and physiology study on feed intake.

7.1.3 Food withdrawal stress

In the food withdrawal stress no change was observed. The time scale within which we measured the fatty acid oxidation rates is almost certainly too short for fish. Capacities to survive extended periods without food varies depending on the species being investigated (Farrell and Munt, 1983). Fish starve more quickly at higher temperatures so we could have increased the circulating temperature to see any impact on metabolic rate. This would not be consistent with the normal physiological temperature of a fish and therefore is probably not relevant. Metabolic response to stress might be better explored by modern genomic techniques using gene array for up regulation of all enzymes involved in fat and CHO oxidation pathways. This approach was not open to us because of the cost.

In conclusion, the fatty acid oxidation rate is dramatically lower than that of mammals and therefore effects did not manifest themselves over time periods that were practical for these studies.

7.2 Regulation of mitochondrial beta-oxidation in fish: do fish use the same strategies as mammals?

The presence of contact sites in rainbow trout was investigated to look at their role in control of fatty acid oxidation. Studies in mammals relatively recently proposed that this may be another point of control. Our experiments were hindered by difficulties in isolating the mitochondrial membrane fractions in fish. We adapted a protocol that had been optimized in mammals and further studies should involve creating an efficient protocol for membrane fractionation in fish. We were unable to determine kinetic values due to low amounts of sample and this is something else that should be considered for further experiments.

Our studies demonstrated for the first time that VDAC is present in trout liver mitochondria and that it does cross-react with antibodies to the mammalian VDAC1. What role it plays in the membrane structure or indeed in the control of fatty acid oxidation remains to be elucidated and further experiments are required to establish its role. We did not see CPT1 enrichment in the contact site in fed or fasted fish. In mammals it has been shown that CPT1 becomes more enriched in the contact sites when food is withheld, this may be a mechanism specific to mammals where the liver produces ketone bodies to supply fuel in order to conserve glucose reserves. Ketosis does not occur in rainbow trout and therefore the lack of enrichment of CPT1 in the contact sites suggests that the contact sites may play an additional role in mammals in the control of fatty acid oxidation beyond what is found in fish.

We looked for upregulation of CPT1 in the study of 14 day fasted fish (Chapter 4). The levels in fed and fasted trout liver were not significantly different in the outer membrane samples but there was double the amount of total CPT in contact sites. However, this did not indicate enrichment in the contact site, so further careful work

should be done to confirm whether the CPT does increase or whether there are more contact sites after 14 days of food deprivation. In mammals, upregulation of CPT1 by 24 hours food deprivation is considerable (Ghadiminejad and Saggerson, 1991; Ramsay, 1993).

7.3 **Peroxisomal COT**

Carnitine acyltransferases are important in the regulation of fatty acid oxidation and have been studied extensively in mammals. More recent studies have looked to improving the knowledge of these enzymes in lower vertebrates (Gutieres et al., 2003; Jackson et al., 1999). Gutieres et al were the first to publish the characterization of an acyltransferase (CPT1) in rainbow trout and determined that like the mammalian enzyme it is inhibited by malonyl-CoA (Gutieres et al., 2003). Protein sequence homology studies revealed that the trout CPT1 is 60% identical to the mammalian enzyme and many of the residues that characterize the enzyme are conserved in the fish enzyme.

Carnitine octanoyltransferase is another enzyme in this family and the aim of our study was to isolate and characterize the enzyme in rainbow trout. The purified protein (detectable as one band by polyacrylamide gel electrophoresis) appeared to have no contamination when stained with coomassie blue. The molecular weight was estimated as 61 KDa, which is in agreement with other COT proteins isolated from mammals. The protein band was sent for mass spectral analysis and eight peptides identified by MALDI and MS/MS were found to be identical to bovine COT (see discussion of sequence below).

Kinetic studies on the trout enzyme revealed that the substrate specificity was comparable with the bovine enzyme. Mammalian COT shows broad chain length specificity among species. Mouse COT is characterized by a high affinity for shorter chain acyl CoAs (Farrell et al., 1984) whereas bovine COT shows high specificity for longer chain acyl CoAs (Ramsay, 1988). Our studies demonstrate that trout COT has highest affinity with acyl chain lengths above C_8. This suggests that the fish enzyme has evolved to transfer the fatty acyl-CoA at a higher chain length so that more energy will be conserved for the more efficient energy-yielding pathway in the mitochondria. On the whole, Km values for L-carnitine remained similar in all species. Any variability could be accounted for by the fact that COT used in the assays came from multiple enzyme preparations of varying purity. COT in trout is not subject to malonyl-CoA regulation.

7.3.1 Sequence

We were successful in sequencing 61% of rainbow trout COT after cloning from a cDNA library. Sequence alignment studies revealed that the trout enzyme is more than 60% homologous with mammalian COT. In comparison with other fish COT sequences, trout showed highest homology with zebra fish (76.1%), suggesting that the enzyme is highly conserved in the fish species.

We established that the residues important in COT catalysis, substrate binding, and enzyme activity and localisation (such as the catalytic H, STS, AHL), which are highly conserved throughout the mammalian species, are also conserved in the trout COT sequence.

The recently published crystal structure of COT revealed that the small size of G553 is important for access to the binding site for the long chain carnitine acyl moiety. This residue is conserved in all species, including trout.

An initial attempt to clone trout COT using degenerate primers was unsuccessful probably owing to lack of sequence data available at the time. COT in *Fugu*, zebrafish and tetraodon has now been fully sequenced and has highlighted conserved residues specific to the fish enzyme and also residues that are not conserved. For example, in designing the primers last time, we assumed that MENQLAK (the amino acids at the start of the COT sequence) were conserved in rainbow trout because it is conserved in most mammalian sequences, however in the three fish sequences that we have data for it is only the methionine that is conserved, all other residues are different. So it may be that a second attempt using this method may enable us to obtain the N-terminal fragment of trout COT yet to be sequenced.

7.4 Conclusions

The work reported in this thesis has established that trout peroxisomal COT is very similar to the mammalian one. This is significant because it means that the function is conserved to a remote branch of evolution.

However, specificity of COT does not support the expected need to metabolise more very long chain fats because of the fish diet of marine fatty acids. Rather, it seems that the mitochondria in trout are able to oxidise these fatty acids too and it is mammals that have specialised to the efficient use of common C16 and C18 fatty acids for energy while retaining the polyunsaturated very long chain fatty acids, C20 and greater, for synthetic use by having slower turnover in peroxisomes. The 40-60 split

in the oxidation contribution of the peroxisomal and mitochondrial oxidation pathways suggests more constant rates in fish than in mammals where 30% in peroxisomes is more usual even in starvation.

Much however remains to be done on the question of upregulation of fatty acid metabolism in stressed fish. Physiological measures of stress, including O_2 consumption need to be co-ordinated with the biochemical studies. Muscle studies (red and white) must also be included as it is the major oxidative organ in fish. Use of both microarray to survey whole fatty acid oxidation pathways, in particular a comparison of CPT1 with the acyl-CoA oxidase of peroxisomes, and of proteomic studies to survey the differences between control and stress fish would be suitable for taking this work further. Such studies are particularly useful because relatively small samples are needed and various tissues from one fish could be studied in parallel.

The question of how fatty acid oxidation in fish is controlled is still not answered. If rates vary little then malonyl-CoA inhibition of CPT1 and gene regulation are likely to be sufficient. PPAR regulation as found in mammals might also regulate CPT1 in fish. Fat is half of the wild fish diet and fishing is a large economy in Scotland. Fish should be a larger part of a healthy diet in modern western society so regulation of fatty acid oxidation and efficient energy production from this energy rich store in fish remains a strategic research topic.

Acknowledgements

Much remains to be done but it requires a budget beyond the minimal postgraduate support that was all available to me. What has been done was made possible by fish from Dr. Valerie J. Smith and an award from the research committee seed fund for

metabolic stress work; cloning and sequencing possible only through the generosity of Dr Nigel Price at the Hannah Institute, Ayr.

References

Adams, V., Bosch, W., Schlegel, J., Wallimann, T., and Brdiczka, D.: Further characterization of contact sites from mitochondria of different tissues: topology of peripheral kinases. Biochim Biophys Acta **981** (2)**:** 213-25, 1989.

Anderson, R. C.: Carnitine palmitoyltransferase: A viable target for the treatment of NIDDM? Current Pharmaceutical Design **4** (1)**:** 1-16, 1998.

Baranska, J., and Wojtczak, L.: Transfer of phophatidic acid between microsomal and mitochondrial outer and inner membranes. Biochimica Biophysica Acta **773:** 23-31, 1984.

Bastrop, R., Jurss, K., and Wacke, R.: Biochemical Parameters as a Measure of Food Availability and Growth in Immature Rainbow-Trout (Oncorhynchus-Mykiss). Comparative Biochemistry and Physiology a-Physiology **102** (1)**:** 151-161, 1992.

Benz, R., Kottke, M., and Brdiczka, D.: The cationically selective state of the mitochondrial outer membrane pore: a study with intact mitochondria and reconstituted mitochondrial porin. Biochim Biophys Acta **1022** (3)**:** 311-8, 1990.

Berg, J. M., Stryer, L., and Tymoczko, J. L.: Biochemistry, W.H Freeman, New York, 2002.

Bergmeyer, H. U.: Methods of Enzymatic Analysis, Academic Press, New York and London, 1974.

Bhaird, N. N. A., Kumaravel, G., Gandour, R. D., Krueger, M. J., and Ramsay, R. R.: Comparison of the Active-Sites of the Purified Carnitine Acyltransferases from Peroxisomes and Mitochondria by Using a Reaction-Intermediate Analog. Biochemical Journal **294:** 645-651, 1993.

Bieber, L. L.: Carnitine. Annual Review of Biochemistry **57:** 261-283, 1988.

Bilinski, E., and Jonas, E.E: Effects of Coenzyme A and Carnitine on Fatty Acid Oxidation by Rainbow Trout Mitochondria. J.Fish.Res.Bd.Canada **27:** 857-864, 1970.

Blok, M. C., Wirtz, K. W. A., and Scherphof, G. L.: Exchange of phospholipids between microsomes and inner and outer mitochondrial membranes of rat liver. Biochimica Biophysica Acta **233:** 61-75, 1971.

Bollag, D. M., Rozycki, M. D., and Edelstein, S. J.: Protein Methods, Wiley-Liss, New York, 1996.

Bonnefont, J. P., Demaugre, F., Prip-Buus, C., Saudubray, J. M., Brivet, M., Abadi, N., and Thuillier, L.: Carnitine palmitoyltransferase deficiencies. Molecular Genetics and Metabolism **68** (4)**:** 424-440, 1999.

Breckenridge, D. G., and Xue, D.: Regulation of mitochondrial membrane permeabilization by BCL-2 family proteins and caspases. Curr Opin Cell Biol **16** (6)**:** 647-52, 2004.

Bremer, J.: Carnitine and its role in fatty acid metabolism. TIBS **2:** 207-209, 1977.

Brown, N. F., Anderson, R. C., Caplan, S. L., Foster, D. W., and McGarry, J. D.: Catalytically Important Domains of Rat Carnitine Palmitoyltransferase-Ii as Determined by Site-Directed Mutagenesis and Chemical Modification - Evidence for a Critical Histidine Residue. Journal of Biological Chemistry **269** (29)**:** 19157-19162, 1994.

Cancio, I., and Cajaraville, M. P.: Cell biology of peroxisomes and their characteristics in aquatic organisms. *In* International Review of Cytology - a Survey of Cell Biology, Vol 199, vol. 199, pp. 201-293, 2000.

Chase, J. F. A., and Tubbs, P. K.: Conditions for the self-catalysed inactivation of carnitine acetyltransferase. Biochem. J. **111:** 225-235, 1969.

Choi, S. J., Oh, D. H., Song, C. S., Roy, A. K., and Chatterjee, B.: Molecular-Cloning and Sequence-Analysis of the Rat-Liver Carnitine Octanoyltransferase Cdna, Its Natural Gene and the Gene Promoter. Biochimica Et Biophysica Acta-Gene Structure and Expression **1264** (2)**:** 215-222, 1995.

Clark, H., Carling, D., and Saggerson, D.: Covalent activation of heart AMP-activated protein kinase in response to physiological concentrations of long-chain fatty acids. European Journal of Biochemistry **271** (11)**:** 2215-2224, 2004.

Clarke, P. R. H., and Bieber, L. L.: Isolation and Purification of Mitochondrial Carnitine Octanoyltransferase Activities from Beef-Heart. Journal of Biological Chemistry **256** (19)**:** 9861-9868, 1981.

Colombini, M.: A candidate for the permeability pathway of the outer mitochondrial membrane. Nature **279:** 643-645, 1979.

Colucci, W. J., and Gandour, R. D.: Carnitine Acetyltransferase - a Review of Its Biology, Enzymology, and Bioorganic Chemistry. Bioorganic Chemistry **16** (3)**:** 307-334, 1988.

Cordente, A. G., Lopez-Vinas, E., Vazquez, M. I., Swiegers, J. H., Pretorius, I. S., Gomez-Puertas, P., Hegardt, F. G., Asins, G., and Serra, D.: Redesign of Carnitine Acetyltransferase Specificity by Protein Engineering. J. Biol. Chem. **279** (32)**:** 33899-33908, 2004.

Crockett, E. L., and Sidell, B. D.: Peroxisomal beta-oxidation is a significant pathway for catabolism of fatty acids in a marine teleost. Am J Physiol **264** (5 Pt 2)**:** R1004-9, 1993a.

Crockett, E. L., and Sidell, B. D.: Substrate selectivities differ for hepatic mitochondrial and peroxisomal beta-oxidation in an Antarctic fish, Notothenia gibberifrons. Biochem J **289 (Pt 2):** 427-33, 1993b.

Crockett, E. L., and Sidell, B. D.: Substrate Selectivities Differ for Hepatic Mitochondrial and Peroxisomal Beta-Oxidation in an Antarctic Fish, Notothenia-Gibberifrons. Biochemical Journal **289:** 427-433, 1993c.

Crompton, M.: The mitochondrial permeability transition pore and its role in cell death. Biochemical Journal **341:** 233-249, 1999.

Cronin, C. N.: cDNA cloning, recombinant expression, and site-directed mutagenesis of bovine liver carnitine octanoyltransferase - Arg505 binds the carboxylate group of carnitine. European Journal of Biochemistry **247** (3)**:** 1029-1037, 1997a.

Cronin, C. N.: The conserved serine-threonine-serine motif of the carnitine acyltransferases is involved in carnitine binding and transition-state stabilization: A site-directed mutagenesis study. Biochemical and Biophysical Research Communications **238** (3)**:** 784-789, 1997b.

Derrick, J. P., and Ramsay, R. R.: L-Carnitine Acyltransferase in Intact Peroxisomes Is Inhibited by Malonyl-Coa. Biochemical Journal **262** (3)**:** 801-806, 1989.

Eaton, S., Bartlett, K., and Pourfarzam, M.: Mammalian mitochondrial beta-oxidation. Biochem J **320 (Pt 2):** 345-57, 1996.

Elgersma, Y., Vanroermund, C. W. T., Wanders, R. J. A., and Tabak, H. F.: Peroxisomal and Mitochondrial Carnitine Acetyltransferases of Saccharomyces-Cerevisiae Are Encoded by a Single-Gene. Embo Journal **14** (14)**:** 3472-3479, 1995.

Farrell, A. P., and Munt, B.: Cholesterol levels in the blood of Atlantic salmonids. Comp Biochem Physiol A **75** (2)**:** 239-42, 1983.

Farrell, S., and Bieber, L. L.: Carnitine Octanoyltransferase of Mouse-Liver Peroxisomes - Purification, Properties and Effect of Hypolipidemic Drugs. Federation Proceedings **42** (4)**:** 1053-1053, 1983.

Farrell, S. O., Fiol, C. J., Reddy, J. K., and Bieber, L. L.: Properties of Purified Carnitine Acyltransferases of Mouse- Liver Peroxisomes. Journal of Biological Chemistry **259** (21)**:** 3089-3095, 1984.

Felig, P., and Wahren, J.: Fuel homeostasis in exercise. New England Journal of Medicine **293:** 1078=1084, 1975.

Ferdinandusse, S., Mulders, J., Ijlst, L., Denis, S., Dacremont, G., Waterham, H. R., and Wanders, R. J. A.: Molecular cloning and expression of human carnitine octanoyltransferase: Evidence for its role in the peroxisomal beta-oxidation of branched-chain fatty acids. Biochemical and Biophysical Research Communications **263** (1)**:** 213-218, 1999.

Ford, T., Graham, J., and Rickwood, D.: Iodixanol - a Nonionic Isosmotic Centrifugation Medium for the Formation of Self-Generated Gradients. Analytical Biochemistry **220** (2)**:** 360-366, 1994.

Fraser, F., Padovese, R., and Zammit, V. A.: Distinct kinetics of carnitine palmitoyltransferase I in contact sites and outer membranes of rat liver mitochondria. Journal of Biological Chemistry **276** (23)**:** 20182-20185, 2001.

Fraser, F., and Zammit, V. A.: Enrichment of carnitine palmitoyltransferases I and II in the contact sites of rat liver mitochondria. Biochemical Journal **329:** 225-229, 1998.

Fraser, F., and Zammit, V. A.: Submitochondrial and subcellular distributions of the carnitine-acylcarnitine carrier. Febs Letters **445** (1)**:** 41-44, 1999.

Fritz, I. B., and Marquis, N. R.: The role of acylcarnitine esters and carnitine palmitoyltransferase in the transport of fatty acyl groups across mitochondrial membranes. Proc. Natl. Acad. Sci. U.S.A. **54:** 1226-1233, 1965.

Froese, R., and Pauly, D.: *FishBase*, World Wide Web electronic publication, www.fishbase.org, 2002.

Froyland, L., Lie, O., and Berge, R. K.: Mitochondrial and peroxisomal beta-oxidation capacities in various tissues from Atlantic salmon Salmo salar. Aquaculture Nutrition **6** (2)**:** 85-89, 2000.

Froyland, L., Madsen, L., Eckhoff, K. M., Lie, O., and Berge, R. K.: Carnitine palmitoyltransferase I, carnitine palmitoyltransferase II, and acyl-CoA oxidase activities in Atlantic salmon (Salmo salar). Lipids **33** (9)**:** 923-30, 1998.

Ghadiminejad, I., and Saggerson, E. D.: A study of properties and abundance of the components of liver carnitine palmitoyltransferases in mitochondrial inner and outer membranes. Effects of hypothyroidism, fasting and a ketotic diabetic state. Biochem J **277 (Pt 3):** 611-7, 1991.

Gobin, S., Thuillier, L., Jogl, G., Faye, A., Tong, L., Chi, M., Bonnefont, J. P., Girard, J., and Prip-Buus, C.: Functional and structural basis of carnitine palmitoyltransferase 1A deficiency. Journal of Biological Chemistry **278** (50)**:** 50428-50434, 2003.

Graham, J., Ford, T., and Rickwood, D.: The Preparation of Subcellular Organelles from Mouse-Liver in Self-Generated Gradients of Iodixanol. Analytical Biochemistry **220** (2)**:** 367-373, 1994.

Gutieres, S., Damon, M., Panserat, S., Kaushik, S., and Medale, F.: Cloning and tissue distribution of a carnitine palmitoyltransferase I gene in rainbow trout (Oncorhynchus mykiss). Comp Biochem Physiol B Biochem Mol Biol **135** (1)**:** 139-51, 2003.

Hackenbrock, C. R.: Chemical and physical fixation of isolated mitochondria in low energy and high energy states. Proc. Natl. Acad. Sci. U.S.A. **61:** 598-605, 1968.

Halestrap, A. P., and Davidson, A. M.: Inhibition of Ca2(+)-induced large-amplitude swelling of liver and heart mitochondria by cyclosporin is probably caused by the inhibitor binding to mitochondrial-matrix peptidyl-prolyl cis-trans isomerase and preventing it interacting with the adenine nucleotide translocase. Biochem J **268** (1)**:** 153-60, 1990.

Halver, J. E.: Lipids and fatty acids. *In* Fish Feed Technology, vol. ADCP/REP/80/11, pp. Chapter 4, UNITED NATIONS DEVELOPMENT PROGRAMME FOOD AND AGRICULTURE ORGANIZATION OF THE UNITED NATIONS, Rome., 1980.

Hardewig, I., Peck, L. S., and Portner, H. O.: Thermal sensitivity of mitochondrial function in the Antarctic Notothenioid Lepidonotothen nudifrons. Journal of Comparative Physiology B-Biochemical Systemic and Environmental Physiology **169** (8)**:** 597-604, 1999.

Hashimoto, N. *In* Fatty acid oxidation, ed. by P. M. Coates, Alan R. Liss, New York, 1990.

Henderson, R. J., and Sargent, J. R.: Chain-Length Specificities of Mitochondrial and Peroxisomal β–oxidation of Fatty Acids in Liver of Rainbow Trout (*Salmo gairdneri*). Comparative Biochemistry and Physiology **82B:** 79-85, 1985a.

Henderson, R. J., and Sargent, J. R.: Chain-Length Specificities of Mitochondrial and Peroxisomal Beta-Oxidation of Fatty-Acids in Livers of Rainbow-Trout (Salmo-Gairdneri). Comparative Biochemistry and Physiology B-Biochemistry & Molecular Biology **82** (1)**:** 79-85, 1985b.

Henderson, R. J., Sargent, J. R., and Pirie, B. J. S.: Peroxisomal Oxidation of Fatty-Acids in Livers of Rainbow-Trout (Salmo-Gairdnerii) Fed Diets of Marine

Zooplankton. Comparative Biochemistry and Physiology B-Biochemistry & Molecular Biology **73** (3)**:** 565-570, 1982.

Henderson, R. J., and Tocher, D. R.: The lipid composition and biochemistry of fresh water fish. Prog. Lipid Res. **26:** 281-347, 1987.

Hoppel, C., Kerner, J., Turkaly, P., and Tandler, B.: Rat liver mitochondrial contact sites and carnitine palmitoyltransferase-I. Arch Biochem Biophys **392** (2)**:** 321-5, 2001.

Hsiao, Y.-S., Jogl, G., and Tong, L.: Structural and Biochemical Studies of the Substrate Selectivity of Carnitine Acetyltransferase. J. Biol. Chem. **279** (30)**:** 31584-31589, 2004.

Jackson, V. N., Cameron, J. M., Zammit, V. A., and Price, N. T.: Sequencing and functional expression of the malonyl-CoA- sensitive carnitine palmitoyltransferase from Drosophila melanogaster. Biochemical Journal **341:** 483-489, 1999.

Jogl, G., Hsiao, Y. S., and Tong, L.: Crystal structure of mouse carnitine octanoyltransferase and molecular determinants of substrate selectivity. J Biol Chem, 2004.

Jogl, G., and Tong, L.: Crystal structure of carnitine acetyltransferase and implications for the catalytic mechanism and fatty acid transport. Cell **112:** 113-122, 2003.

Johnston, I. A., Calvo, J., Guderley, H., Fernandez, D., and Palmer, L.: Latitudinal variation in the abundance and oxidative capacities of muscle mitochondria in perciform fishes. Journal of Experimental Biology **201** (1)**:** 1-12, 1998.

Kiessling, A., Larsson, L., Kiessling, K.-H., Lutes, P. B., Storebakken, T., and Hung, S. S. S.: Spawning Induces a Shift in Energy Metabolism from Glucose to Lipid in

Rainbow Trout (*Oncorhynchus mykiss*). Fish Physiol. Biochem **14:** 439-448, 1995a.

Kiessling, A., Larsson, L., Kiessling, K. H., Lutes, P. B., Storebakken, T., and Hung, S. S. S.: Spawning induces a shift in energy metabolism from glucose to lipid in rainbow trout white muscle. Fish Physiology and Biochemistry **14** (6)**:** 439-448, 1995b.

Kiessling, K. H., and Kiessling, A.: Selective Utilization of Fatty-Acids in Rainbow-Trout (Oncorhynchus-Mykiss Walbaum) Red Muscle Mitochondria. Canadian Journal of Zoology-Revue Canadienne De Zoologie **71** (2)**:** 248-251, 1993.

Kolodziej, M. P., and Zammit, V. A.: Reevaluation of the Interaction of Malonyl-Coa with the Rat- Liver Mitochondrial Carnitine Palmitoyltransferase System by Using Purified Outer Membranes. Biochemical Journal **267** (1)**:** 85-90, 1990.

Lazarow, P. B.: Rat liver peroxisomes catalyze the beta-oxidation of fatty acids. J. Biol. Chem. **253:** 1522-1528, 1978.

Lazarow, P. B.: Assay of peroxisomal beta-oxidation of fatty acids. *In* Methods in Enzymology, vol. 72, pp. 315-317, Academic Press, 1981.

Lazarow, P. B., and DeDuve, C.: A fatty acyl-CoA oxidising system in rat liver peroxisomes: enhancement by clofibrate, a hypolipidemic drug. Proc.Natl. Acad. Sci. U.S.A. **73:** 2043-2046, 1976.

Lin, L. N., Hasumi, H., and Brandts, J. F.: Catalysis of proline isomerization during protein-folding reactions. Biochim Biophys Acta **956** (3)**:** 256-66, 1988.

Love, R. M.: The chemical biology of fishes, Academic Press, London, 1970.

Lynen, F., and Ochoa, S.: Enzymes of fatty acid metabolism, 1953. Biochimica Biophysica Acta **1000:** 281-296, 1989.

Mannella, C. A.: Structural analysis of mitochondrial pores. Experientia **46** (2)**:** 137-45, 1990.

Markwell, M. A., McGroarty, E. J., Bieber, L. L., and Tolbert, N. E.: The subcellular distribution of carnitine acyltransferases in mammalian liver and kidney. A new peroxisomal enzyme. J Biol Chem **248** (10)**:** 3426-32, 1973a.

Markwell, M. A. K., McGroarty, E. J., Bieber, L. L., and Tolbert, N. E.: Journal of Biological Chemistry **248:** 3426-3432, 1973b.

McClelland, G. B., Khanna, S., Gonzalez, G. F., Butz, C. E., and Brooks, G. A.: Peroxisomal membrane monocarboxylate transporters: evidence for a redox shuttle system? Biochemical and Biophysical Research Communications **304** (1)**:** 130-135, 2003.

McGarry, J. D., and Foster, D. W.: Regulation of hepatic fatty acid oxidation and ketone body production. Annual Review of Biochemistry **49:** 395-420, 1980.

McGarry, J. D., Leatherman, G. F., and Foster, D. W.: The site of inhibition of fatty acid oxidation by malonyl-CoA. Journal of Biological Chemistry **253:** 4128-4136, 1978.

Meed, J. F., and Kayama, M.: Lipid metabolism in fish. *In* Fish oils, ed. by M. E. Stansby, pp. 289-99, Avi Publ. Co., Westport, Conn.,, 1967.

Miyazawa, S., Ozasa, H., Osumi, T., and Hashimoto, T.: Purification and properties of carnitine octanoyltransferase and carnitine palmitoyltransferase from rat liver. Journal of Biochemistry **94:** 529-542, 1983.

Morillas, M., Clotet, J., Rubi, B., Serra, D., Asins, G., Arino, J., and Hegardt, F. G.: Identification of the two histidine residues responsible for the inhibition by malonyl-CoA in peroxisomal carnitine octanoyltransferase from rat liver. Febs Letters **466** (1)**:** 183-186, 2000.

Morillas, M., Gomez-Puertas, P., Roca, R., Serra, D., Asins, G., Valencia, A., and Hegardt, F. G.: Structural model of the catalytic core of carnitine palmitoyltransferase I and carnitine octanoyltransferase (COT) - Mutation of CPT I histidine 473 and alanine 381 and COT alanine 238 impairs the catalytic activity. Journal of Biological Chemistry **276** (48)**:** 45001-45008, 2001.

Morillas, M., Gomez-Puertas, P., Rubi, B., Clotet, J., Arino, J., Valencia, A., Hegardt, F. G., Serra, D., and Asins, G.: Structural model of a malonyl-CoA-binding site of carnitine octanoyltransferase and carnitine palmitoyltransferase I - Mutational analysis of a malonyl-CoA affinity domain. Journal of Biological Chemistry **277** (13)**:** 11473-11480, 2002.

Morillas, M., Lopez-Vinas, E., Valencia, A., Serra, D., Gomez-Puertas, P., Hegardt, F. G., and Asins, G.: Structural model of carnitine palmitoyltransferase I based on the carnitine acetyltransferase crystal. Biochemical Journal **379:** 777-784, 2004.

Moser, H. W.: Pathogenetic mechanisms in peroxisomal disorders. Current Opinion in Neurology **9** (6)**:** 473-476, 1996.

Moyes, C. D., Suarez, R. K., Brown, G. S., and Hochachka, P. W.: Peroxisomal Beta-Oxidation - Insights from Comparative Biochemistry. Journal of Experimental Zoology **260** (2)**:** 267-273, 1991.

Mynatt, R. L., Greenhaw, J. J., and Cook, G. A.: Cholate extracts of mitochondrial outer membranes increase inhibition by malonyl-CoA of carnitine palmitoyltransferase-I by a mechanism involving phospholipids. Biochem J **299 (Pt 3):** 761-7, 1994.

Nic a'Bhaird, N., Kumaravel, G., Gandour, R. D., Krueger, M. J., and Ramsay, R. R.: Comparison of the Active-Sites of the Purified Carnitine Acyltransferases from

Peroxisomes and Mitochondria by Using a Reaction-Intermediate Analog. Biochemical Journal **294:** 645-651, 1993.

Nic a'Bhaird, N., and Ramsay, R. R.: Malonyl-Coa Inhibition of Peroxisomal Carnitine Octanoyltransferase. Biochemical Journal **286:** 637-640, 1992.

Nic a'Bhaird, N., Yankovskaya, V., and Ramsay, R. R.: Active sites residues of beef liver carnitine octanoyltransferase (COT) and carnitine palmitoyltransferase (CPT-II). Biochemical Journal **330:** 1029-1036, 1998.

Osmundsen, H., Bremer, J., and Pedersen, J. I.: Metabolic Aspects of Peroxisomal Beta-Oxidation. Biochimica Et Biophysica Acta **1085** (2)**:** 141-158, 1991.

Patey, C. P., and Driedzic, W. R.: Cold acclimation increases activities of mitochondrial long-chain acyl-CoA synthetase and carnitine acyl-CoA transferase I in heart of rainbow trout (*Oncorhynchus mykiss*). Canadian Journal of Zoology-Revue Canadienne De Zoologie **75:** 324-331, 1997.

Petersen, A. L.: Analytical Biochemistry **83:** 346-356, 1977.

Ramsay, R. R.: The Soluble Carnitine Palmitoyltransferase from Bovine Liver - a Comparison with the Enzymes from Peroxisomes and from the Mitochondrial Inner Membrane. Biochemical Journal **249** (1)**:** 239-245, 1988.

Ramsay, R. R.: A comparison of the malonyl-CoA sensitive carnitine palmitoyltransferase activities acting on cytoplasmic substrates and their distribution in mitochondria, peroxisomes and microsomes. Life Science Advances **12:** 23-29, 1993.

Ramsay, R. R.: A brief history of carnitine and its presence in the CNS. Journal of Neurochemistry **66:** S64-S64, 1996.

Ramsay, R. R.: The role of the carnitine system in peroxisomal fatty acid oxidation. American Journal of the Medical Sciences **318** (1)**:** 28-35, 1999.

Ramsay, R. R.: The carnitine acyltransferases: modulators of acyl-CoA- dependent reactions. Biochemical Society Transactions **28:** 182-186, 2000.

Ramsay, R. R., and Arduini, A.: The Carnitine Acyltransferases and Their Role in Modulating Acyl-Coa Pools. Archives of Biochemistry and Biophysics **302** (2)**:** 307-314, 1993.

Ramsay, R. R., and Bhaird, N. N.: Malonyl-CoA Inhibits Purified Peroxisomal Carnitine Octanoyl- Transferase at the Active-Site. Faseb Journal **6** (4)**:** A1383-A1383, 1992.

Ramsay, R. R., Derrick, J. P., Friend, A. S., and Tubbs, P. K.: Purification and Properties of the Soluble Carnitine Palmitoyltransferase from Bovine Liver-Mitochondria. Biochemical Journal **244** (2)**:** 271-278, 1987.

Ramsay, R. R., and Gandour, R. D.: Selective modulation of carnitine long-chain acyltransferase activities - Kinetics, inhibitors, and active sites of COT and CPT-II. *In* Current Views of Fatty Acid Oxidation and Ketogenesis, vol. 466, pp. 103-109, 1999.

Ramsay, R. R., Gandour, R. D., and van der Leij, F. R.: Molecular enzymology of carnitine transfer and transport. Biochimica Et Biophysica Acta-Protein Structure and Molecular Enzymology **1546** (1)**:** 21-43, 2001.

Ramsay, R. R., Tubbs, P.K.: The mechanism of fatty acid uptake by heart mitochondria: an acylcarnitine-carnitine exchange. FEBS Letters **54** (1)**:** 21-25, 1975.

Reed, J. C., Jurgensmeier, J. M., and Matsuyama, S.: Bcl-2 family proteins and mitochondria. Biochim Biophys Acta **1366** (1-2)**:** 127-37, 1998.

Reichert, A. S., and Neupert, W.: Contact sites between the outer and inner membrane of mitochondria - role in protein transport. Biochimica Et Biophysica Acta-Molecular Cell Research **1592** (1): 41-49, 2002.

Rickwood, D., Ford, T., and Graham, J.: Nycodenz - a New Non-Ionic Iodinated Gradient Medium. Analytical Biochemistry **123** (1): 23-31, 1982.

Rinaldo, P., and Matern, D.: Fatty acid oxidation disorders. Annual Review of Physiology **64:** 477-502, 2002.

Robinson, A. M., and Williamson, D. H.: Comparison of glucose metabolism in the lactating mammary gland of the rat in vivo and in vitro. Effects of starvation, prolactin or insulin deficiency. Biochem J **164** (1): 153-9, 1977.

Robinson, I. N., and Zammit, V. A.: Sensitivity of Carnitine Acyltransferase-I to Malonyl-Coa Inhibition in Isolated Rat-Liver Mitochondria Is Quantitatively Related to Hepatic Malonyl-Coa Concentration Invivo. Biochemical Journal **206** (1): 177-179, 1982.

Rodnick, K. J., and Sidell, B. D.: Cold acclimation increases carnitine palmitoyltransferase I activity in oxidative muscle of striped bass. Am J Physiol **266** (2 Pt 2): R405-12, 1994.

Saddler, J. B., and Cardwell, R.: The effect of tagging upon the fatty acid metabolism of juvenile pink salmon. Comparative Biochemistry and Physiology **39A:** 709-721, 1971.

Schlegel, J., Wyss, M., Schurch, U., Schnyder, T., Quest, A., Wegmann, G., Eppenberger, H. M., and Wallimann, T.: Mitochondrial creatine kinase from cardiac muscle and brain are two distinct isoenzymes but both form octameric molecules. J Biol Chem **263** (32): 16963-9, 1988.

Schmidt-Nielsen, K.: Animal Physiology, Cambridge University Press, Cambridge, MA, 1975.

Schnyder, T., Engel, A., Lustig, A., and Wallimann, T.: Native mitochondrial creatine kinase forms octameric structures. II. Characterization of dimers and octamers by ultracentrifugation, direct mass measurements by scanning transmission electron microscopy, and image analysis of single mitochondrial creatine kinase octamers. J Biol Chem **263** (32)**:** 16954-62, 1988.

Schultz, H.: Beta-oxidation of fatty acids. Biochimica Biophysica Acta **1081:** 109-120, 1991.

Segner, H., Dolle, A., and Bohm, R.: Ketone body metabolism in the Carp Cyprinus carpio: biochemical and 1H NMR spectroscopical analysis. Comp Biochem Physiol B Biochem Mol Biol **116** (2)**:** 257-62, 1997.

Sergeant, J. R., McIntosh, R., Bauermeister, A., and Blaxter, J. H. S.: Assimilation of the wax esters of marine zooplankton by herring (*Clupea harengus*) and rainbow trout (*Slamo gairdnerii*). Marine Biology **51:** 203-207, 1979.

Singh, H., Beckman, K., and Poulos, A.: Evidence of two catalytically active carnitine medium/long chain acyltransferases in rat liver peroxisomes. Journal of Lipid Research **37** (12)**:** 2616-2626, 1996.

Singh, H., Derwas, N., and Poulos, A.: Very long chain fatty acid beta-oxidation by rat liver mitochondria and peroxisomes. Arch Biochem Biophys **259** (2)**:** 382-90, 1987.

Singh, I., Lazo, O., Dhaunsi, G. S., and Contreras, M.: Transport of fatty acids into human and rat peroxisomes. Differential transport of palmitic and lignoceric acids and its implication to X-adrenoleukodystrophy. J Biol Chem **267** (19)**:** 13306-13, 1992.

Singh, I., Pahan, K., Dhaunsi, G. S., Lazo, O., and Ozand, P.: Phytanic Acid Alpha-Oxidation - Differential Subcellular- Localization in Rat and Human Tissues and Its Inhibition by Nycodenz. Journal of Biological Chemistry **268** (14): 9972-9979, 1993.

St-Pierre, J., Charest, P. M., and Guderley, H.: Relative contribution of quantitative and qualitative changes in mitochondria to metabolic compensation during seasonal acclimatisation of rainbow trout Oncorhynchus mykiss. Journal of Experimental Biology **201** (21): 2961-2970, 1998.

Stryer, L.: Biochemistry, W.H. Freeman, New York, 1988.

Szabo, I., De Pinto, V., and Zoratti, M.: The mitochondrial permeability transition pore may comprise VDAC molecules. II. The electrophysiological properties of VDAC are compatible with those of the mitochondrial megachannel. FEBS Lett **330** (2): 206-10, 1993.

Tang, D. G., La, E. H., Kern, J., and Kehrer, J. P.: Fatty acid oxidation and signaling in apoptosis. Biological Chemistry **383** (3-4): 425-442, 2002.

Taroni, F., Verderio, E., Fiorucci, S., Cavadini, P., Finocchiaro, G., Uziel, G., Lamantea, E., Gellera, C., and Didonato, S.: Molecular Characterization of Inherited Carnitine Palmitoyltransferase-Ii Deficiency. Proceedings of the National Academy of Sciences of the United States of America **89** (18): 8429-8433, 1992.

Tatton, W. G., and Olanow, C. W.: Apoptosis in neurodegenerative diseases: the role of mitochondria. Biochim Biophys Acta **1410** (2): 195-213, 1999.

Tran, T. N., and Christophersen, B. O.: Partitioning of polyunsaturated fatty acid oxidation between mitochondria and peroxisomes in isolated rat hepatocytes studied by HPLC separation of oxidation products. Biochimica Et Biophysica Acta-Molecular and Cell Biology of Lipids **1583** (2): 195-204, 2002.

Venkatesh, B.: Evolution and diversity of fish genomes. Curr Opin Genet Dev **13** (6): 588-92, 2003.

Verhoeven, N. M., Roe, D. S., Kok, R. M., Wanders, R. J. A., Jakobs, C., and Roe, C. R.: Phytanic acid and pristanic acid are oxidized by sequential peroxisomal and mitochondrial reactions in cultured fibroblasts. Journal of Lipid Research **39** (1): 66-74, 1998.

Volkl, A., Mohr, H., and Fahimi, H. D.: Peroxisome subpopulations of the rat liver. Isolation by immune free flow electrophoresis. J Histochem Cytochem **47** (9): 1111-8, 1999.

Wanders, R. J. A., Vreken, P., Ferdinandusse, S., Jansen, G. A., Waterham, H. R., van Roermund, C. W. T., and Van Grunsven, E. G.: Peroxisomal fatty acid alpha- and beta-oxidation in humans: enzymology, peroxisomal metabolite transporters and peroxisomal diseases. Biochemical Society Transactions **29:** 250-267, 2001.

Weber, J. M., and Haman, F.: Pathways for metabolic fuels and oxygen in high performance fish. Comparative Biochemistry and Physiology a-Physiology **113** (1): 33-38, 1996.

Zammit, V. A., and Newsholme, E. A.: Activities of enzymes of fat and ketone body metabolism and effect of starvation on blood concentrations of glucose and fat fuels in teleost and elasmobranch fish. Biochemical Journal **184:** 313-322, 1979.